National Library of Canada

Acquisitions and Bibliographic Services Branch

395 Wellington Street
Ottawa, Ontario
K1A 0N4

Bibliothèque nationale du Canada

Direction des acquisitions et des services bibliographiques

395, rue Wellington
Ottawa (Ontario)
K1A 0N4

Your file Votre référence

Our file Notre référence

NOTICE

The quality of this microform is heavily dependent upon the quality of the original thesis submitted for microfilming. Every effort has been made to ensure the highest quality of reproduction possible.

If pages are missing, contact the university which granted the degree.

Some pages may have indistinct print especially if the original pages were typed with a poor typewriter ribbon or if the university sent us an inferior photocopy.

Reproduction in full or in part of this microform is governed by the Canadian Copyright Act, R.S.C. 1970, c. C-30, and subsequent amendments.

AVIS

La qualité de cette microforme dépend grandement de la qualité de la thèse soumise au microfilmage. Nous avons tout fait pour assurer une qualité supérieure de reproduction.

S'il manque des pages, veuillez communiquer avec l'université qui a conféré le grade.

La qualité d'impression de certaines pages peut laisser à désirer, surtout si les pages originales ont été dactylographiées à l'aide d'un ruban usé ou si l'université nous a fait parvenir une photocopie de qualité inférieure.

La reproduction, même partielle, de cette microforme est soumise à la Loi canadienne sur le droit d'auteur, SRC 1970, c. C-30, et ses amendements subséquents.

Canada

University of Alberta

The hydrology and hydrochemistry of a high Arctic glacier

by

Mark Leslie Skidmore

©

A thesis submitted to the Faculty of Graduate Studies and Research in partial fulfillment of the requirements of Master of Science

Department of Geography

Edmonton, Alberta

Fall 1995

National Library
of Canada

Acquisitions and
Bibliographic Services Branch

395 Wellington Street
Ottawa, Ontario
K1A 0N4

Bibliothèque nationale
du Canada

Direction des acquisitions et
des services bibliographiques

395, rue Wellington
Ottawa (Ontario)
K1A 0N4

Your file Votre référence

Our file Notre référence

THE AUTHOR HAS GRANTED AN IRREVOCABLE NON-EXCLUSIVE LICENCE ALLOWING THE NATIONAL LIBRARY OF CANADA TO REPRODUCE, LOAN, DISTRIBUTE OR SELL COPIES OF HIS/HER THESIS BY ANY MEANS AND IN ANY FORM OR FORMAT, MAKING THIS THESIS AVAILABLE TO INTERESTED PERSONS.

L'AUTEUR A ACCORDE UNE LICENCE IRREVOCABLE ET NON EXCLUSIVE PERMETTANT A LA BIBLIOTHEQUE NATIONALE DU CANADA DE REPRODUIRE, PRETER, DISTRIBUER OU VENDRE DES COPIES DE SA THESE DE QUELQUE MANIERE ET SOUS QUELQUE FORME QUE CE SOIT POUR METTRE DES EXEMPLAIRES DE CETTE THESE A LA DISPOSITION DES PERSONNE INTERESSEES.

THE AUTHOR RETAINS OWNERSHIP OF THE COPYRIGHT IN HIS/HER THESIS. NEITHER THE THESIS NOR SUBSTANTIAL EXTRACTS FROM IT MAY BE PRINTED OR OTHERWISE REPRODUCED WITHOUT HIS/HER PERMISSION.

L'AUTEUR CONSERVE LA PROPRIETE DU DROIT D'AUTEUR QUI PROTEGE SA THESE. NI LA THESE NI DES EXTRAITS SUBSTANTIELS DE CELLE-CI NE DOIVENT ETRE IMPRIMES OU AUTREMENT REPRODUITS SANS SON AUTORISATION.

ISBN 0-612-06540-5

Canada

University of Alberta

Library Release Form

Name of Author: Mark Leslie Skidmore

Title of Thesis: The hydrology and hydrochemistry of a high Arctic glacier.

Degree: Master of Science

Year this Degree Granted: 1995

Permission is hereby granted to the University of Alberta Library to reproduce single copies of this thesis and to lend or sell such copies for private, scholarly, or scientific research purposes only.

The author reserves all other publication and other rights in association with the copyright in the thesis, and except as hereinbefore provided, neither the thesis nor any substantial portion thereof may be printed or otherwise reproduced in any material form whatever without the author's prior written permission.

Mark Skidmore

128, Vicarage Road,
Wollaston, Stourbridge,
West Midlands, DY8 4QY,
England

6/October/1995

University of Alberta

Faculty of Graduate Studies and Research

The undersigned certify that they have read, and recommend to the Faculty of Graduate Studies and Research for acceptance, a thesis entitled "The hydrology and hydrochemistry of a high Arctic glacier" submitted by Mark Leslie Skidmore in partial fulfillment of the requirements for the degree of Master of Science

Dr. M. J. Sharp

Dr. R. B. Rains

Dr. B. E. Nesbitt

5 october 1995

Abstract

The chemical characteristics of the outflowing waters from a high Arctic glacier indicate significant subglacial drainage and hence, polythermal ice conditions. The release of the subglacial water is catastrophic, occurring initially as a sudden outburst-break flood event, followed by a jökulhlaup. Mineral weathering in the ice-marginal and proglacial environment is a rapid process and the majority of subglacial waters are saturated with respect to calcite. Calcite precipitation and minor dedolomitisation occur subglacially due to the common ion effect with gypsum. These results have two important implications. First they provide direct evidence on the manner of subglacial water storage and release in polythermal ice masses and therefore, may provide useful information for the current debate on the manner of water release from the former mid-latitude ice sheets. Second the results may be used to improve the parameterisation of global chemical weathering models, which currently assume that chemical erosion beneath the Wisconsinan ice sheets was zero, and negligible in proglacial areas. Correctly parameterising these models is important in assessing the role of glacially-driven chemical weathering in controlling atmospheric CO_2 levels.

Acknowledgements

I would like to thank Dr. Martin Sharp for encouraging my interests in glaciology over the past six years and for the initial invitation to work with him and pursue an MSc. at the University of Alberta. Thanks also go to Dr. John England for stimulating and encouraging my interests in Arctic based research, Dr. John Shaw for advice on glacial hydrology and other matters, Dr. Bruce Rains for broadening my horizons in physical geography, Dr. Bruce Nesbitt for improving my understanding of water chemistry and Dr. Karlis Muehlenbachs for encouragement in my academic studies.

I am deeply indebted to my field assistant Joel Barker, for collection of field data, since without his help this thesis would not have been possible. John Woodward and Anthony Arendt also provided invaluable assistance both in the field and in Edmonton. Ideas in the thesis were sharpened through useful discussions with Scott Lamoureux. Craig Coburn solved the majority of my computing nightmares. Advice on ion chromatography came from Patrick Steffes and Mike Callaghan both of Dionex Incorporated and on water quality analyses from Ernie Perkins at the Alberta Research Council. Finally thanks to Michael Fisher in the drawing office for Figures 2.1 and 2.3

Financial support for the MSc. was provided in part by an Ministry of Advanced Education International Education Award from the Government of Alberta. Field research was supported by a grant from the Canadian Circumpolar Institute, and from NSERC and CRF (University of Alberta) grants to Dr. Martin Sharp. Logistical support in the field was provided by the Polar Continental Shelf Project, Department of Energy, Mines and Resources. The fieldwork was carried out with the kind permission of the Science Institute of the Northwest Territories, and the peoples of Resolute Bay and Grise Fiord.

I would also like to thank those individuals whose friendship has seen me through trying times during the course of my thesis: Shandy, Jeff, Vince, Andy P., Mandy, Shul, Scott, Anne, Olaf, Jason, Shaun, Jenn, Leslie, Greg, Louise and Andy S. Finally I would like to thank my brother and my parents for their encouragement and financial support.

TABLE OF CONTENTS

CHAPTER 1 : INTRODUCTION 2

Ice dynamics and hydrology 2

Temperate glacier hydrology 3

Arctic glacier hydrology 4

Water storage and release in larger polythermal ice masses 6

Wider implications of the study 7

Site selection 9

Approach to the study 10

Glacial hydrochemistry 11

Solute sources in a glacial catchment 12

Hydrochemistry in polar environments. 14

The application of hydrochemical techniques at John Evans Glacier 15

Outline of the thesis 15

CHAPTER 2: SITE DESCRIPTION, FIELD AND LABORATORY METHODS 16

Site description 16

Hydrology 16

Glacier geometry 19

Geology 23

Climate 24

Field methods 27

Gauging station location 27

Stream gauging 29

Continuous water quality monitoring 29

Discrete water quality sampling 30

Alkalinity 31

Laboratory methods 31

Suspended sediment 31

Ion Chromatography 32

CHAPTER 3 : CHEMICAL WEATHERING PROCESSES IN A HIGH ARCTIC GLACIAL CATCHMENT 36
Introduction 36
Glacially-driven chemical weathering 36
Heinrich events and erosion in glaciated carbonate_terrains 37
Solute sources in a glacial catchment 38
Weathering of catchment minerals. 38
Solute acquisition by glacial meltwaters. 44
Field and laboratory methods 47
Analytical methods 47
Results 51
Average stream water composition. 51
Solute provenance in stream waters. 51
Temporal changes in the composition of waters in individual streams. . . . 55
Characterisation of Weathering Environments 60
Supraglacial weathering environment 60
Proglacial weathering environment 63
Ice marginal weathering environment 64
Subglacial weathering environments 66
Quantification of calcite precipitation 67
Dissolved oxygen variations in the meltwaters 70
Sulphide oxidation as a proton source for weathering reactions 71
Sulphide oxidation in type 1 waters 71
Sulphide oxidation in type 2 waters 72
Sulphide sources in the catchment 73
Conclusions 73
Implications 74

CHAPTER 4 : SUBGLACIAL HYDROLOGICAL VARIATIONS 76
Introduction 76
Observations on the hydrology of glaciers in the Canadian Arctic 76
Observations on the hydrology of ice sheets 77
Water storage mechanisms in polythermal ice masses 78
Catastrophic flood types 79
Field methods 81
Results 81
Mode and location of water release 81
Proglacial stream 86
Outburst event 86
Fountain 91
Subglacial stream 91
The chemical composition of the subglacial waters. 94
Comparison of modes of outflow 97
Interannual variability of the subglacial drainage system 98
Conclusions 99

CHAPTER 5 : CONCLUSIONS 100
Implications 101
Hydrology 101
Hydrochemistry 102

REFERENCES 104

APPENDICES 114

LIST OF TABLES

Table 2.1 Geological formations of the catchment bedrock 23

Table 2.2 Average charge balance (CB) error for the water analyses of the six streams studied 34

Table 3.1 The mean and standard deviation of values for SIc, SId and SIg in the five studied streams. 50

Table 3.2 Mean concentrations in μeq/l and coefficients of variance for each ionic species in the six studied streams. 52

Table 3.3 Selected ion ratios for crustally sourced and atmospherically sourced solute. . . 54

Table 3.4 Seawater ratios of various crustal minerals relative to chloride concentrations . 55

Table 3.5 Composition of perfect charge balance waters for the subglacial stream (July 27th, 1994) 67

Table 3.6 Theoretical cation composition of the gypsum following scenario 1 68

Table 3.7 Mean and coefficients of variation of dissolved oxygen saturation levels in the five meltwater streams studied 71

LIST OF FIGURES

Figure 1.1 John Evans Glacier 1

Figure 2.1 Location of John Evans Glacier, eastern Ellesmere Island, N.W.T., Canada . . 17

Figure 2.2 a) Proportion of rock, glacier ice and lakes within the catchment
b) Sub catchment basins and areal extents 18

Figure 2.3 Configuration of the outflowing streams at the glacier snout 20

Figure 2.4 a) Area elevation distribution of John Evans Glacier
b) Long profiles of the three main glacier subcatchments 21

Figure 2.5 Bedrock geology of the catchment and the supraglacial hydrological network 22

Figure 2.6 Average daily air temperatures at Allman Bay and Alert, 1st July 1988 - 1st July 1989. 25

Figure 2.7 a) Summer length at Alert (1951-1994)
b) Positive degree days at Alert (1951-1994). 26

Figure 2.8 Timetable of water quality sampling in the six outflowing streams 28

Figure 3.1 a) Major cation and b) Major anion concentrations in the supraglacial stream. 56

Figure 3.2 a) Major cation and b) Major anion concentrations in the west marginal stream. 57

Figure 3.3 a) Major cation and b) Major anion concentrations in the proglacial stream 58

Figure 3.4 a) Plot of pP_{CO2} v $SI_{calcite}$ for five of the studied streams
b) Plot of alkalinity v pH for five of the studied streams 62

Figure 4.1 Characteristic hydrographs for a) sudden-break outburst flood, b) jökulhlaup and c) schematic diagram of a "stepped" jökulhlaup. 80

Figure 4.2 The artesian fountain on 9th July, 1994 83

Figure 4.3 Upwelling of subglacial waters through sediments at the ice-sediment interface 10th July, 1994 83

Figure 4.4 View of the proglacial stream channel on a) July 8th, b) July 9th, c) July 10th 84

Figure 4.5 View of the proglacial stream channel on a) July 11th,
b) July 12th, c) July 13th 85
Figure 4.6 a) Discharge, b) EC and c) SSC variations in the proglacial stream June
15th - August 6th, 1994. 87
Figure 4.7 a) Discharge v SSC for the proglacial stream July 10th - July15th
b) EC v SSC for the proglacial stream July 10th - July15th. 90
Figure 4. 8 SSC and EC variations in the fountain stream July 9th - July13th 92
Figure 4.9 a) Discharge, b) EC and c) SSC variations in the subglacial
stream July 15th - August 7th, 1994. 93
Figure 4.10 Nitrate concentrations in the supraglacial, proglacial, fountain
and subglacial streams from June 15th - August 7th.
. 95

Figure 1.1 John Evans Glacier.

CHAPTER 1 : INTRODUCTION

This thesis presents the results of a study of the hydrology of a high Arctic glacier (John Evans Glacier, Ellesmere Island, N.W.T., Canada). The research focuses on the measurement and analysis of the chemical characteristics of six streams draining the glacier. Using the meltwater chemistry, the major processes of solute acquisition in the different components of the drainage system are identified as are the major factors controlling these processes. Temporal variations in the hydrochemistry are used to demonstrate seasonal changes in the balance of solute sources and processes of solute acquisition which can be linked to changes in flow routing through the glacier. The wider implications of the study in terms of (a) the links between hydrology and dynamics in larger polythermal ice masses; contemporary ice sheets, and the mid-latitude Quaternary ice sheets and (b) the influence of glacially-driven chemical weathering on global biogeochemical cycles are discussed.

Ice dynamics and hydrology

During the past two decades there has been increasing realisation of the importance of the internal hydrology of glaciers and larger ice masses in controlling their dynamics (e.g. Iken, 1981; Iken and Bindschadler, 1986). The flow of an ice mass can have three components. The first is internal: plastic deformation of the ice; the second and third are basal: sliding of the ice over its bed and deformation of the bed itself (Paterson, 1994). Significant sliding and bed deformation can occur only where the basal ice is temperate (at the pressure melting point) and water is present. Plastic deformation can occur in ice at any temperature, however, the viscosity of the ice decreases as the ice temperature approaches 0°C. The distribution of temperate basal ice in an ice mass is controlled by ice thickness and the thermal regime.

Temperate glacier hydrology

Traditionally, it has been argued that basal motion is responsible for the majority of flow in temperate glaciers (Paterson, 1994). Studies of temperate glacier flow have identified changing subglacial water pressures (Pw) as a key variable in determining velocity fluctuations on a variety of timescales (e.g. Iken *et al.*, 1983 - increased summer flow velocities; Kamb, 1987 - glacier surges). Pw depends upon the meltwater flux, the ice mass geometry (which controls the hydraulic gradient and the tendency for ice flow to close down drainage pathways), the structure of the drainage system and the hydraulic geometry, sinuosity and boundary roughness of the major drainage routeways (Sharp, 1991). There are two primary sources of water at the base of an ice mass: meltwater derived from the melting of basal ice layers and surface derived meltwater. A small contribution to the total subglacial discharge comes from internal melt. The input of surficial runoff to the glacier bed is controlled primarily by the extent of crevassing and the number of moulins on the glacier surface, since they provide the pathways via which the majority of supraglacial water reaches the bed. Some additional meltwater may reach the glacier bed from marginal streams. Once at the glacier bed, water movement is controlled by the configuration of the basal hydrological system. Theoretical analyses of glacier hydrology for temperate glaciers now identify at least six possible components to subglacial drainage systems. These include subglacial water films (Weertman, 1972), R-channels incised upwards into the glacier sole (Röthlisberger, 1972), Nye channels incised into bedrock (Nye, 1973), linked cavity systems (Walder, 1986), permeable subglacial sediments (Shoemaker, 1986), and broad canals incised into the surface of such sediments (Walder and Fowler, 1994). Both the magnitude of Pw for a given discharge and the direction of the Pw/discharge relationship vary with drainage system type (Walder, 1986; Kamb, 1987; Walder and Fowler, 1994). Where the glacier is underlain by bedrock, rising subglacial water pressures lead to ice-bed decoupling and as Pw approaches Pi (ice overburden pressure) basal sliding increases. The closer Pw is to Pi the more rapid the sliding velocity. Where the glacier is underlain by sediment, the subglacial water can saturate the sediments, reducing their shear strength and thus allowing flow by sediment

deformation. If water pressures are high enough, basal sliding may also contribute to glacier velocity due to ice-sediment decoupling induced by high Pw (Iverson *et al.*, 1995). Clearly then, an understanding of the internal hydrological system of an ice mass is fundamental to studies of its dynamics.

Arctic glacier hydrology

Studies on glacier hydrology in polar regions are extremely limited. However, the large difference in mean annual air temperatures and seasonal temperature distribution between Arctic and Alpine environments would be expected to modify ice temperatures and seasonal runoff patterns. The few glacial hydrological studies that have been conducted in the Canadian Arctic note that runoff is not observed to penetrate to the glacier bed, being confined to supraglacial and ice marginal channels. Furthermore, runoff is highly seasonal being confined to the months when there is meltwater generation (May - August), (Adams, 1966; Østrem *et al.*, 1967; Ballantyne and McCann, 1981; Wolfe, 1995). These observations highlight two key differences between Arctic and Alpine glaciers.

First, the absence of subglacial drainage suggests that water does not penetrate to the beds of Arctic glaciers in large quantities. Arctic glaciers are often composed wholly or largely of cold ice. As a consequence, flow is largely the result of internal deformation alone and velocities are significantly lower than in Alpine glaciers. Consequently crevassing tends to be more limited, and this restricts the number of routeways by which surficial water may reach the glacier bed. In addition, if the glacier ice is largely cold (i.e. <0°C) it is impermeable on the intergranular scale. Moreover, it seems unlikely that water entering small surface cracks can carry or generate enough heat to develop a network of conduits within cold ice (Paterson, 1994). Water might reach the glacier bed by penetration from the sides; however, the sides are likely frozen to the bed since the ice there is thin. Second the reduced intensity and duration of the meltseason at Polar latitudes as compared to temperate latitudes will result in a reduction in surficial runoff for a given

glacier size. The lower water fluxes may not generate enough heat to penetrate to the glacier bed even if crevasses are present.

Despite these factors which might be expected to limit the extent of subglacial drainage in Arctic glaciers, there is indirect evidence that such drainage occurs. Müller and Iken, (1973) observed increased summer ice flow velocities in the ablation zone of White Glacier, Axel Heiberg Island, and they attributed these to seasonal basal motion. This implies that the basal ice is at the melting point and that surface meltwaters penetrate to the bed, even though the bulk of the ice is well below melting point. Iken (1972) argued that meltwater flowing down moulins penetrated to the bed and spread out over an area large enough to affect the basal velocity. Subsequent studies by Blatter (1987) show White Glacier has a polythermal regime, such that there is a central core of temperate ice at the bed, surrounded by cold ice at the surface, margins and glacier snout. Meltwater that does reach the bed will thus be limited spatially to the zone of basal ice at the pressure melting point. Discharge of turbid "englacial" water was observed from both the eastern and western margins of the glacier, but not from the glacier snout (Iken, 1974). This suggests that at White Glacier there may be a barrier of cold ice which prevents the drainage of such waters to the glacier snout.

Following Blatter and Hutter (1991), it appears that some Arctic glaciers are polythermal and that surficial water reaching the glacier bed is restricted to the basal zone where ice is temperate. If the basal hydraulic gradient is downglacier, then basal water will flow towards the snout, being ponded behind the cold ice barrier. The growth of the water pocket will depend on the rate of input of supraglacial waters and the permeability of the underlying substrate which controls groundwater outflow. If meltwater input significantly exceeds the output then water storage will occur until a critical point is reached when Pw is close enough to Pi to create bed separation and a breach of the cold ice dam. Release of the stored water will likely occur as a sudden outburst - break flood (Haeberli, 1983) similar to that of water pocket ruptures in Alpine glaciers. If the cold ice dam is thinner at the margins than at the snout then subglacial water may exit ice marginally (e.g. White

Glacier, Iken, 1974). The overall size of the water pocket and the subsequent flood will be controlled by the meltwater flux, the subglacial bedrock geometry and the thickness of the cold ice barrier. If annual water fluxes are low and the ice barrier is thick, interannual storage of water may occur.

Water storage and release in larger polythermal ice masses

Currently there is much debate about the nature of storage and release of water from within the former Laurentide ice sheet (Shaw, 1989; Shaw *et al.*, 1989; Shoemaker, 1991, 1992; Rains *et al.*, 1993). Evidence of water storage and release from beneath current ice sheets is limited. Here follows a synthesis of observations to date on Greenland and Antarctica.

Oswald and Robin (1973) interpret radio echo sounding traces from the base of the Antarctic Ice Sheet to indicate the presence of subglacial lakes. These lakes are found c. 1000 kilometres from the ice sheet margin beneath c. 2 kilometres of ice and have formed in bedrock depressions tens of kilometres in diameter. Since the lakes fill bedrock depressions and the rate of water input is limited to basal melt, they are considered to be stable features and therefore unlikely to drain catastrophically. At Law Dome east Antarctica, Goodwin (1988) observed "jökulhlaup"[1] events during the austral winters of 1985 and 1986. Detailed chemical and isotopic analysis of the outflowing waters indicate that they had been stored subglacially for a significant time period prior to their release. The outflowing waters issued from the glacier abruptly and continued to flow more or less continuously for a period of 6 months each winter. Thus, it would appear that the discharge event may be more accurately described as being of the sudden outburst-break

[1] A jökulhlaup is the catastrophic drainage of either an ice dammed or subglacial lake, via a subglacial drainage routeway which is enlarged progressively during the event. During the jökulhlaup, discharge increases exponentially until a point is reached when the reservoir of water is exhausted and a rapid decline in discharge is observed, resulting in a distinctive flood hydrograph.

type[2] rather than a jökulhlaup. In contrast to the lakes described by Oswald and Robin (1973), the location of the subglacial water pocket at Law Dome is considered to be c. 3 kilometres from the ice margin.

Observations of meltwater drainage at the margin of the Greenland ice sheet have noted catastrophic releases of water both during the meltseason (Sugden *et al.*, 1985; Scholtz *et al.*, 1988) and during the winter (Russell, 1990). The sources for the summer flood events are proglacial ice dammed lakes. Russell (1990) suggests that the drainage of an englacial/subglacial lake is the source of the water for the winter event. However, in a subsequent paper Russell (1993) argued that the water source is two large supraglacial lakes c. 20km from the ice margin. The supporting evidence for this theory is, however, circumstantial. The above studies show evidence for 'unusual' drainage events from polythermal ice masses. However, the sampling strategy for the studies was opportunistic, as were the majority of the observations. Therefore, the storage and release of water from beneath polythermal ice masses remains a poorly understood phenomenon, especially in the wider context of Arctic glacier hydrology.

Wider implications of the study

During the Quaternary up to 21 glacial and interglacial periods have been inferred from the $\delta^{18}O$ record in foraminifera in deep ocean sediment cores (van Donk, 1976). Direct evidence on the age of the present day ice sheets is available from ice core records at Summit, Greenland (Dansgaard *et al.*, 1993) and Vostok, Antarctica (Jouzel *et al.*, 1987). Both core records indicate that ice from the last interglacial exists at the base of the ice sheet. Modelling studies on the Greenland ice sheet (Letreguilly *et al.*, 1991) suggest that ice was still prevalent over the majority of the continent during the last interglacial. Denton *et al.*, (1970) state that the East Antarctic ice sheet has covered the continent for

[2] A sudden outburst break type event is the catastrophic drainage of either an ice dammed or subglacial lake resulting from the rupture of the ice dam. Discharge is at a maximum initially and shows an exponential decline as the reservoir drains.

at least the last 4 million years. In contrast, Zotikov (1986) notes that the mid-latitude ice sheets are relatively short-lived phenomena and do not persist during interglacial periods. Accordingly, he suggests that reconstructions of mid-latitude ice sheets and their dynamics should not be based upon assumptions derived from the current 'polar' ice sheets, since they have fundamentally different thermophysical characteristics.

Current reconstructions of the extent and dynamics of the mid-latitude ice sheets are largely based on geomorphic evidence (e.g. Clark 1994; Punkari, 1982). Both authors suggest that there were numerous fast flowing lobes on the southern margins of the ice sheets. Mathews (1974) suggests that these lobes had very low surface angles. With low surface angles the driving stress will be low and thus it is necessary to invoke basal ice motion and thus polythermal ice conditions to account for the fast flow. Borehole studies on ice streams[3] at the margins of present day ice sheets indicate that the ice is polythermal (i.e. the presence of temperate ice at the base). Kamb and Englehardt, (1991) argue that the rapid ice motion of Ice Stream B, West Antarctica, is caused by deformation of the underlying saturated sediments and/or basal sliding. In contrast, Iken *et al.*, (1993) argue that the rapid flow of Jakobshavn Isbrae, Greenland, is a result of enhanced ice deformation of weaker temperate basal ice. However, it is likely that Ice Stream B is the better analogy for the lobes on the southern margin of the Laurentide ice sheet since unlike Jakobshavn Isbrae it is not topographically constrained. Modelling studies (Arnold, 1994) that generate a lobate pattern in general agreement with the geomorphological evidence, stress the importance of hydrology in controlling the dynamics of the Fennoscandian ice sheet. Clearly then, polythermal ice conditions must have been prevalent along parts of the southern margins of the mid-latitude ice sheets during deglaciation.

---

[3] Following the definition of Paterson (1994, p301) I use 'ice stream' in the broad sense that it includes fast-flowing outlet glaciers.

Both Ice Stream B and Jakobshavn Isbrae are over two kilometres thick and have non-terrestrial termini. Jakobshavn Isbrae has a calving margin and Ice Stream B flows into the Ross Ice Shelf. Hence, studies on the nature of the subglacial hydrological system and the manner in which water may be released subglacially are inherently difficult. However, using borehole temperature measurements Blatter and Hutter (1991) show that high Arctic glaciers (e.g. White Glacier, Axel Heiberg Island) may also exhibit polythermal characteristics, suggesting that they have the potential for subglacial drainage. This suggests that high Arctic glaciers which are thick enough to be polythermal in character and which have terrestrial termini may be useful small-scale analogues for studying subglacial hydrological conditions in polythermal ice masses.

Site selection

Selection of a suitable field site was based on the following criteria :-

1. Hodgkins (1994) suggests that there is a critical thickness that an Arctic glacier must achieve before polythermal conditions can exist. In the case of Scott Turnerbreen, Svalbard, this is calculated to be 101 metres. In contrast White Glacier, Axel Heiberg Island, N.W.T., is 240 metres thick in the mid-ablation area where polythermal conditions are inferred (Müller, 1963).
2. The glacier terminus must be on land, rather than in tidewater, in order to allow monitoring of the outflowing streams.
3. The glacier should ideally occupy a single well-defined self-contained basin such that all the runoff drains to the snout to allow daily monitoring of multiple outflowing streams.

Since field reconnaissance was impractical due to logistical costs, the study glacier had to be selected on the basis of observations of maps and aerial photographs. More than 200 aerial photographs of glaciers in eastern Ellesmere Island were examined. John Evans Glacier is a large valley glacier located at 79°40'N 74° 00'W on an unnamed peninsula, south of Dobbin Bay, eastern Ellesmere Island, and was chosen for three basic reasons.

Analysis of map sheet 39H&29G and aerial photographs A-16607-193, 194 and 195 (1959) indicated:-

1. The glacier has an areal extent of over c. 110 square kilometres and an altitudinal range of 1300 metres (cf. White Glacier: area 38.7 square kilometres and altitudinal range 1700 metres; Ommanney, 1969). The size of the glacier suggests that polythermal ice conditions are highly likely to occur within it.
2. A number of supraglacial streams terminate in crevasse fields c. 4km from the glacier snout. A large turbid stream, which exits from the glacier mid-snout and is not linked directly to any supraglacial stream, may be the outflow for these streams. This suggests that the glacier may have an englacial/subglacial drainage system.
3. The glacier has a reasonably well defined watershed, where all runoff eventually drains to the snout of the glacier, allowing daily monitoring of multiple outflowing streams.

Approach to the study

Direct observations of contemporary subglacial drainage systems are extremely limited due to their physical inaccessibility. Direct observations of the morphology of englacial channels have been made on numerous Alpine and Arctic glaciers (Holmlund, 1988; Hagen *et al.*, 1991; Rehak and Rehak, 1995; Reynaud and Moreau, 1995; Schroder, 1995). However, most of the studies describe only a minute part of the glacier drainage system. Moreover, this mapping method is only useful in empty conduits that are large enough for people to move through. Direct observation of subglacial conditions has been attempted using down-borehole video cameras (Pohjola, 1994); however, views of the subglacial environment were extremely limited due to cloudy water at the base of the boreholes. The morphology of paleosubglacial drainage systems has been mapped in the forefields of retreating glaciers (e.g. Hallet and Anderson, 1980; Sharp *et al.*, 1989). Again, the method is limited by substrate type and to retreating glaciers. Although useful, all the above methods have a common limitation, that they are static observations, made at a specific point in time and can only be effectively applied to a small part of the glacier drainage system.

To assess the dynamics of subglacial hydrological systems, indirect methods of determining drainage system characteristics and their variation in space and time have to be applied (Sharp, 1991). The ideal research programme for monitoring the glacial hydrological system should include combined water quality measurements, of both dissolved and suspended load, dye tracer experiments and borehole investigations. Dye tracer and water quality techniques can be applied in tandem so that the validity of the results inferred from the water chemistry can be compared to those from dye tracing experiments. Moreover, borehole investigations provide a direct method of observing dynamic processes in the subglacial environment. As such they also provide independent verification of inferences made from both water quality and dye tracer studies. Both dye tracer studies and borehole investigations are most successfully executed once a basic knowledge of the glacier morphology and drainage system has been established. They are both only applicable if it has been established that there is a subglacial hydrological system to investigate. Since this study was an exploratory one to be completed in a single field season, and no direct field observations existed for John Evans Glacier, neither borehole nor dye tracer studies were considered appropriate strategies for investigation. However, it was believed that water quality measurements could be used to answer a number of basic questions about the hydrology of the glacier, for example the crucial question of whether or not there was subglacial drainage.

Glacial hydrochemistry

The basic premise of glacier hydrochemistry is that the chemical composition of the outflowing waters can provide information on the drainage pathway that those waters have followed. To correctly interpret the data on the chemical composition of the outflowing waters it is important to determine the likely sources of solute within the catchment.

Solute sources in a glacial catchment

Solute is defined as all the dissolved aqueous species, comprising positively charged species (cations - e.g. Ca^{2+}, Na^{+}), negatively charged species (anions - e.g. SO_4^{2-}, Cl^{-}) and neutral species (e.g. O_2^0,). In a glacial catchment, solute can be derived from two primary sources, the atmosphere and the weathering of crustal material. Biogenic inputs are largely unknown, but are assumed to be negligible due to the cold temperatures and sparse occurrence of biota. Solute input of charged species to the catchment from precipitation has two sources, the seasalt aerosol (comprising primarily Na^{+}, Mg^{+}, Ca^{2+}, K^{+}, Cl^{-}, SO_4^{2-}, HCO_3^{-}) and the anthropogenic (pollutant) aerosol, (H^{+}, Cl^{-}, NO_3^{-}, SO_4^{2-}). Input of neutral species (CO_2, O_2, N_2) from the atmosphere is controlled by rates of gaseous diffusion, and is not restricted to precipitation events.

Solute derived from crustal material can come from weathering of rock minerals derived from within the catchment or from weathering of wind-blown foreign particulate material deposited in the catchment. The main weathering reactions in glacial catchments have been identified by (Tranter *et al.*, 1993) as the acid hydrolysis of carbonate and silicate minerals, the simple dissolution of evaporite minerals and the oxidation of sulphides. The dominant weathering reactions in a particular catchment are therefore dependent on the minerals available for weathering in the catchment bedrock and on the solubility of the minerals. For example, Thomas and Raiswell (1984) note that in the Argentière catchment in the French Alps the acid hydrolysis of calcite is the dominant weathering reaction by which meltwaters acquire solute, even though calcite comprises only 1% of the minerals available for weathering.

The primary factors governing the extent of solute acquisition by glacial meltwaters have been identified by Sharp, (1991) as:

(i) the chemistry of the source waters;

(ii) the availability of protons (H^+) derived from snowpack leaching, carbonation or oxidation reactions;

(iii) the duration of contact between meltwaters and weatherable rock material;

(iv) the grain size, shape and mineralogical properties of particulate rock material; and

(v) the ratio between meltwater volume and the surface area of rock material available for weathering.

Different types of drainage system may be characterised by different proton sources, rock availability and weatherability, and water-rock contact times, and hence by differing magnitudes and processes of solute acquisition (Sharp, 1991). Temporal changes in these properties of any one type of system may result from varying source water composition and water flux. Where different parts of a single glacier are underlain by different types of drainage system, (e.g. Humphrey *et al.*, 1986; Willis *et al.*, 1990; Nienow, 1993) bulk water chemistry reflects mixing of waters from the different systems, which will often be non-conservative (Raiswell, 1984; Brown *et al.*, 1994).

Certain ionic species (eg. nitrate) are present in the atmospheric input but are unlikely to be derived by crustal weathering processes. Nitrate is derived from the nitric acid aerosol. If halite is not present in the catchment, then chloride also can only be derived as an atmospheric input from the seasalt aerosol. Tranter *et al.*, (1994) have observed much higher concentrations of nitrate and chloride in snowmelt than in icemelt both on Alpine and sub-polar glaciers. Therefore, it is reasonable to use nitrate and chloride as tracer ions to indicate a snowmelt source for particular waters.

Hydrochemistry in polar environments.

To the author's knowledge this is the first hydrochemical study on glacial meltwaters in the Canadian Arctic. Observations on glacial meltwaters in other polar regions of the northern hemisphere are limited and have only recorded drainage and water quality in supraglacial and ice marginal/proglacial streams (Andreason, 1984; Hodgkins, 1994; Hodson, 1994). According to Hodgkins (1994) both his study and that of Hodson (1994), on valley glaciers in Svalbard, indicate that at the start of the meltseason, high concentrations of solute are observed in the first fractions of snowmelt, declining as the snow cover is reduced. Andreason (1984) reports similar findings from two outlet glaciers in West Greenland. These results are similar to the findings of Johannessen and Henriksen (1978) and Bales (1992), from laboratory experiments on snow column melting.

Andreason (1984) showed that electrical conductivity (a surrogate measure for solute concentration) values in an ice marginal stream were consistently higher than in a supraglacial stream. Following the discharge of concentrated snowmelt, both streams show little diurnal variability for the remainder of the meltseason. Hodson (1994) observed similar trends in the solute concentrations in supraglacial and proglacial streams at Austre Broggerbreen, Svalbard. The proglacial meltwaters were dominated by Ca^{2+} and HCO_3^-, indicating solute acquisition by rock weathering. The only observations on the chemical composition of subglacially sourced waters in polar regions are at Law Dome, Antarctica (Goodwin, 1988). Goodwin (1988) shows that the total solute concentration of subglacially stored water in a polar environment is twice that of the maximum value for glacial meltwaters reported by Raiswell (1984) following his analysis of 40 temperate melt-water systems. The stored waters released in an outburst event were preferentially enriched in alkali metals (Na^+ and K^+), and thus are interpreted to have been squeezed through subglacial sediments for an extensive period (Goodwin, 1988).

The application of hydrochemical techniques at John Evans Glacier

The glacier has been selected on the premise that there may be a subglacial drainage system due to its size and likely polythermal characteristics. Aerial photographs show that there is circumstantial evidence to support this hypothesis. The aim is then to establish whether a subglacial drainage system exists, and if so under what conditions does it operate. It is likely that hydrochemistry should be a useful method of discriminating between waters which have drained, and perhaps been stored, at the bed and those which have drained more rapidly by supraglacial/ice marginal routes. Hence, monitoring hydrochemistry of the multiple outflow streams over the course of the melt season allows changes in the observed water characteristics to be linked to changing patterns of meltwater outflow.

Outline of the thesis

Chapter 1 has discussed the rationale behind the study, outlining its aims and the general approach to be taken. Chapter 2 introduces the study site, focusing on the hydrology, and bedrock geology of the catchment and pertinent climatic variables. Field methods and water sampling strategies are discussed, as are the laboratory methods. Chapter 3 identifies the predominant chemical weathering processes in the various outflowing streams, and assesses the balance of crustal versus atmospheric solute sources for the waters. Chapter 4 uses the results of the chemical analysis to interpret the subglacial hydrology of the glacier. Chapter 5 presents the conclusions of the study.

CHAPTER 2: SITE DESCRIPTION, FIELD AND LABORATORY METHODS

Site description

John Evans Glacier is a large valley glacier located at 79°40'N; 74° 00'W on an unnamed peninsula, south of Dobbin Bay, eastern Ellesmere Island, N.W.T., Canada. (Figure 2.1). Its total catchment area is approximately 220 km^2 of which 74% is glaciated (Figure 2.2a). The western part of the catchment area is occupied by a main trunk glacier which spans an altitudinal range from 100 - 1750 m, while the eastern part of the catchment comprises 8 small valley glaciers feeding into an ice marginal lake c. 4 km from the snout of the trunk glacier.

Hydrology

The catchment can be divided into three main sub-drainage basins (Figure 2.2 b). The eastern sub basin is the largest, with an areal extent of c. 131 km^2. It drains the eastern side of the trunk glacier and the 8 small valley glaciers. The majority of the runoff is channelled into the ice marginal lake and then flows in an ice marginal channel, which occasionally is routed beneath the ice margin. This stream is referred to in the thesis as the east marginal stream.

The central sub basin is the second largest with an area of approximately 50 km^2. This basin drains the majority of the upper part of the trunk glacier, and thus contains only a very small percentage of exposed bedrock. Runoff is concentrated into three large supraglacial streams which terminate in a large crevasse field at an altitude of c. 500 metres.

The western sub basin is the smallest of the three sub basins and has an area of 28 km^2. It drains the western part of the trunk glacier and the adjacent valley sides. Streams draining this catchment initially flow supraglacially, and converge at the margin to form

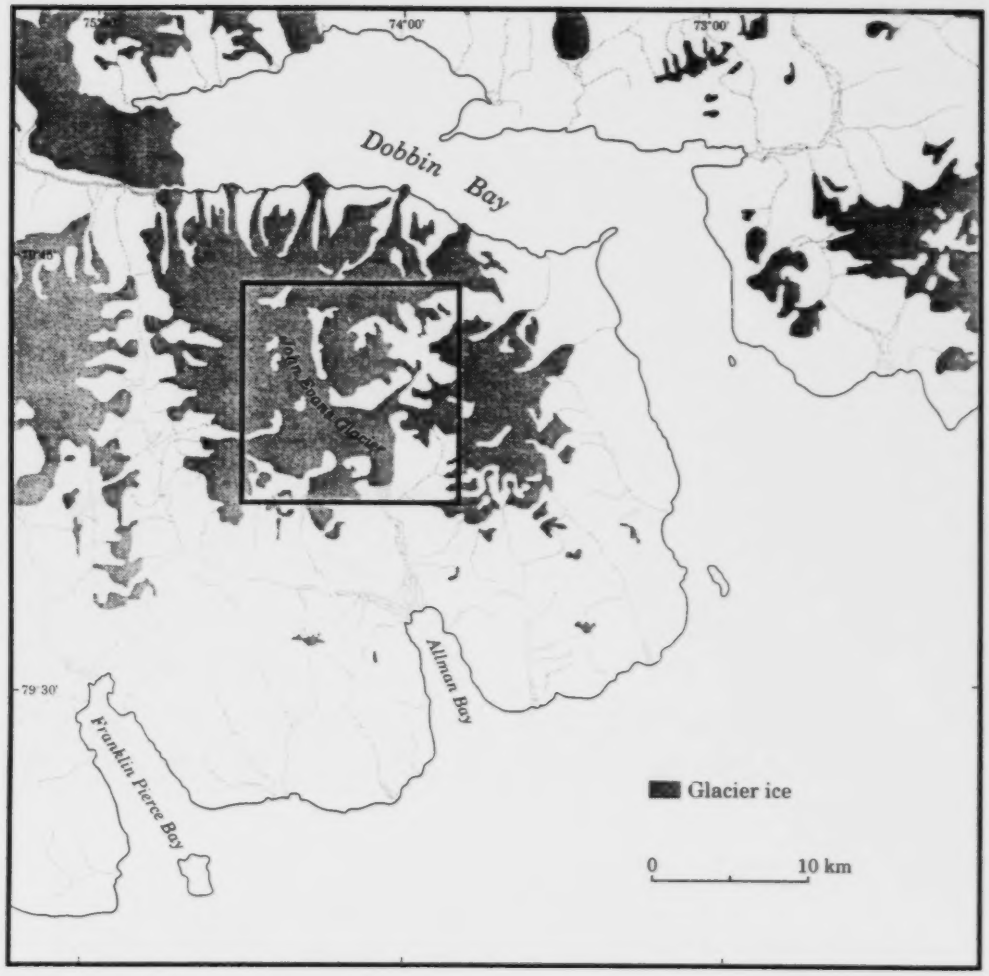

Figure 2.1 Location of John Evans Glacier, eastern Ellesmere Island, N.W.T., Canada. Note, outlined area is shown in more detail in Figures 2.2a and b.

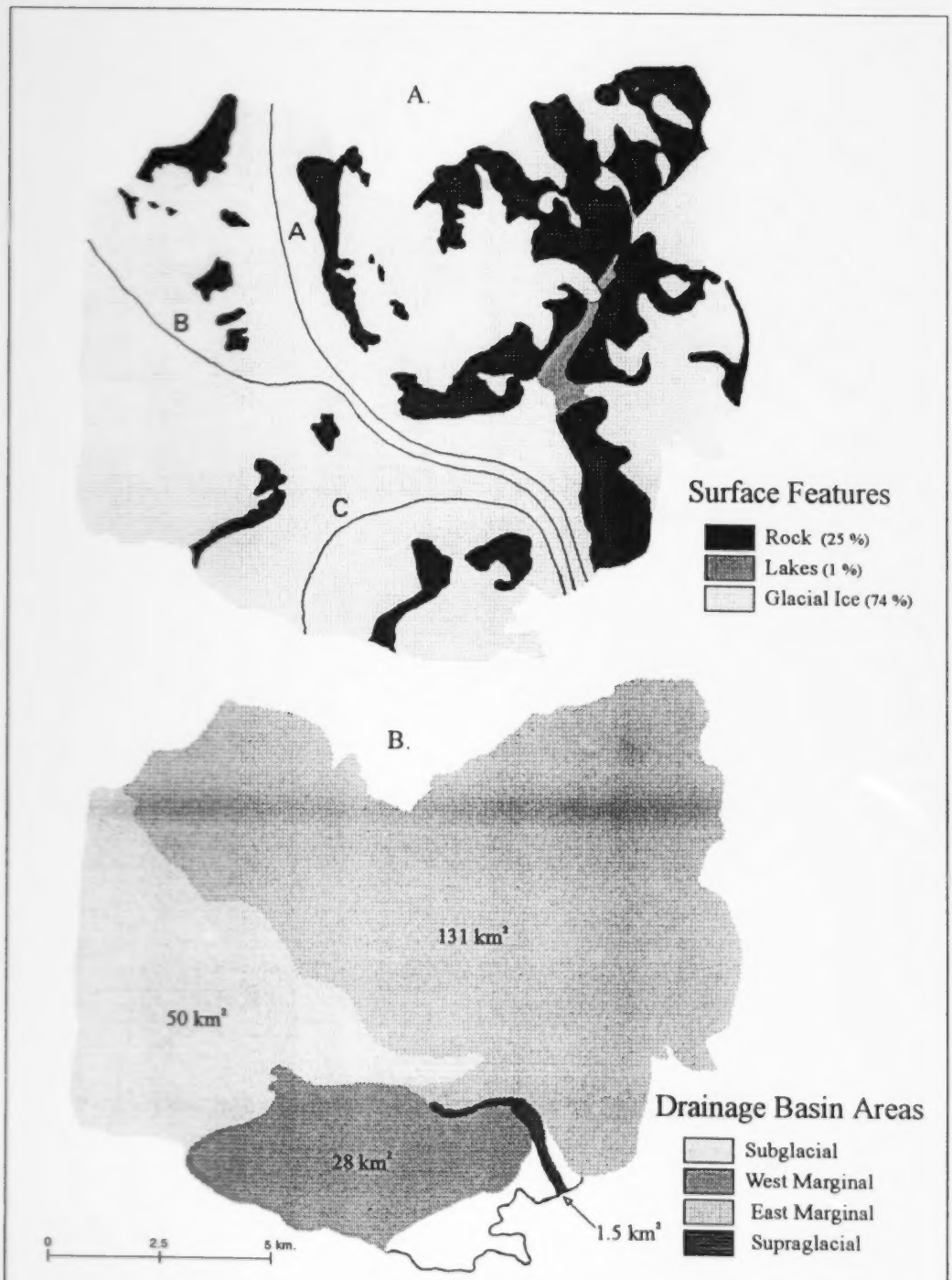

Figure 2.2 A. Proportion of rock, glacier ice and lakes within the catchment.
B. Sub catchment basins and areal extents.

a single large channel. This marginal channel is predominantly ice-walled and subaerial for the initial 2.5 km, after which the channel is routed subglacially for 1 km before exiting the glacier snout. Although routed subglacially, the channel is still located at the margin of the main glacier as it simply flows beneath the confluence between the main glacier and a small tributary glacier. This stream is referred to in the thesis as the west marginal stream. Also shown on Figure 2.2b is the very small catchment of the supraglacial stream.

Figure 2.3 shows the configuration of the main streams at the glacier snout. Glacier drainage at the snout is dominated by the two marginal streams and the subglacial stream. The subglacial stream is believed to be the outflow for runoff from the central sub-basin that enters the glacier in the major crevasse field. Also shown are the locations of the other streams studied, the "proglacial", "supraglacial" and "fountain" streams. The proglacial area is covered with a layer of unconsolidated sediments at least 4m thick, dissected by a large braided channel network.

Glacier geometry

The main trunk glacier occupies c. 50% of the total catchment area and is the focus of this study. 95% of the glacier lies below 1300 m, with the majority of the glacier lying between the elevations of 500 - 1000 m. (Figure 2.4a) The glacier has a maximum length of 21 kilometres and a stepped surface profile, with a major step at an elevation of c.500 m. The average gradients of profiles constructed along the glacier (see Figure 2.2a)in each of the *glacial* subcatchments are as follows; profile A, 6.3°, profile B, 4.9° and profile C, 7.4° giving an overall average gradient of 6.2° for the glacier (Figure 2.4b). The glacier surface is dissected by numerous supraglacial streams, which have carved deeply incised meandering channels (Figure 2.5). The glacier surface is relatively debris free and no significant medial or lateral moraines are evident.

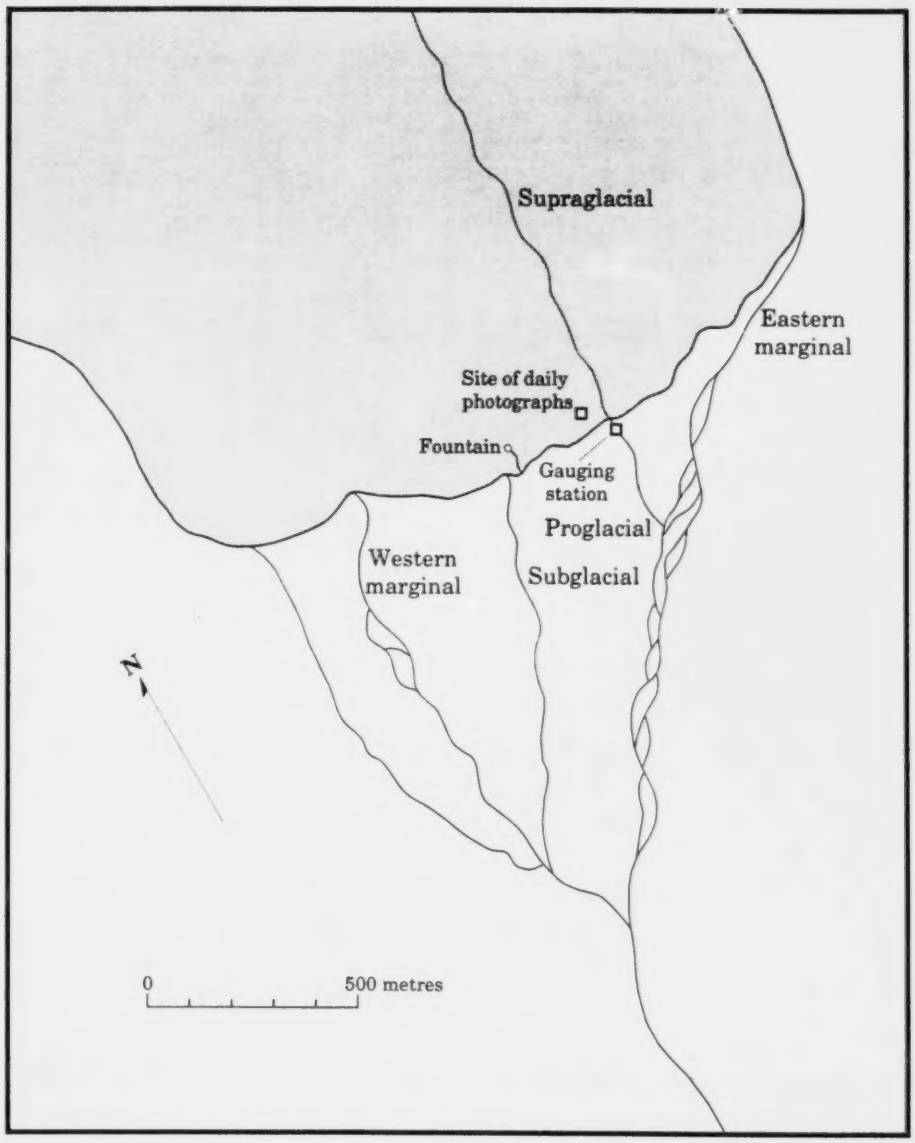

Figure 2.3 Configuration of the outflowing streams at the glacier snout.

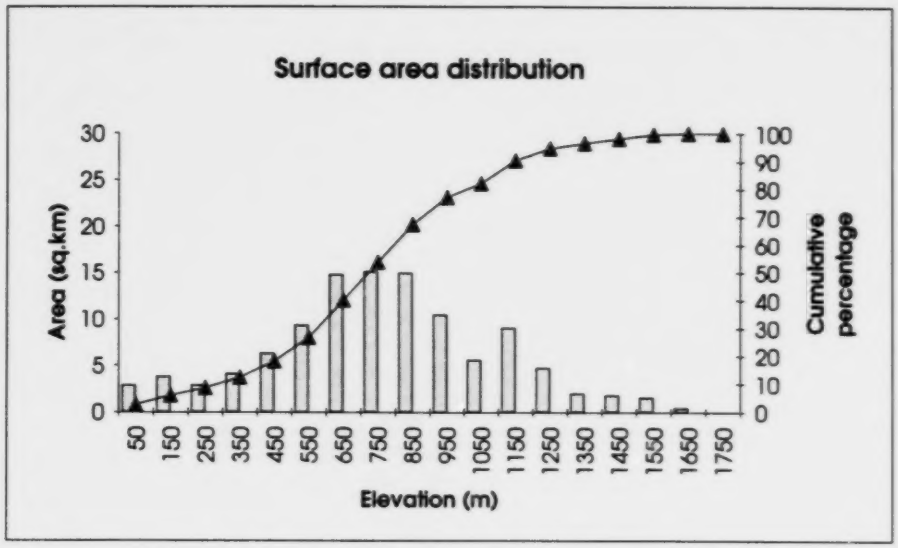

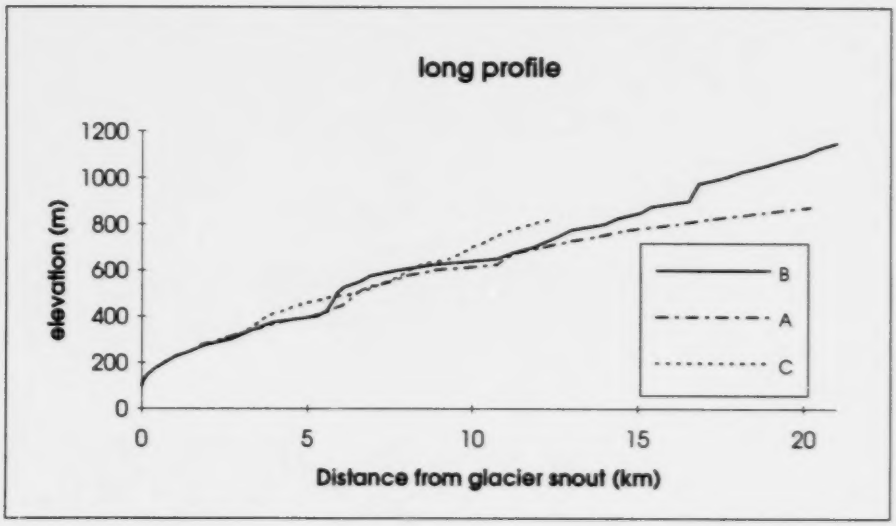

Figure 2.4 a. Area elevation distribution of John Evans Glacier

b. Long profiles of the three main glacier subcatchments

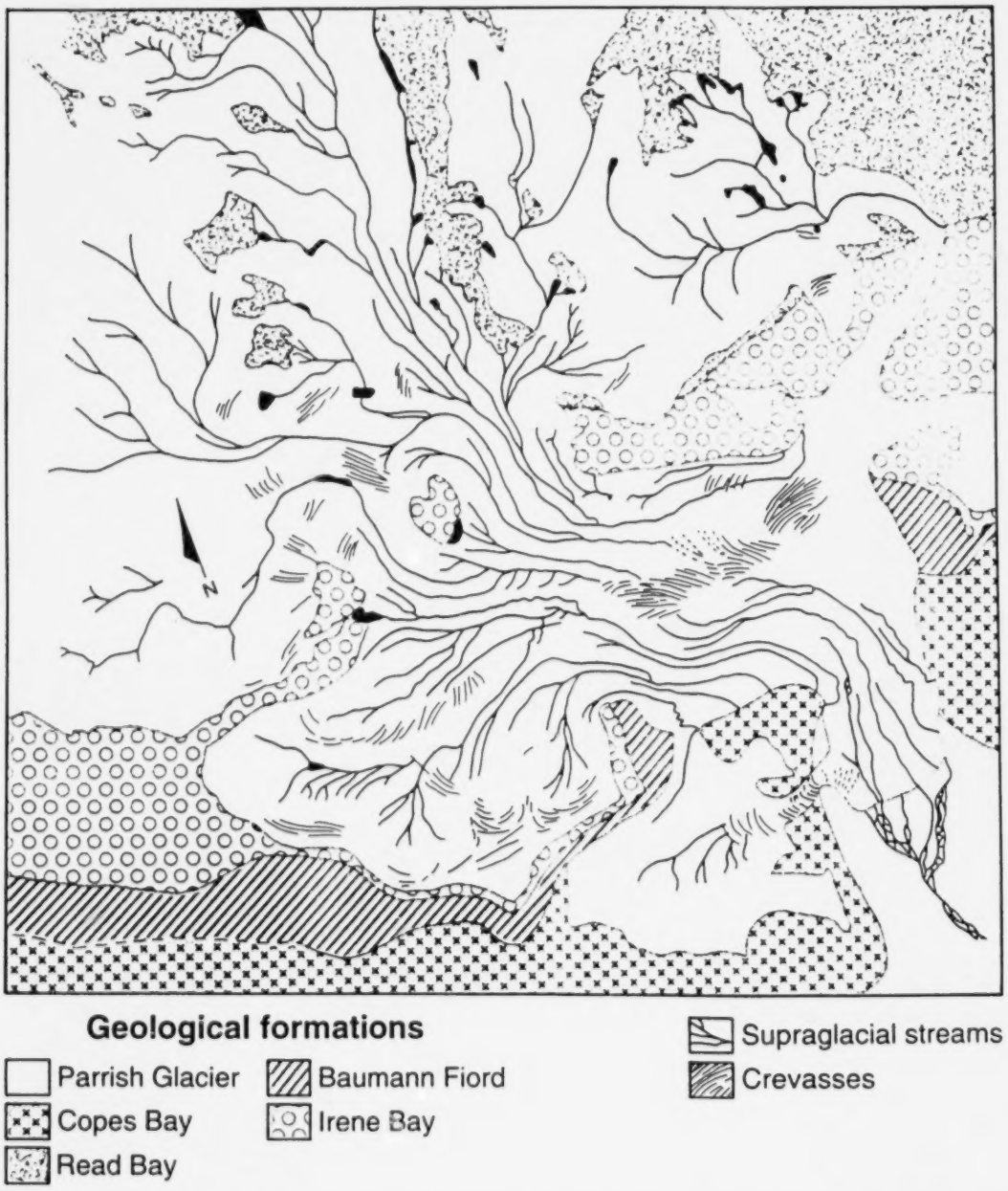

Figure 2.5 Bedrock geology of the catchment and the supraglacial hydrological network

Geology

Figure 2.5 shows the geology of the bedrock outcropping marginal to John Evans Glacier. The formations shown in Figure 2.5 continue uninterrupted eastward along the peninsula

---

Table 2.1 Geological formations of the catchment bedrock

Period	Group	Formation
Middle Cambrian:		Parrish Glacier : limestone, shale interbeds minor sandstone and flat-pebble conglomerate.
Lower Ordovician:		Copes Bay : limestone; minor flat-pebble conglomerate, anhydrite and dolomite. Baumann Fiord : anhydrite, gypsum; minor limestone (recessive).
Lower and Middle Ordovician: (undivided)	Cornwallis (Middle Ordovician)	Irene Bay : limestone, argillaceous limestone, dolomite. Thumb Mountain : limestone, minor dolomite. Bay Fiord : limestone, anhydrite and gypsum, siltstone. Eleanor River (Lower and Middle Ordovician): limestone.
Upper Ordovician, Lower, Middle and Upper Silurian, and Lower Devonian:		Read Bay (undivided) : limestone, siltstone Allen Bay : dolomite, minor limestone

(Figure 2.1). Thus, the eastern part of the main catchment is underlain by the same geological formations that outcrop marginal to the glacier. On Figure 2.5 the formation labelled Irene Bay actually represents the whole of the Cornwallis Group; comprising the Irene Bay, Thumb Mountain, Bay Fiord and Eleanor River Formations (see Table 2.1). Similarly, the formation labelled Read Bay actually represents both the Read Bay and Allen Bay Formations. Detailed descriptions of the formations are given in Table 2.1, (Kerr, 1972).

Climate

The nearest weather stations that have a continuous record of weather data for any substantial period are Eureka (230 km west of John Evans Glacier) and Alert (300 km north of John Evans Glacier). Daily air temperatures measured at a meteorological station placed in Allman Bay (c. 5 km south of the glacier snout) for the year July 1988 - July 1989 (G. Henry pers. comm., 1995), compare well with those recorded at Alert over the same time period (Figure 2.6). Arendt (1995) notes that at Allman Bay the average July temperature for the 1988 - 1989 period is c. 3°C higher than at Alert, whereas mean annual average air temperatures are very similar. On this basis it would seem that air temperature data from Alert is a good proxy for air temperatures at the snout of John Evans Glacier. Air temperatures actually on the glacier probably decline with altitude at an estimated rate of 0.4°C/100m based on the only available observations of lapse rates in the high Arctic at Storstrømmen, N.E. Greenland (Bøggild *et al.*, 1994). For the forty year period 1950 - 1990, mean annual and mean July temperatures at Alert were -18°C and 3.6°C respectively (Arendt, 1995). Figures 2.7a and b show the length and intensity (measured by the number of positive degree days) of the melt season at Alert over the last forty years. In comparison to previous years it appears that in 1994 the meltseason was of relatively long duration but of low intensity.

Data for other climatic variables, such as precipitation, are not available from the 1988-89 dataset. However, interpolation of Koerner's (1979) map of precipitation distribution in

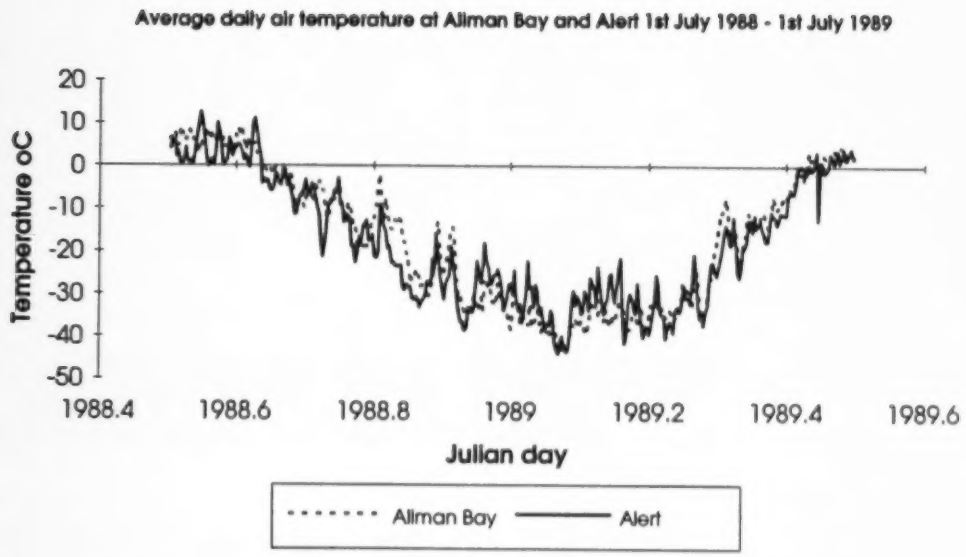

Figure 2.6 Average daily air temperatures at Allman Bay and Alert 1st July 1988 - 1st July 1989.

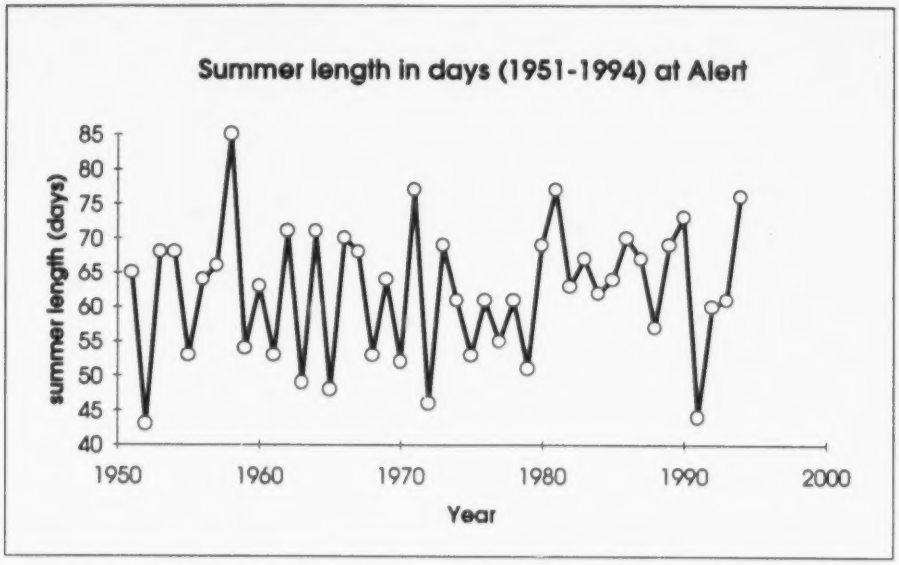

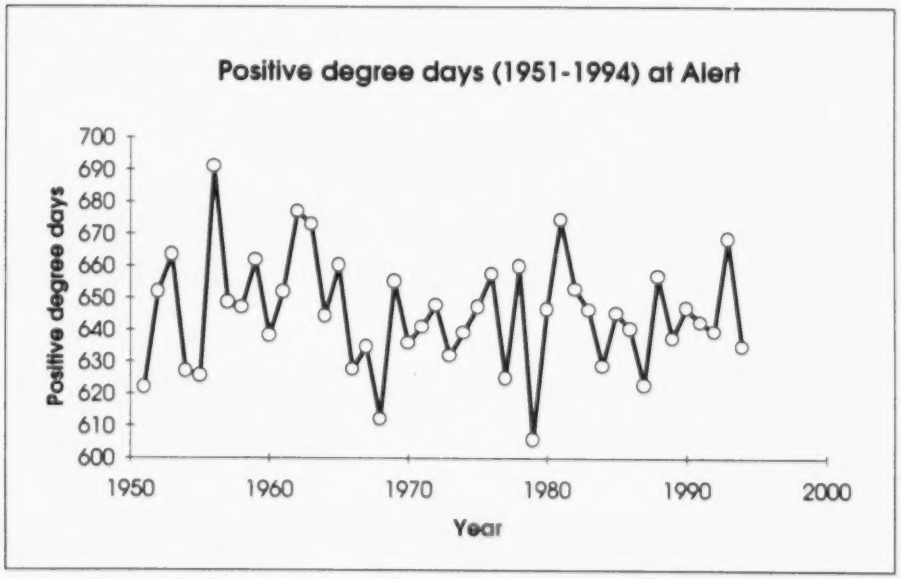

Figure 2.7 a) Summer length at Alert (1951-1994)

b) Positive degree days at Alert (1951-1994).

the eastern Arctic, suggests that John Evans Glacier receives on average 200-300mm water equivalent (WE) a^{-1}, which is c. 50-150mm (WE) a^{-1} more precipitation than at Alert. This is due to the glacier's closer proximity to the moisture source of Baffin Bay.

Field methods

The 1994 field season commenced on June 15th (Julian Day (JD) 166), and ended on August 7th (JD219). Appendix 1 (fold out page) is a Julian Day Calendar, which may be useful as a reference aid throughout the thesis. During that period water quality measurements were made on six meltwater streams draining the glacier. The supraglacial and west marginal streams were monitored for the duration of the field season, and the proglacial, fountain, east marginal and subglacial streams for parts thereof (Figure 2.8). During the periods when streams were sampled; measurements were made at least once daily, except when high discharges in the east marginal stream prevented access to the other streams. The discharge of the proglacial stream was measured both manually at least once a day, and continuously from July 15th - August 6th. Manual measurements of discharge in the subglacial stream were made at least once daily from July 27th-August 7th. The methods employed for collecting these various data are outlined in detail below.

Gauging station location

Aerial photographs taken in 1959 appeared to show a large, highly turbid meltstream draining from the glacier mid-snout, although no large supraglacial stream was observed feeding it from immediately up-glacier. The highly turbid stream was, therefore, interpreted as being of subglacial origin due to the high levels of suspended sediment. As part of the sampling programme, it was intended to set up a gauging station to continuously monitor the stage and electrical conductivity (EC) variations of the possible subglacial stream. On arrival in the field, however, no obvious dry channel was evident at the location in which the stream appeared on the aerial photographs. However, a large dry channel was observed immediately in front of the glacier snout c. 300m to the east

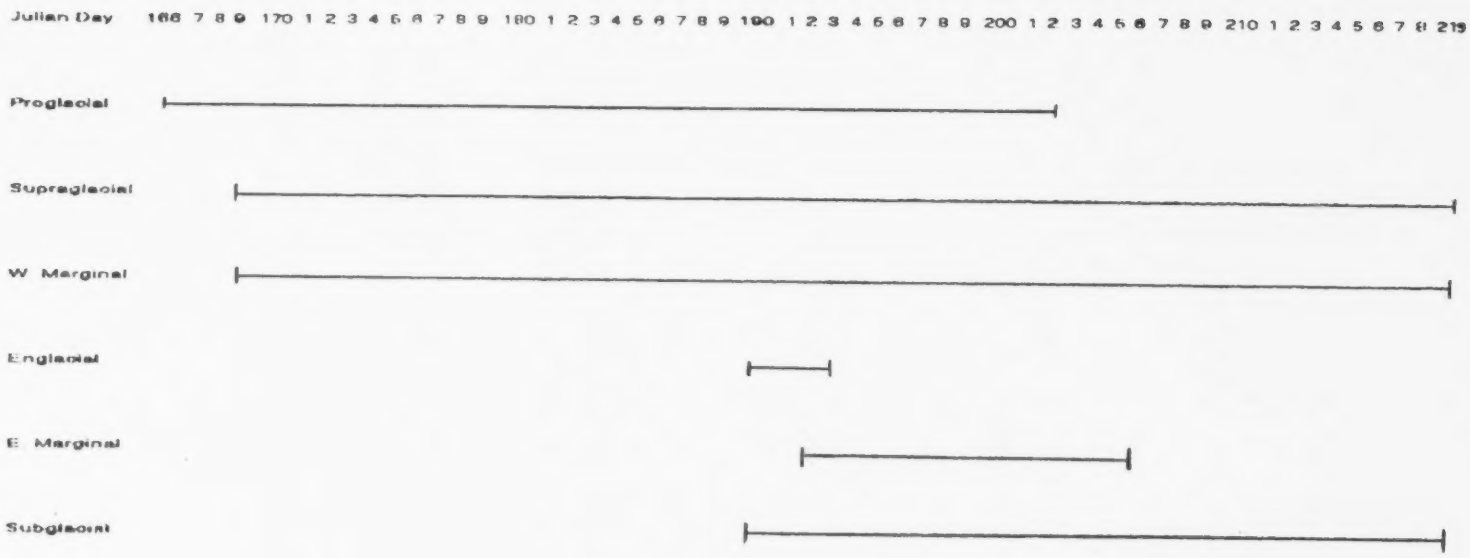

Figure 2.8 Timetable of water quality sampling in the six outflowing streams

of the expected position. The banks of this channel were c.1.5 m high and well defined, commencing c. 20 m from the glacier snout. Therefore, it was decided that this would be the site of the permanent gauging station unless subglacial drainage was observed in another location.

Stream gauging

Stage of the proglacial stream was recorded continuously using a Keller Series 169 pressure transducer. Readings were taken every ten seconds and the half hourly averaged values were stored on a Campbell CR10 datalogger. To provide an independent check on the accuracy of the logger readings, manual readings of stage were taken twice daily using a meter rule mounted on the gauging station. Discharge values were calculated from manual measurements of channel cross sectional area and velocity (which were taken at the same time as water quality samples) using the velocity area method (Gardiner and Dackcombe, 1983, p. 127). Velocity measurements were made using a Gurley current meter.

Continuous water quality monitoring

The EC of the proglacial stream waters was recorded continuously using a Nickel conductivity probe. Readings were taken every ten seconds and the half hourly averages stored on a Campbell CR10 datalogger. The probe was mounted on a dexion stake inserted into the stream bed such that the tip of the probe was c. 3cm above the bed. For the probe to function the electrodes must be fully immersed in water in order to complete the electrical circuit. Hence, breaks in the EC record reflect episodes when the probe was not fully immersed during very low discharges.

The conductivity probe was calibrated in the field, prior to installation, using Fisher Conductivity standards of 10.4 and 98.3 $\mu s\ cm^{-1}$. The calibration was checked twice during the field season and again at the end. Raw values from the datalogger sometimes

exceeded those for the 98.3 μs cm^{-1} standard. In the laboratory a 10 point calibration curve from 0 - 400 μs cm^{-1} at 20°C was established (using dilutions of the 985 μs cm^{-1} Fisher Conductivity standard), to extend the range of the calibration to include the high datalogger values recorded in the field. The Cole Palmer conductivity meter automatically corrects the conductivity values recorded to 25°C. Logger values were corrected to a temperature of 2°C following Hemm, (1982).

Discrete water quality sampling

Where possible, water samples were taken from the centre of the stream channel. However, high stream flow velocities sometimes prevented this, in which case samples were taken from as close to the centre of the channel as safety considerations allowed. The sampling bottle was rinsed 3 times with stream water and then a 500ml aliquot was taken. The pH and EC of the waters were measured immediately on a sub sample of the aliquot. The pH was measured using a Ross Sure-flow electrode, connected to an Orion 290A pH meter. The instrument was calibrated 4 times daily using fresh Orion Low ionic strength buffer solutions - pH 7.01 and 4.10 - on each occasion. Calibration was performed before and after the morning and afternoon sampling sessions to ascertain if there was any noticeable drift in the pH values recorded by the electrode. None was observed. The EC was measured using a Cole Palmer conductivity meter. This meter was calibrated twice a week using Fisher Scientific 10.4 and 98.3 μs cm^{-1} conductivity standards. The remainder of the aliquot was filtered through a 0.45 micron cellulose nitrate filter membrane using a hand pumped vacuum filtration system. Four 30ml filtered samples were retained, three for analysis of bicarbonate concentrations in the field, and the other for laboratory analysis of major anion and cation concentrations by ion chromatography. On return from the field all samples were stored in a refrigerator. Filter papers were folded and stored in Ziploc bags to allow calculation of the suspended sediment concentrations. A further 500ml aliquot of water was taken for determination of dissolved oxygen (DO) levels. Dissolved oxygen concentrations were measured immediately after collection using an Orion Model 97-08 Oxygen Electrode connected to

an Orion 290A pH/ISE Meter. Samples were stirred using a magnetic stirrer to ensure a regular flow of water past the DO membrane. Temperature of the water was also recorded. The meter was standardised prior to sample measurement in a flask containing water saturated air at a barometric pressure of 746 mm (the pressure at an elevation of 500 feet a.s.l. assuming sea level barometric pressure is 760mm and constant). The probe has a reported accuracy of ± 0.05 parts per million (DO) or 2% of the reading.

Alkalinity

Total alkalinity was determined in the field within 24 hours of sampling by titration using a Hach digital titrator. Phenolphthalein powder pillows were added to the sample to ascertain whether any carbonate alkalinity was present. The initial pH of the sample was recorded, and titrant (0.16N sulphuric acid) added to an endpoint of pH 5.1 as specified by the manufacturer. Titrant volumes were converted to give bicarbonate (HCO_3^-) concentration in µeq/l.

Laboratory methods

Suspended sediment

Filter papers were not individually weighed prior to fieldwork. Instead, 5 filter papers from each box of 100 were retained unused to be tested as blanks. Filter papers generally show consistency in weight within a box. However, there may be measurable differences between boxes, (G.H.Brown, pers. comm., 1994). In order to achieve comparability between the blanks and the field filter papers, 500ml of deionised water was passed through the filter paper using the same vacuum filtration apparatus. All filter papers (blanks and field samples) were dried at 105°C for 24 hours, and left to cool for 30 minutes in a desiccator prior to weighing. A Mettler AE100 balance was used for all the weight determinations and has a reported accuracy of +/- 0.0001g. In some cases where suspended sediment concentrations were high, sediment leaked from the filter paper into

the Ziploc bag. When this occurred, the bag was rinsed with deionised water until free of sediment and the slurry was poured into pre-weighed crucibles along with the filter paper. The crucibles were subjected to the same drying procedures as the filter papers. To calculate the weight of sediment on the filter paper, the average weight of the five blanks was subtracted from the dried weights. Weights of less than 0.0005g were reported as zero. Since the sample volume was only 500ml all sediment weights were multiplied by 2 and reported as a concentration in g/l.

Ion Chromatography

All cation and anion determinations were made using a Dionex DX 500 ion chromatograph. Anion concentrations (Chloride (Cl^-), Nitrate (NO_3^-), Sulphate (SO_4^{2-})) were determined using a Dionex Ionpac AS4 column and 1.7mM Sodium Carbonate/1.8mM Sodium Bicarbonate eluent. Cation concentrations (Sodium (Na^+), Potassium (K^+), Magnesium (Mg^{2+}), and Calcium (Ca^{2+})) were determined using a Dionex Ionpac CS12 column and 20mM Methanesulphonic Acid (MSA) eluent.
Samples for laboratory analysis were not acidified in the field, since sufficient bottles were not available to allow separate samples to be taken for anion and cation determination. Anion determinations were carried out first and the residual samples were acidified using 25µl of 99% pure MSA prior to cation analysis.

Sample preparation: All eluents were prepared using deionised (18 megaohm) water. Prior to addition of the sample, all vials were washed three times using deionised water and the filter caps were rinsed with 30ml of deionised water. A "blank" vial prepared in an identical manner to the samples containing deionised water was analysed at the end of every sample run to check for any contamination in the water supply or during sample preparation. Of the 15 blanks run for cation analysis 7 samples showed very slight contamination; <1µeq/l Na^+ was observed in 4 of the samples and < 1.5 µeq/l Ca^{2+} in 3 of the samples. All other ion concentrations were zero. Of the 7 blanks run for anion analysis only 1 showed slight contamination (with 0.25 µeq/l Cl^-). Contamination of

samples during the preparation process was thus considered to be insignificant. Samples were analysed in a random order to prevent any systematic errors appearing as trends within the time series data. Prior to sample analysis, the baseline conductivity of the eluent must be stable. Therefore, the chromatograph was run until less than 0.2μs cm^{-1} drift / 10 minutes was observed.

Calibration : Dionex 'six cation' (Li^+, Na^+, NH_4^+, K^+, Mg^{2+}, Ca^{2+}) and 'five anion' (F^-, Cl^-, NO_3^-, PO_4^{3-}, SO_4^{2-}) standards were used to construct 10 point calibration curves, over a range appropriate for each individual ion. The anion calibrations were checked independently using standards prepared using the appropriate mineral salts ($NaNO_3$, NaCl and Na_2SO_4) and deionised water.

Repeat analyses: At least one sample from each stream was analysed nine times to check the repeatability of the results over a wide range of ion concentrations. Eleven samples were analysed for cations and seven for anions. For certain ions the level of repeatability varies with concentration. The standard errors for individual ions are as follows:
Na^+, < 2%, (>7μeq/l); K^+, 10% (<1μeq/l), 1% (>5μeq/l); Mg^{2+}, < 2% (>8μeq/l); Ca^{2+}, 5% (<20μeq/l), <1% (>40μeq/l); Cl^-, 2% (>10μeq/l); NO_3^-, 5% (>0.4μeq/l); SO_4^{2-}, 2% (5μeq/l). Even at very low concentrations the reproducibility of the results was very good.

Charge balance: The charge balance (CB) of each sample was calculated using equation 1

$$(\Sigma^+ - \Sigma^-)/ (\Sigma^+ + \Sigma^-) \times 100 \qquad (1)$$

Calculations of HCO_3^- from field titrations were also included in equation 1. The average charge balance error for each of the six streams is shown in Table 2.2. Analyses of very dilute waters (e.g. supraglacial and proglacial stream) often have fairly high charge balance errors. However, if the source of the charge balance error was due to a constant error in the analytical technique, it would be expected that as solutions become more

concentrated the overall charge balance would improve since absolute errors would become proportionately less important.

Table 2.2 Average charge balance (CB) error for the water analyses of the six streams studied

Stream	mean (CB) error %	mean total solute μeq/l
Supraglacial	+ 15	129
Proglacial	+ 7	534
West marginal	+ 24	1283
East Marginal	+ 17	1341
Fountain	+ 1.4	5411
Subglacial	- 2	4040

Therefore, the charge balances for the west and east marginal streams are somewhat unusual in two ways. The errors are higher than for the more dilute waters and in all the analyses cation concentrations are greater than anion concentrations, suggesting a systematic error. If it is assumed that the results from ion chromatography are reliable as indicated by the blanks and the reproducibility of the results, the bicarbonate concentrations are the likely source of error. The titration procedure for alkalinity has a number of possible sources of error and the accuracy of the HCO_3^- determination method itself is limited by the accuracy of the pH meter (± 0.1 pH units). HCO_3^- is the dominant anion in the waters of the west and east marginal streams and occurs in much higher concentrations than in the other streams. This suggests that the error scales with concentration. Given this, a possible source of error may be that the digital titrator calibration is itself incorrect such that 1 turn on the titrator releases a slightly larger volume of acid than the 1/800ml it is supposed to. An alternative explanation may be that

the acid was actually stronger than the reported concentration of 0.08M on the cartridge. However, as all the cartridges were used in the field, testing of the acid strength was not possible. Assuming perfect charge balance in the marginal streams, and that the excess cations are all balanced by bicarbonate, the saturation indices for calcite (SI_c) and dolomite (SI_d) and the partial pressure of CO_2 (P_{CO2}) would all be changed, (details on the calculations of (SI_c), (SI_d) and (P_{CO2}) are given in Chapter 3). On average the perfect charge balance figures would result in an increase in SI_c by 0.2 units, SI_d by 1.4 units and P_{CO2} would be increased by an average of 0.2 units. Such differences would not change the interpretation of the variations in these parameters and therefore the field values were used since the source of the error remains unidentified.

CHAPTER 3 : CHEMICAL WEATHERING PROCESSES IN A HIGH ARCTIC GLACIAL CATCHMENT

Introduction

In this chapter the major chemical weathering processes occurring in the supraglacial, proglacial, marginal and subglacial environments at John Evans Glacier, Ellesmere Island, N.W.T. are identified. This provides the basis for grouping waters into two categories on the basis of their weathering pathways.

Glacially-driven chemical weathering

It is recognised that atmospheric CO_2 levels are a major factor in determining climatic conditions, through various feedback mechanisms (e.g. Hansen *et al.*, 1981). Kump and Alley (1994) show that on glacial/interglacial timescales ($<10^4$-10^5 years) changes in rates of chemical erosion have the potential to affect atmospheric CO_2 levels through the process of acid hydrolysis. During glacial times, ice cover on the earth's surface greatly increased and runoff regimes were significantly modified in the newly glaciated terrains. Glacial erosion produced large volumes of highly comminuted sediment by the processes of abrasion and crushing (Sugden and John, 1976). The interaction of this sediment with large volumes of relatively dilute glacial meltwaters provided a favourable environment for chemical weathering.

Sharp *et al.*, (1995) show that chemical denudation rates in temperate valley glacier systems are 1.5-3 times the continental average, and that CO_2 consumption due to chemical weathering increases linearly with meltwater runoff. If this relationship is valid on larger scales, it would suggest that the deglaciation of major ice sheets would be an important event in terms of CO_2 consumption due to the massive increases in runoff in glaciated areas. However, temperate valley glaciers are not good analogues for Pleistocene ice sheets due to their thermal regime and limited areal extent.

In modelling global chemical erosion during the last glaciation and at present, Gibbs and Kump (1994) assumed that all areas covered by Pleistocene ice sheets had an effective chemical erosion flux of zero, since they assume that the ice sheets were likely predominantly cold based. They also assume that the immediate channelisation of meltwater from the ice sheets would limit the extent to which waters have access to weatherable sediment and thus prevent extensive chemical erosion. However, they note that rates of chemical erosion at ice margins are largely unknown at present and that there may possibly be high transient rates of chemical erosion during deglaciations. Due to their predominantly cold thermal regime, high Arctic glaciers may provide better analogues for drainage conditions in Pleistocene ice sheets than the temperate alpine glaciers which have been more widely studied. Therefore, they provide a better basis for testing the assumptions of Gibbs and Kump.

Heinrich events and erosion in glaciated carbonate terrains

Deep sea sediment cores in the North Atlantic contain a series of layers that are rich in ice-rafted debris (Heinrich, 19 88). The ice rafted debris layers that mark these "Heinrich events" are rich in detrital carbonate. Bond *et al.*, (1992) interpret these layers to reflect massive discharges of icebergs from the Palaeozoic carbonate terrains of eastern Canada. The cause of the extreme events is puzzling, but Bond *et al.*, (1992) suggest that they may reflect rapid advances of the Laurentide ice sheet. Clearly, to understand the formation of these layers, knowledge of glacial erosion processes in carbonate terrains is required. The key question must focus on the incorporation of detrital carbonate into the basal ice layers of the Laurentide ice sheet. This will have been dependent on the thermal regime of the ice mass. If, as suggested previously (Chapter 1), John Evans Glacier may be a reasonable small scale analogue for marginal areas of the Laurentide Ice sheet, due to the similarity between its thermal characteristics and those of the ice sheets, then it may provide a suitable environment for studying the processes of carbonate erosion beneath polythermal ice masses.

Solute sources in a glacial catchment

The basic premise of glacier hydrochemistry is that the chemical composition of the outflowing waters can provide information on the drainage pathway that those waters have followed. To correctly interpret data on the chemical composition of the outflowing waters it is important to determine the likely sources of solute within the catchment.

Solute is defined as all the dissolved aqueous species, comprising positively charged species (cations - e.g. Ca^{2+}, Na^{+}), negatively charged species (anions - e.g. SO_4^{2-}, Cl^{-}) and neutral species (e.g. O_2^0,) (Stumm and Morgan, 1981). In a glacial catchment, solute can be derived from two primary sources, the atmosphere and the weathering of crustal material. Biogenic inputs are largely unknown, but are assumed to be negligible due to the cold temperatures and sparse occurrence of biota. Solute input of charged species to the catchment from precipitation has two sources, the seasalt aerosol (comprising primarily Na^{+}, Mg^{+}, Ca^{2+}, K^{+}, Cl^{-}, SO_4^{2-}, HCO_3^{-}) and the anthropogenic (pollutant) aerosol, (H^{+}, Cl^{-}, NO_3^{-}, SO_4^{2-}). Input of neutral species (CO_2, O_2, N_2) from the atmosphere is controlled by rates of gaseous diffusion and is not restricted to precipitation events. Solute derived from crustal material can come from weathering of rock minerals derived from within the catchment or from weathering of wind-blown foreign particulate material deposited in the catchment.

Weathering of catchment minerals.

To identify the likely aqueous species it is useful to identify the minerals available for weathering in the solid phase and their solubility (Raiswell, 1984). From Table 2.1 it is evident that the catchment geology is dominated by carbonate and evaporite minerals, most notably, calcite, dolomite, gypsum and anhydrite. In the three large sub-catchments, west marginal, east marginal and subglacial (inferred) all the above minerals are present in the bedrock. Thus, intuitively it would be expected that if chemical weathering is occurring then the weathering products of these minerals will be evident in the

meltwaters.

Tranter *et al.*, (1993) define two major types of reaction which supply base cations to meltwater, simple dissolution and acid hydrolysis. Anhydrite ($CaSO_4$) may dissociate directly in the presence of water. In field conditions it normally hydrates first, becoming gypsum which dissolves by dissociation (Ford and Williams, 1989).

$$CaSO_4.2H_20_{(s)} \rightleftharpoons Ca^{2+}_{(aq)} + SO_4^{2-}{}_{(aq)} + 2H_20_{(l)} \quad (2)$$

gypsum

A double dissociation reaction describes the reaction of calcite with water as follows:

$$CaCO_{3(s)} + H_20_{(l)} \rightleftharpoons Ca^{2+}_{(aq)} + CO_3^{2-}{}_{(aq)} + H^+_{(aq)} + OH^-_{(aq)} \quad (3)$$

calcite

Acid hydrolysis requires the exchange of aqueous protons for base cations

$$CaCO_{3(s)} + H^+_{(aq)} \rightarrow Ca^{2+}_{(aq)} + HCO_3^-{}_{(aq)} \quad (4)$$

calcite

$$CaMg(CO_3)_{2(s)} + 2H^+_{(aq)} \rightarrow Ca^{2+}_{(aq)} + Mg^{2+}_{(aq)} + 2HCO_3^-{}_{(aq)} \quad (5)$$

dolomite

The solubilities of the above minerals in water at 25°C, 1 bar and $P_{CO2} = 10^{-3}$ bar are as follows; gypsum 2400mg/l, calcite, 100mg/l, dolomite 90mg/l (Freeze and Cherry, 1979). In glacial meltwaters, where temperatures are close to 0°C, calcite and dolomite are more soluble than at 25°C, whereas gypsum is slightly less soluble (Garrels and Christ, 1965; Plummer and Busenberg, 1982). Since the weathering of gypsum is by simple dissociation its solubility will be unaffected by changes in pH. However, at 0°C dolomite and calcite

both become more soluble as pH rises (Palmer, 1984). Where total ionic strength of the water is much less than 0.1 (e.g. glacial meltwaters), the solubility of calcite and dolomite is considerably reduced (up to 40%), if waters have already had substantial contact with gypsum (Ford and Williams, 1989).

There are four possible sources of H^+ in the meltwaters:

1) Dissociation of water

Pure water itself dissociates to a certain extent

$$H_2O_{(l)} \rightleftharpoons H^+_{(aq)} + OH^-_{(aq)} \qquad (6)$$

2) Acid aerosol in precipitation

$$HCl_{(aq)} \rightarrow H^+_{(aq)} + Cl^-_{(aq)} \qquad (7)$$

hydrochloric acid

$$HNO_{3(aq)} \rightarrow H^+_{(aq)} + NO_3^-{}_{(aq)} \qquad (8)$$

nitric acid

$$H_2SO_{4(aq)} \rightarrow 2H^+_{(aq)} + SO_4^{2-}{}_{(aq)} \qquad (9)$$

sulphuric acid

Supply of aqueous protons from the acid aerosol is likely to occur during melting of the snowpack early in the meltseason and during or after summer precipitation events (after the precipitation falls as snow).

3) Carbonation reaction

$$CO_{2(g)} + H_20_{(l)} \rightleftharpoons H_2CO_3^*{}_{(aq)} \quad (10)$$

$$H_2CO_3^*{}_{(aq)} \rightleftharpoons H^+_{(aq)} + HCO_3^-{}_{(aq)} \quad (11)$$

$$HCO_3^-{}_{(aq)} \rightleftharpoons H^+_{(aq)} + CO_3^{2-}{}_{(aq)} \quad (12)$$

The equilibrium constants for the above reactions are used in subsequent equations and are as follows :

For reaction (10) $K_H = \{H_2CO_3^*\}/ P_{CO2}$ (13)

For reaction (11) $K_1 = \{H^+\}\{HCO_3^-\} / \{H_2CO_3^*\}$ (14)

For reaction (12) $K_2 = \{H^+\}\{CO_3^{2-}\}/ \{HCO_3^-\}$ (15)

Where {} = activities of the species and P_{CO2} = the partial pressure of CO_2 in the atmosphere. (Stumm and Morgan, 1981)

Supply of aqueous protons by the carbonation reaction is controlled physically by the extent to which water has access to atmospheric carbon dioxide and kinetically by the rate of CO_2 dissolution into the water, and the rate of dissociation of $H_2CO_3^*$ and HCO_3^-. In the pH range 4.5 - 8.3 HCO_3^- is the dominant anion in the carbonate system (equations 10 & 11). Above pH 8.3 enough HCO_3^- dissociation is occurring such that CO_3^{2-} becomes important as an aqueous species (and in measurable quantities). As pH rises above 8.3 more of the HCO_3^- present in solution will dissociate giving CO_3^{2-} and H^+ (equation 12).

"In the aqueous carbonate system the concentration (activity) of CO_2 (aq) can be expressed either in terms of concentration units or in terms of the 'partial pressure of the gas in solution,' that is, that pressure of CO_2 in the gas phase with which the sample would be in equilibrium. $CO_{2(aq)}$ and P_{CO2} are interrelated by Henry's Law $[CO_{2(aq)}] = K_H P_{CO2}$. Where K_H is the Henry's Law constant. If the aqueous system is in equilibrium

with the gas phase, the' partial pressure of the gas in solution' is equal to the partial pressure of the gas phase. " (Stumm and Morgan, 1981).

The partial pressure of CO2 (P_{CO2}) of the atmosphere is $10^{-3.5}$ atm. Therefore, waters in equilibrium with the atmosphere will have a concentration of dissolved CO2 that is in equilibrium with a partial pressure of CO_2 of the atmosphere ($10^{-3.5}$ atm.) In the following analysis the P_{CO2} of the atmosphere with which the water would be in equilibrium with is calculated and compared to the theoretical equilibrium value of $10^{-3.5}$ atm. Waters where the P_{CO2} value is not equal to $10^{-3.5}$ are considered to be in disequilibrium with the atmosphere since the atmospheric P_{CO2} is constant at $10^{-3.5}$. This not to suggest however that there is physically an atmosphere overlying the waters where the P_{CO2} is greatly variant from $10^{-3.5}$.

Waters with a P_{CO2} of $10^{-3.5}$ are in equilibrium with the overlying atmosphere and are termed "open" (Raiswell, 1984). By contrast waters with P_{CO2} values $< 10^{-3.5}$ or $>10^{-3.5}$ are in disequilibrium with the overlying atmosphere and are termed "closed" system waters (Raiswell, 1984). This terminology has been accepted in both the glacial meltwater chemistry and karst hydrology literature for at least the past 11 years. However, thermodynamically the terms "open" and "closed" system have very strict meanings. Thermodynamically an "open" system is a system where there is free transfer of energy and mass and a "closed" system is system where there is no transfer of energy or mass. Clearly, then, both the systems described by Raiswell are "open" thermodynamically. Thus a more useful definition may be that waters which have an atmospheric P_{CO2} of $10^{-3.5}$ are *equilibrium* systems and waters which have a corresponding atmospheric P_{CO2} which is not $10^{-3.5}$ are *disequilibrium* systems.

Fairchild *et al.* (1994), in analysis of c.200 water samples from glaciated carbonate terrains, note that there are trends in the P_{CO2} values of groups of water samples. Therefore, following the terminology of Raiswell (1984) they characterise waters as evolving either along 'opening' or 'closing' system pathways. In 'opening' systems there

is net addition of CO_2, whereas in 'closing' systems there is net removal of CO_2. Thermodynamically these terms are again confusing, since the plots are of individual water samples and therefore, there is strictly no evolution of specific samples. Therefore, although there may be trends in the P_{CO2} values for specific streams waters are simply described as being either close to equilibrium with atmospheric CO_2 or far from equilibrium with atmospheric CO_2.

Waters with P_{CO2} values of $>10^{-3.5}$ indicate a high P_{CO2} and CO_2 must outgas from the water for equilibrium with the atmosphere to be achieved. High P_{CO2} waters can occur if the rate of supply of H^+ to the waters is greater than their rate of consumption by weathering reactions. In the natural system this would require an input of H^+ from a source other than the carbonation reaction. Low P_{CO2} waters occur when the rate of H^+ consumption in the weathering reaction is faster than the rate of supply from the carbonation reaction. Waters with P_{CO2} values $<10^{-3.5}$ indicate a low P_{CO2} and thus CO_2 must dissolve into the water for equilibrium with the atmosphere to be attained.

Since the dissociation of $H_2CO_3^*$ and HCO_3^- (equations 11 & 12) are pH dependent then so is the P_{CO2} (equation 16). Calcite and dolomite solubility are also dependent on pH, underlining the importance of pH in controlling weathering reactions in the aqueous carbonate system. From field titrations, only HCO_3^- was detected in the waters, therefore the following equation for calculation of P_{CO2} was used.

$$\log_{10}P_{CO2}(\text{atmospheric}) = \log_{10}(HCO_3^-) - pH + pK_1 + pK_H \qquad (16)$$

where $pK_1 = 6.58$ at 0^oC, $pK_H = 1.12$ at 0^oC and HCO_3^- (moles/L) (Ford and Williams, 1989). However, the pH values of the waters were often in the range 9-10, therefore, it is likely that some of total carbonate alkalinity would have existed as CO_3^{2-}. Given the pH and the HCO_3^- concentration the chemical speciation program WQ4F calculates the CO_3^{2-} concentration and incorporates this into its calculation of P_{CO2}. For the same input values (pH 9.3 and a HCO_3^- concentration of 140 μeq/l) the $\log_{10}P_{CO2}$ value from equation

16 is -5.34, whereas from WQ4F it is -5.58. Therefore, it indicates that the approximation method calculates values that are slightly closer to equilibrium with the atmosphere than is actually the case. At pH values higher than 9.3 the discrepancy between the two methods will increase as more of the carbonate alkalinity will be in the form of CO_3^{2-} ,and at pH values lower than 9.3 the discrepancy will decrease since the majority of the carbonate alkalinity will be in the form of HCO_3^-. The differences between the approximation method and the more accurate WQ4F method are however, not particularly significant since the analysis is concerned with trends in the dataset rather than specific values.

4) Sulphide oxidation

For example:-

$$4FeS_{2(s)} + 15O_{2(aq)} + 14H_2O_{(l)} \rightarrow 4Fe(OH)_{3(s)} + 16H^+_{(aq)} + 8SO_4^{2-}{}_{(aq)} \quad (17)$$

pyrite

Supply of aqueous protons by sulphide oxidation is to a first order dependent on whether there are sulphide minerals available for weathering within the catchment. If sulphide minerals are present, the reaction is then dependent on the supply of dissolved oxygen. However, reaction kinetics may also be important. If the rate of reaction is slow and the water-rock contact time is very limited then the effects of the reaction may be limited even if the waters have dissolved oxygen levels close to saturation.

Solute acquisition by glacial meltwaters.

The primary factors governing the extent of solute acquisition by glacial meltwaters have been identified by Sharp (1991) as:

(i) the chemistry of the source waters;

(ii) the availability of protons (H^+) derived from snowpack leaching, carbonation or oxidation reactions;

(iii) the duration of contact between meltwaters and weatherable rock material;
(iv) the grain size, shape and mineralogical properties of particulate rock material; and
(v) the ratio between meltwater volume and the surface area of rock material available for weathering.

Different streams may be characterised by different proton sources, rock availability and weatherability, and water-rock contact times, and hence by differing magnitudes and processes of solute acquisition (Sharp, 1991). To assess the influence of these controlling factors, six streams in the catchment were selected for detailed study. Streams were selected on the basis of anticipated differences in the controlling factors, and examined for any differences in the water chemistry. Figure 2.1 shows the sub-catchments within the main basin that are the source areas for the streams studied. The catchment areas for the east marginal, west marginal, and subglacial/fountain streams are significantly larger than for the supraglacial and proglacial streams.

The "**supraglacial**" stream drains a small area of the glacier snout, flows in an ice walled channel and leaves the glacier via a waterfall over the ice cliff at the glacier margin. Suspended sediment concentrations were extremely low (<0.005g/l) so little weathering of crustal material would be expected.

Beyond the glacier, the supraglacial stream flows into a well defined channel, the bed and banks of which are composed of unconsolidated sediments, but it is significantly underfit. This stream is called the "**proglacial**" stream. Some additional meltwater is contributed to this stream from melting of glacier ice on the face of the ice cliff at the glacier snout and from large snowpatches at the base of the ice cliff. Suspended sediment concentrations are very low (<0.01g/l), but water-rock ratios are greater than in the supraglacial stream, so some modification of the water chemistry would be expected.

On 10th July, 1994, large quantities of turbid water issued from the ice/sediment interface at the base of the glacier across a 30 m wide section of the snout (see Figure 4.3). The

turbid water exited the glacier directly beneath the waterfall of the supraglacial stream. The mixed waters then flowed into the proglacial stream channel. Initially this discharge was c. 10 times that of the supraglacial stream, but it declined exponentially over the next 6 days until it ceased. The pattern of release of the water resembled that of an outburst break type flood event (Haeberli, 1983). During the outburst event, suspended sediment concentrations in the proglacial stream rose as high as 0.4g/l. These waters then have higher rock/water ratios and may have had limited access to the atmosphere, since access of waters to the atmosphere may be limited physically in the subglacial environment due to the overlying ice. Following the outburst event, waters draining via the proglacial stream had a similar provenance to those which drained via the same routeways prior to the event. Thus, in subsequent analyses of the water chemistry of the proglacial stream, the measurement record is split into three time periods; proglacial (a) June 15th - am July 9th: pre-outburst event, proglacial (b) pm July 9th - July 16th: outburst event, (c) July 17th - July 22nd post-outburst event.

At the same time that the outburst occurred in the proglacial stream, a fountain of turbid water was observed exiting from a point on the glacier snout some 20 m above the glacier bed. Waters issuing from this point are referred to as "**fountain**" in subsequent discussions. These waters were also interpreted to have drained across the glacier bed, on the basis of its high suspended sediment concentrations (c. 0.1 g/l). The fountain only existed for 4 days. On the evening of July 15th, a small stream was observed issuing from the ice-sediment interface at the base of the glacier but occupying a well defined stream channel. At the same time, the subglacial water input to the proglacial stream ceased, suggesting a change in the point of efflux for the subglacial waters. Waters issuing from this new location are thus referred to as the "**subglacial**" stream. Suspended sediment concentrations in this stream were on the order of 0.1g/l.

Waters flowing into the **western marginal stream** were initially supraglacial. The stream flowed subaerially at the ice margin for 2.5 km, with additional supraglacial discharge being added as the stream flowed downvalley. For the last 1 km it flowed beneath the

glacier. The stream flowed mainly in ice walled channels but there was significant sediment input by rockfall from the valley sides. Suspended sediment concentrations averaged 0.117g/l. Little is known about the catchment of the **eastern marginal stream**, and most of the available information is derived from aerial photographs. It is significantly larger than the western marginal catchment and contains a small ice-dammed lake. Suspended sediment concentrations in the eastern marginal stream were not measured, but the stream always appeared "clearer" than either the subglacial or western marginal streams, since the ice marginal lake is likely an effective sediment trap.

Field and laboratory methods

Water samples were taken from the six outflowing streams during the period June 15th - August 7th. Figure 2.8 shows the specific periods over which each stream was monitored. pH, EC (electrical conductivity) and the dissolved oxygen content of each water sample were immediately measured. Filtered water samples were retained for determination of HCO_3^- concentrations by titration with acid in the field and for concentrations of major cations (Ca^{2+}, Mg^{2+}, Na^+, K^+) and anions (Cl^-, SO_4^{2-}, NO_3^-) by ion chromatography in the laboratory. The filter papers from each water sample were dried and weighed in the laboratory to determine suspended sediment concentrations. Full details of the analytical techniques are provided in Chapter 2.

Analytical methods

A very significant parameter in water chemistry analysis is the P_{CO2} with which an analysed sample would be in equilibrium. This reveals information on whether water samples are close to or far from equilibrium with an atmospheric P_{CO2} value of $10^{-3.5}$ atm. P_{CO2} values for the waters were calculated using equation 16.

Another measure of the weathering potential of a water sample is its degree of saturation with respect to a saturated solution of a given mineral. Saturation indices for the major minerals in the catchment (calcite, dolomite and gypsum) were thus calculated. From

Fairchild *et al.* (1994) the saturation index of calcite (SIc) is as follows:

$$SIc = \log(IAP/Keq) \quad (18)$$

where:

IAP(ionic activity product) = (activity Ca^{2+}) x (activity CO_3^{2-})

IAP applies to any solution of interest, whereas Keq is the same product of activities but in a solution which is saturated with calcite, and hence in equilibrium with it. Activities are conceptual parameters which are within a few per cent of concentrations in moles/l in dilute solutions (Stumm and Morgan, 1981). Since the concentration of CO_3^{2-} is not easily measured (Ford and Williams, 1989); the SIc can be calculated using known or measurable parameters:-

$$SIc = \log (Ca^{2+})(HCO_3^-)K_2 / (H^+)(K_c) \quad (19)$$

or

$$SI_{calcite} = \log_{10}(Ca^{2+}) + \log_{10}(HCO_3^-) + pH - pK_2 + pK_c \quad (20)$$

where Ca^{2+} and HCO_3^- (moles/L) and $pK_2 = 10.63$ at 0°C and $pK_c = 8.38$ at 0°C. (Ford and Williams,1989).

Equivalent equations, which follow the same basic principles, can be written for saturation of the sample waters with respect to a solution saturated with respect to either dolomite or gypsum. (From Ford and Williams, 1989)

$$SI_{dolomite} = \log_{10}(Ca^{2+}) + \log_{10}(Mg^{2+}) + 2\log_{10}(HCO_3^-) + 2pH - 2pK_2 + pK_d \quad (21)$$

where Ca^{2+}, Mg^{2+}, HCO_3^- (moles/l) and $pK_2 = 10.63$ at 0°C and $pK_d = 16.56$

$$SI_{gypsum} = \log_{10}(Ca^{2+}) + \log_{10}(SO_4^{2-}) + pK_g \quad (22)$$

where Ca^{2+} and SO_4^{2-} (moles/l) and at 0°C $pK_g = 4.38$

If SI < 0, the sample water is undersaturated with respect to the mineral and further mineral dissolution can occur.
If SI = 0, the sample water is saturated with respect to the mineral.
If SI > 0, the sample water is supersaturated with respect to the mineral and net precipitation of the mineral is possible.

Whether dissolution or precipitation actually occurs will depend on the kinetics of the reaction.

The above equations for saturation indices are only approximations since they do not take into account activities. For example, not all of the Ca^{2+} and HCO_3^- will exist as free aqueous species. Some will exist as $CaHCO_3^+{}_{(aq)}$ and $CaCO_3^\circ{}_{(aq)}$. Consequently it would be expected that the above calculations would tend to overestimate the level of saturation. To determine the magnitude of this overestimation, saturation indices for calcite, dolomite and gypsum were also determined for two of the most concentrated water analyses using the chemical speciation program WQ4F (Rollins, 1989) which does take into account the ion pairs. For the selected samples, the approximate methods overestimate the WQ4F values by 0.2 units for SIc and by 0.4 units for SId and SIg. Whether such corrections are appropriate for all samples is unknown. Over 250 water analyses exist for the various streams and as input of data into WQ4F is a time-consuming process it was impossible to calculate SI for all samples using this program. Currently, work is being undertaken to construct both a spreadsheet layout and a conversion programme to create WQ4F input files from spreadsheet data. However, to allow comparison between streams, the simpler and quicker approximation method was used for the current water analyses. As no pH

data exist for the east marginal stream, P_{CO2} values and saturation indices were calculated only for the supraglacial, proglacial, west marginal, subglacial and fountain streams (Table 3.1).

Table 3.1 The mean and standard deviation values for SIc, SId and SIg in the five studied streams. (Proglacial(a) = June 15th - am July 9th, Proglacial(b)= pm July 9th - July 16th, Proglacial(c) = July 17th - July 22nd. n = sample size.

	SI_c			SI_d			SI_g		
Stream	$\bar{x}$	s.d.	n	$\bar{x}$	s.d.	n	$\bar{x}$	s.d.	n
Supraglacial	-3.86	0.65	78	-8.34	1.28	78	-5.40	0.48	91
Proglacial(a)	-0.59	0.42	32	-2.39	0.88	32	-3.78	0.39	39
Proglacial(b)	-0.04	0.47	10	-1.29	0.87	10	-1.29	0.18	12
Proglacial(c)	-0.19	0.2	7	-1.66	0.57	7	-3.75	0.16	10
W.Marginal	-0.39	0.45	41	-2.93	0.89	41	-3.27	0.26	63
Subglacial	0.27	0.33	36	-0.63	0.69	36	-1.48	0.16	41
Fountain	-0.12	0.22	6	-1.91	0.44	6	-1.22	0.21	7

From Table 3.1 it is evident that there are temporal trends in the SIc of the subglacial waters. The initial subglacial waters (fountain and proglacial (b)) are closer to saturation with respect to gypsum and less saturated with respect to carbonates when compared to the later season "subglacial" waters. This may suggest that the initial waters there may have been more marked calcite precipitation, thus moving the waters away from supersaturation.

Results

Average stream water composition.

Table 3.2 shows the mean and coefficients of variation of the measured anion and cation concentrations in the six streams studied. Using the mean values it is possible to identify similarities between certain streams on account of their average ionic composition. In all streams the dominant cation is Ca^{2+}, followed by Mg^{2+}, Na^{+} and K^{+} in order of decreasing concentration. In the supraglacial stream, proglacial (a) and (c), west and east marginal streams the dominant anion is HCO_3^-.

Waters from these streams are referred to as type 1 waters. In the proglacial (b), fountain and subglacial streams the dominant anion is SO_4^{2-}. Waters from these streams are referred to as type 2 waters. Total solute concentrations in type 2 waters are on average four times higher then the most concentrated type 1 waters.

Solute provenance in stream waters.

(i) The balance between atmospheric and crustal sources.

To assess the balance between atmospheric and crustal sources of anions to the meltwaters the following expression can be used, $(NO_3^- + Cl^-)/ \Sigma-$ where $\Sigma-$ is the sum of the anions (see Table 3.3). Since halite is not present in the catchment, $NO_3^- + Cl^-$ represents the proportion of the anions that are atmospherically derived from the acid nitrate aerosol and the seasalt aerosol. It indicates that in the supraglacial stream the atmospheric component is on average c. 30% of the total anion concentration. The atmospheric component of total anions decreases in the the other streams significantly indicating an increase in the crustal component.

Water Type	stream	Ca^{2+}		Mg^{2+}		Na^{+}		K^{+}		HCO_3^{-}		SO_4^{2-}		Cl^{-}		NO_3^{-}		Sum solute	
		$\bar{x}$	c.v.	$\bar{x}$	c.v.	$\bar{x}$	c.v.	$\bar{x}$	c.v.	$\bar{x}$	c.v.	$\bar{x}$	c.v.	$\bar{x}$	c.v.	$\bar{x}$	c.v.	$\bar{x}$	c.v
1	supraglacial	47	45	16	27	11	71	1.2	129	31	51	9	65	15	62	0.1	334	129	34
1	proglacial(a)	232	24	22	52	9	84	0.4	164	171	29	41	33	18	70	0.1	286	494	23
1	proglacial(c)	287	30	26	64	6	29	0.4	140	190	20	79	74	12	14	0.3	100	574	36
1	west marginal	712	18	74	43	22	51	3.5	67	449	18	71	44	22	50	0.9	112	1283	27
1	east marginal	663	9	122	10	15	7	3.1	64	443	9	109	14	16	19	1.8	15	1341	13
2	proglacial(b)	2211	21	219	37	77	32	7.9	38	215	18	2189	23	28	21	1.8	28	4949	21
2	fountain	2391	25	252	59	87	36	10.2	56	230	8	2402	30	31	24	2.2	23	5411	27
2	subglacial	1702	17	180	24	75	61	11.1	61	219	10	1812	20	24	47	1.1	30	4040	17

Table 3.2 Mean concentrations in μeq/l and coefficients of variation for each ionic species. Note the values in the supraglacial, proglacial (a) and west marginal have been calculated for the period after June 25th since the effects of the ionic flush, due to the melting of the snowpack, would tend to skew the results.

Assuming that the seasalt aerosol has a similar composition to seawater itself, it should be possible to calculate the solute input to the catchment using standard seawater ratios from Holland (1978) for the major ionic species relative to Cl^- concentrations (see table 3.4). it is evident then that the dominant cation by far in the seasalt aerosol is Na^+. Given that the concentrations of Cl^- are low in most streams the contribution of the seasalt aerosol to the concentrations of the other ions (K^+, Mg^{2+}, Ca^{2+}, SO_4^{2-} and HCO_3^-) is likely negligible. If Na^+ concentrations significantly exceed Cl^- it suggests that there is a crustal source of Na^+ in addition to the atmospheric source. From Table 3.2 it is evident that it is only in type 2 waters that Na^+ concentrations exceed Cl^- concentrations. In type 2 waters Na/Cl ratios are on average 3:1, indicating a significant Na^+ input from crustal sources.

(ii) Seasalt/acid aerosol balance in the atmospheric solute input.

Assuming that Cl^- is derived solely from the seasalt aerosol, and that NO_3^- is derived solely from the nitric acid aerosol, then the NO_3^-/Cl^- ratio provides a measure of the pollutant input to individual streams (see Table 3.3). On average, all the streams show significantly more Cl^- than NO_3^- indicating that the seasalt aerosol is the predominant source for atmospherically derived solute. Moreover, it has been established that in a number of glacial catchments NO_3^- is present in snowmelt and not in icemelt (Tranter *et al.*, 1994), therefore, the Cl^-/ NO_3^- ratio may provide information on the relative inputs from icemelt and snowmelt. At the snout of John Evans Glacier this observation appears to be valid. However, it may be that in very cold years where there is minimal runoff and therefore, leaching of ions from the snowpack nitrate may be incorporated into the glacier ice during the firnification process. If however, it is assumed that NO_3^- is predominantly from a snowmelt source, it suggests that there is a greater input of snowmelt relative to icemelt in the eastern marginal and subglacial waters. This is not surprising since both catchments rise to high elevations c. at least 1100m and therefore there will likely be a snowmelt input to these streams for the duration of the fieldseason.

(iii) Differences in crustal solute input in the individual streams.

The predominant cations in both type 1 and type 2 waters are Ca^{2+} and Mg^{2+}, and the predominant anions are HCO_3^- and SO_4^{2-}. Within type 1 waters there are marked differences in the average Ca/Mg ratio between the different streams (see table 3.3). The supraglacial stream has the lowest Ca/Mg ratio, suggesting that dolomite dissolution is important relative to both gypsum and calcite dissolution in this environment. The next highest Ca/Mg ratio is in the east marginal stream. The proglacial ((a) and (c)) and west marginal streams have the highest Ca/Mg ratios. Type 2 waters have a relatively high Ca/Mg ratio, similar to that observed in the proglacial and west marginal streams.

Only in type 2 waters, which are dominated by Ca^{2+} and SO_4^{2-}, is there evidence for a crustal source of Na^+. Moreover, highest K^+ concentrations are also observed in type 2 waters (Table 3.2). Since the concentrations of K^+ from the seasalt aerosol are likely negligible (Table 3.4) then the low concentrations of K^+ in type 1 waters are probably crustally derived.

Table 3.3 Selected ion ratios for crustally sourced and atmospherically sourced solute.

Water type	Stream	Ca^{2+}/ Mg^{2+}	c.v. %	(NO_3^- + Cl^-) / Σ^-	c.v. %	NO_3^-/ Cl^-	c.v. %
1	Supraglacial	2.90	35	0.30	40	0.01	360
1	Proglacial (a)	10.33	25	0.08	44	0.02	147
1	Proglacial (c)	13.23	27	0.05	35	0.02	104
1	West Marginal	10.41	21	0.04	35	0.03	92
1	East Marginal	5.50	4	0.03	13	0.11	17
2	Proglacial (b)	10.84	24	0.01	19	0.07	19
2	Fountain	10.14	19	0.01	31	0.07	14
2	Subglacial	9.75	17	0.01	45	0.05	28

Table 3.4 Seawater ratios of various crustal minerals relative to chloride concentrations (Holland, 1978).

Ion	ratio relative to Cl^- concentration
Na^+	0.86
K^+	0.018
Mg^{2+}	0.19
Ca^{2+}	0.038
SO42-	0.104
HCO_3^-	0.0044

Temporal changes in the composition of waters in individual streams.

Without good discharge data, caution must be applied in interpreting temporal changes in the chemistry of the meltwaters. However, in the streams that flow subaerially there are three types of temporal change in the water chemistry that are unlikely to be due to fluctuations in the discharge of the individual streams:

(i) *The ionic pulse associated with the first fractions of snowmelt.* June 15th - June 25th (JD166-176) supraglacial/proglacial stream, June 18th - July 9th (JD169-JD190) west marginal stream. (Figures 3.1, 3.2 and 3.3)

In the supraglacial and marginal streams, concentrations of all the ions were initially high, but then declined to a relatively constant level for the remainder of the melt season. In contrast, concentrations of ions in the proglacial stream were initially low, but then rose to a peak before declining to reasonably constant levels.

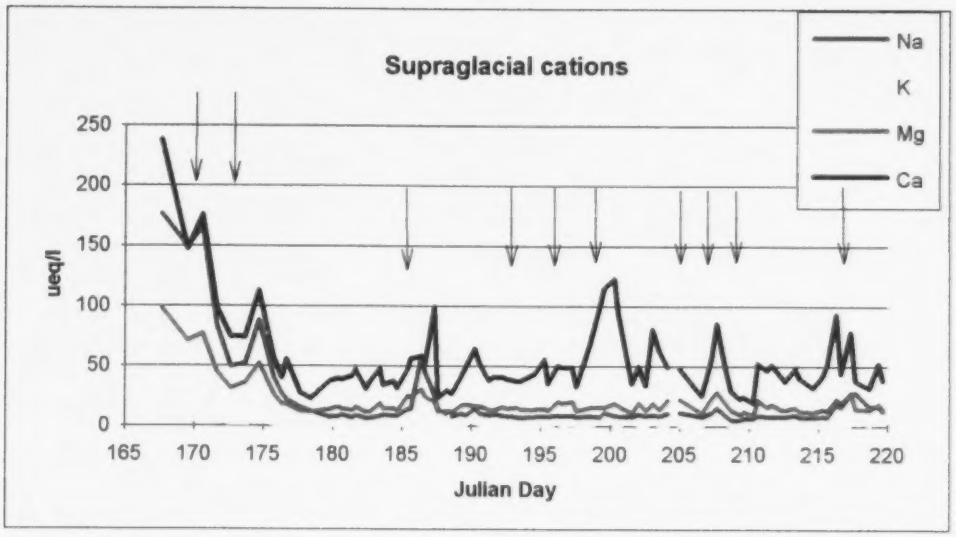

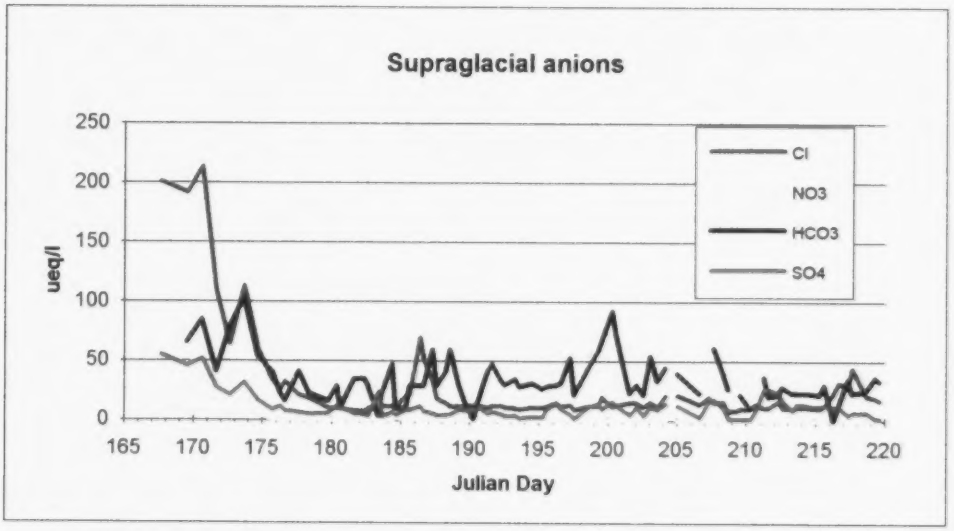

Figure 3.1 a) Major cation and b) Major anion concentrations in the supraglacial stream. Note vertical arrows indicate precipitation events.

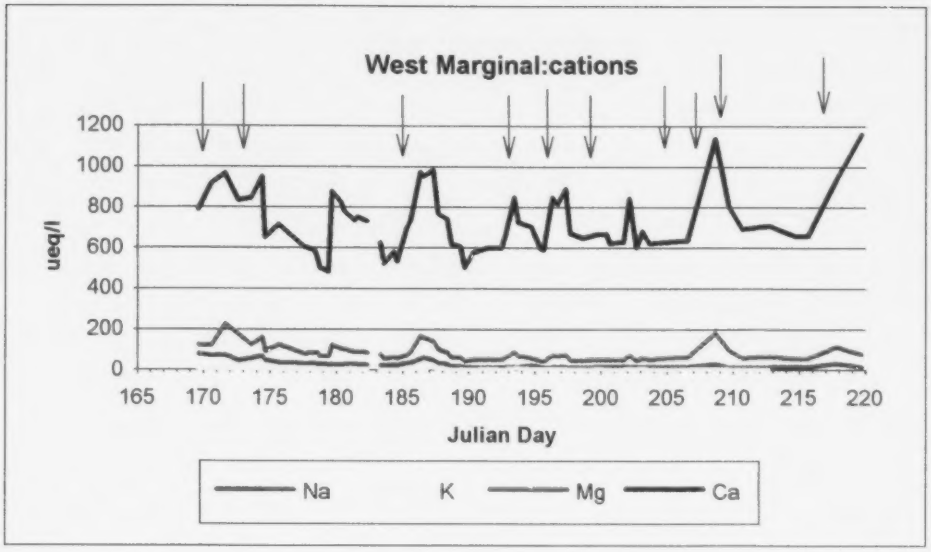

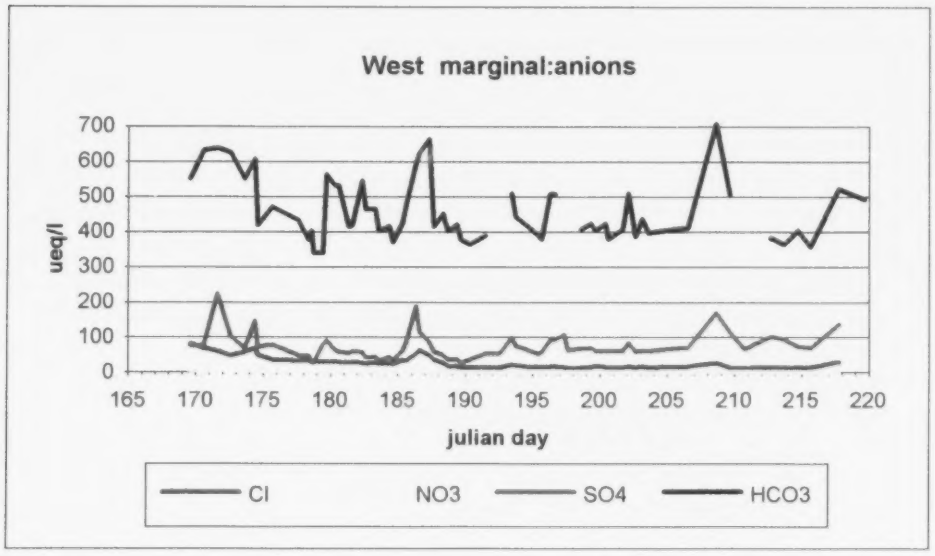

Figure 3.2 a) Major cation and b) Major anion concentrations in the west marginal stream. Note vertical arrows indicate precipitation events.

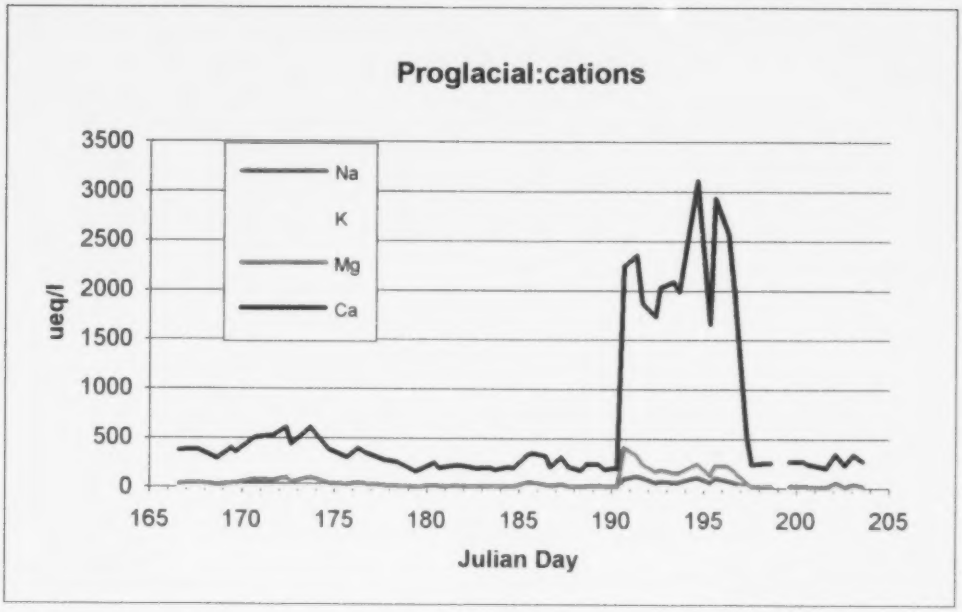

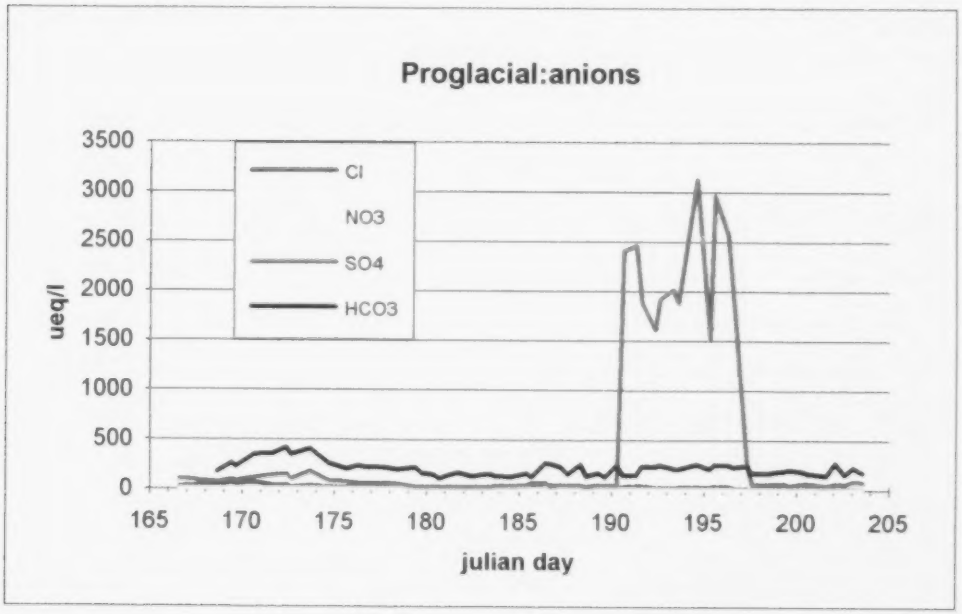

Figure 3.3 a) Major cation and b) Major anion concentrations in the proglacial stream.

In the supraglacial (and proglacial) stream the ionic pulse lasted for 12 days after monitoring started. In the west marginal stream the ionic pulse lasted for 20 days after monitoring started, and the decline from the peak value was more attenuated. The difference observed between the two streams can be explained by the fact that the west marginal stream catchment spans a greater altitudinal range than that of the supraglacial stream, so that the snowpack persisted for longer in this catchment.

(ii) Precipitation inputs to the subaerial streams later in the meltseason. (see Figures 3.1, 3.2 and 3.3)

Since, the proglacial stream is fed directly by the supraglacial stream and it has additional subglacial input and a shorter monitoring record, the observations will focus on the supraglacial and west marginal streams as they were monitored for the entire field season. After the snowpack had melted the marginal and supraglacial streams were fed by icemelt and precipitation when it occurred. Ten precipitation events were recorded during the field season (shown as arrows on Figures 3.1a and 3.2a). Some were more prolonged than others, but no quantitative data were collected on relative rainfall amounts. Peaks in the concentrations of major cations (Ca^{2+}, Mg^{2+}) and anion concentrations (HCO^{3-}, SO_4^{2-}) which have predominantly crustal sources in the two streams appear to lag precipitation events by 12-24 hours. Generally, however, increases in concentrations of the major constituents in the seasalt aerosol (Na^+ and Cl^-) are low in comparison. Using the ratios in table 3.4 for the average composition of the seasalt aerosol, it is evident that the increases in Ca^{2+}, Mg^{2+}, HCO_3^- and SO_4^{2-} are not due to the direct input of solute from the seasalt aerosol. However, it suggests that when precipitation events occur there may be significant input of crustal material to the west marginal stream catchment due to increased runoff from the valley sides.

A key difference between the supraglacial and west marginal streams is that following the precipitation event on JD199 the largest peak in ionic concentrations during the "icemelt" fed section of the meltseason was observed on JD200 in the supraglacial stream.

However, no such peak was recorded in the marginal stream record following this precipitation event. This peak most likely represents the input of dust into the catchment which is then weathered by the supraglacial waters. By contrast, there are peaks in the major ion concentrations in the marginal stream on JD180 and JD202, that do not directly follow precipitation events. The former peak is larger and more prolonged that the latter. These peaks may reflect increased mobilisation of sediment into the stream, thus providing more material available for weathering.

(iii) The input of subglacial waters to the proglacial stream (Figure 3.3).

The effect of the input of subglacial waters on solute concentrations in the proglacial stream is immediately evident on Figures 3.3a and b. With the exception of HCO_3^-, concentrations of all the ions increased by at least five times with the input of subglacial waters. After the burst ended, slightly elevated levels of Ca^{2+} and SO_4^{2-} were observed in the proglacial stream, possibly suggesting a slow and continuous leakage of small amounts of high Ca^{2+}/ SO_4^{2-} water through the sediments for the remainder of the meltseason.

Characterisation of Weathering Environments

Supraglacial weathering environment

In the supraglacial weathering environment, suspended sediment concentrations in the stream waters are very low (<0.005g/l), so solute acquisition due to weathering processes would be expected to be minimal. Total solute concentrations in the supraglacial stream are very low, as are the saturation indices for the major catchment minerals (see Tables 3.1 and 3.2). However, examination of the ratios of crustally/atmospherically derived solute, reveals that on average 70% of $\Sigma-$ and 85% of $\Sigma+$ are crustally derived (the discrepancy is due to charge balance errors in the water analysis). Therefore, it appears that even in the supraglacial environment solute is derived primarily from the weathering of crustal material. At the start of the meltseason this relationship is modified by the ionic

pulse associated with snowmelt. Initially, the atmospheric component of $\Sigma-$ was 70% when the snowpack first started to melt, declining over the subsequent 12 days to 30% when the snowpack in the stream catchment had completely melted and waters were derived primarily from icemelt. Similarly, the atmospheric component of $\Sigma+$ was initially 55%, declining to 15% as the snowpack was removed.

The high concentration of solutes, especially those with an atmospheric source, in the first fractions of snowmelt is a well recognised phenomenon (e.g. Johannessen and Henriksen, 1978; Bales, 1992). Typically, 50-80% of the total snowpack solute load is released in the first 30% of the meltwater. Without data on the chemical composition of the bulk snow prior to melt it is not possible to calculate concentration factors for the individual ions. Using nitrate as a tracer for snowmelt-derived waters, it is evident that the snowpack in the supraglacial stream catchment had melted by JD176.

For the remainder of the meltseason the supraglacial stream was supplied by icemelt waters and by precipitation when it occurred. Since the composition of icemelt appears reasonably constant over a range of discharges, it seems likely that the chemical composition of the ice is reasonably constant too, or that there is effective homogenisation of waters during runoff. The peaks observed in calcium and bicarbonate concentrations occur after precipitation events and probably reflect the weathering of particulate material blown on to the glacier from the surrounding catchment rocks. Alternatively more vigorous runoff and sediment entrainment may occur on the ice surface. The Ca/Mg ratio in the waters shows little variation around a mean value of 2:1. Given that some calcium may be derived from gypsum dissolution, this suggests that the predominant carbonate mineral being weathered in the supraglacial environment is dolomite. During the solute concentration peaks, however, the Ca/Mg ratio rises to a maximum of 7:1 suggesting that the additional crustal input is from calcite rather than from dolomite.

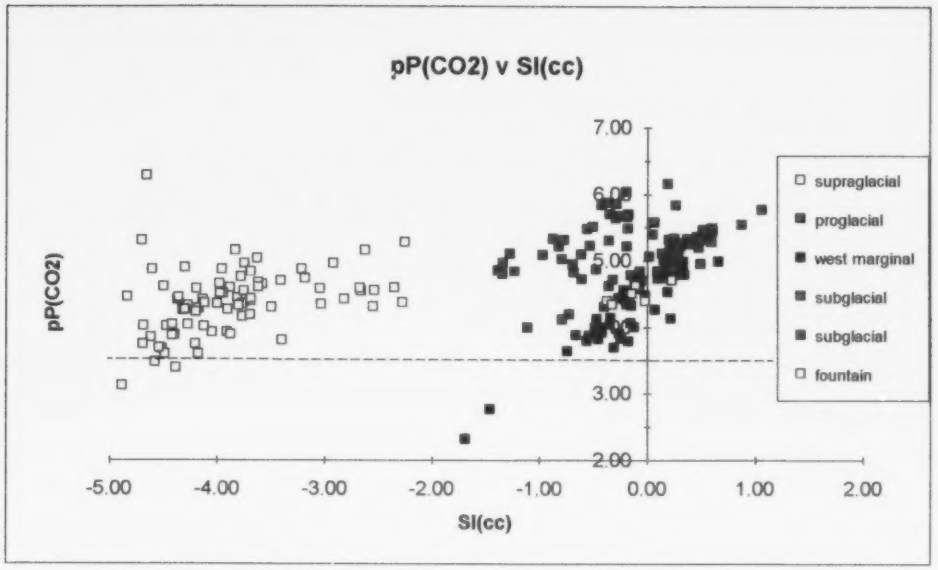

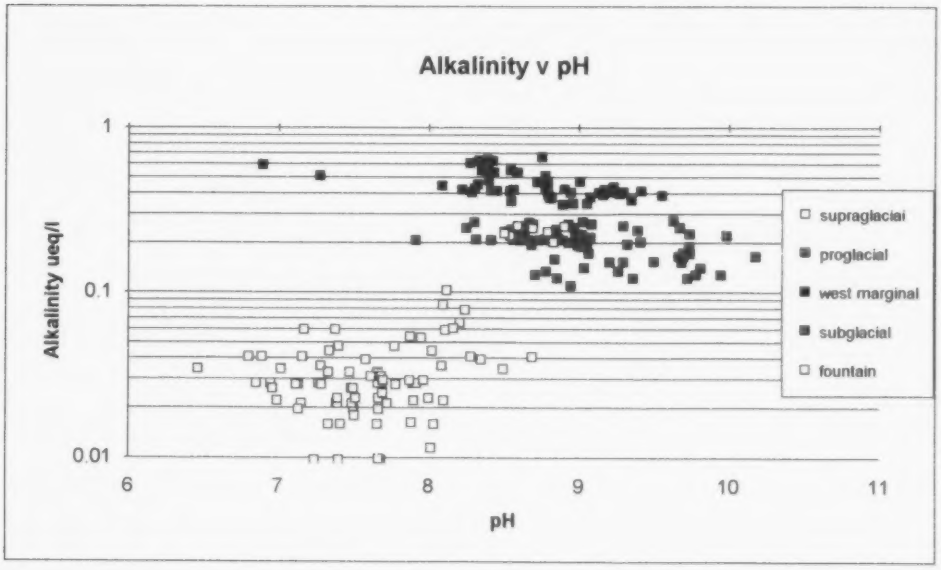

Figure 3.4 a) Plot of pPco2 v SI calcite for five of the studied streams.
b) Plot of alkalinity v pH for five of the studied streams.

Saturation indices for the individual mineral species are all very low, reflecting that in absolute terms weathering in the supraglacial environment is limited (Figure 3.4a). The primary rate-limiting factor in this environment appears to be the lack of particulate material to weather. However, where minerals are available the weathering is likely to be rapid. pP_{CO2} values in the supraglacial stream are below atmospheric but are relatively close to equilibrium. (Figure 3.4a). This suggests that the limited reactions that occur in the supraglacial environment consume protons faster than they are supplied by CO_2 diffusion into the waters.

Proglacial weathering environment

The proglacial stream is fed primarily by the supraglacial stream. Accordingly, the ionic pulse associated with snowmelt in the supraglacial stream is also evident in the proglacial stream (Figure 3.3 a and b). In the proglacial weathering environment, however, dilute snow and ice melt come into contact with sediment at the base and banks of the stream channels, although concentrations of suspended sediment remain low (<0.01g/l except when there is subglacial input). The observed increase in the concentration of HCO_3^- relative to the supraglacial stream can largely be accounted for by an increase in calcite weathering. The increase in SO_4^{2-} is attributable to an increase in gypsum dissolution because the major cation to balance the increases in HCO_3^- and SO_4^{2-} is Ca^{2+}. There is a very small increase in Mg^{2+} when compared to the supraglacial waters, suggesting either that Mg^{2+} is present as an impurity in the calcite or gypsum (the former seems more likely; Deer *et al.*, 1965, p. 206) or that very limited dolomite weathering is occurring. Ca/Mg ratios of 10:1 in the proglacial stream reflect this change in the dominant minerals to be weathered.

The increased amounts of weathering result in increases in SIc, SId and SIg in the proglacial stream waters (Table 3.1). The pP_{CO2} of the proglacial waters is higher than that of the supraglacial waters (Figure 3.4a), indicating that they are further from equilibrium with respect to atmospheric CO_2. The pH of the proglacial waters is significantly higher

than in the supraglacial stream waters (Figure 3.4b), showing net consumption of H^+ ions. The higher pP_{CO2} and pH values suggest that weathering reactions are consuming H^+ ions more rapidly than they are supplied by the dissolution of atmospheric CO_2 into the water.

Ice marginal weathering environment

Waters in the ice marginal environments exhibit a dominant Ca^{2+} - HCO_3^- chemistry. Concentrations of both ions are slightly lower in the east marginal stream than in the west marginal stream. By contrast, both Mg^{2+} and SO_4^{2-} concentrations are higher in the east than in the west marginal stream. Ca/Mg ratios are only 5.5:1 in the east marginal stream compared to 10:1 in the west marginal stream. The most simple explanation for this difference is that relative to the west marginal stream there is more dolomite and gypsum dissolution and less calcite dissolution than in the east marginal stream.

There are also differences in the concentrations of the atmospherically derived solutes (Cl^- and NO_3^-) between the two streams. In the west marginal stream, nitrate input to the waters ceases on July 9th, reflecting removal of the snowpack from the stream catchment. Subsequent nitrate input to the stream waters is a result of precipitation events. By contrast, nitrate concentrations in the east marginal stream are relatively constant, with a mean value of 1.8 ueq/l. This suggests that the snowmelt input to the east marginal stream catchment persists throughout the season. Ionic concentrations in the east marginal stream showed little variability, in contrast to the other streams studied (see Table 3.2). The east marginal catchment is large in comparison to the other stream catchments and the majority of the runoff drains into the small ice marginal lake c. 4 km from the glacier snout. It appears that this lake effectively homogenises input waters of potentially varying composition, such that the output has a fairly constant composition. This suggests that the majority of solute acquisition occurs in the upper reaches of the catchment or in the lake.

The Ca^{2+} and HCO_3^- chemistry of both streams suggests that the major weathering reaction is the acid hydrolysis of calcite with some limited dolomite and gypsum dissolution to account for the Mg^{2+} and SO_4^{2-}. The increased concentrations of Ca^{2+} and HCO_3^-, and of the secondary ions, Mg^{2+}, K^+ and SO_4^{2-} relative to the proglacial stream (a) and (c) suggest that weathering in these environments has proceeded to a greater extent.

The peaks observed in Ca^{2+} and HCO_3^- concentrations in the west marginal stream following precipitation events probably reflect the input of solute from runoff from the valley sides where solute acquisition processes are likely to be considerable due to the longer water-rock contact times and the increased water-rock area ratio(cf. the ice walled marginal stream channel). The west marginal stream has both subaerial and subglacial sections. In order to assess the degree of solute acquisition occurring in the subglacial section, simultaneous measurements of EC were made before the waters went beneath the glacier and in the proglacial area. These indicate that little solute acquisition occurs in the subglacial section. Similar to the findings for the east marginal stream, it appears that the majority of the solute is acquired in the upper subaerial section. This is probably because SIc is close to saturation and therefore the reaction rates have slowed down.

The pP_{CO2} and SIc data for the west marginal stream (Figure 3.4a) show that on average, the SIc values are slightly higher than those for proglacial stream waters. However, pP_{CO2} values are much lower, and approach atmospheric values. From Figure 3.4b it is evident that HCO_3^- concentrations are increasing, while pH is falling, hence the rate of H^+ ion supply is faster than the rate of consumption and therefore the P_{CO2} of the waters is driven closer to atmospheric values (Figure 3.4a).

Subglacial weathering environments

In this section, waters from the proglacial (b), fountain and subglacial streams are discussed together because of the similarity in their chemistry. The fountain and proglacial (b) waters have an almost identical chemistry since they exited the glacier at the same time. In contrast to the type 1 waters (proglacial (a) and (c) and marginal waters) the predominant cation and anion species are Ca^{2+} and SO_4^{2-} respectively. Moreover, there are also elevated levels of Mg^{2+} and K^+ derived from weathering sources. There also appears to be a weathering source for Na^+ in the subglacial environment as Na^+ concentrations are significantly higher than Cl^- concentrations. By contrast, HCO_3^- concentrations are only slightly higher than in the proglacial stream and much lower than in the marginal streams. They also show the least variability of all the ions. The dominant weathering reaction in the subglacial environment thus appears to be the dissolution of gypsum/anhydrite, accounting for the high concentrations of Ca^{2+} and SO_4^{2-}. In addition, there must also be some weathering of calcite and/or dolomite to account for the HCO_3^- concentrations. It is possible that Mg^{2+}, Na^+ and K^+ are found as impurities in the gypsum, but it is more likely that they come from calcite or dolomite (Deer *et al.*, 1965).

Subglacial waters exhibit a similar relationship between pP_{CO2} and SIc to the west marginal waters (Figure 3.4a). However, the majority of the subglacial waters are supersaturated with respect to calcite. If the effect of ion pairing is taken into account, and all SIc values are reduced by 0.2 units, at least half of the subglacial waters are still supersaturated with respect to calcite. This suggests that the precipitation of calcite is likely to be an active process in subglacial environment. HCO_3^- values remain virtually constant even though there is a trend of decreasing pH values (Figure 3.4b). The waters are relatively close to equilibrium with atmospheric CO_2 but exhibit virtually constant HCO_3^- concentrations due to precipitation of calcite due to the common ion effect.

Quantification of calcite precipitation

Using a mass balance approach, the amount of calcite precipitation occurring for a single water sample is calculated. Two different scenarios are adopted which result in maximum and minimum estimates of the quantity of calcite precipitated from each litre of solution.

The calculations are performed for the subglacial waters sampled on July 26th. These waters have a SIc value of 0.55 by the approximate method, so that if they are corrected by 0.2 units they still have a SIc value of 0.35. Plummer and Busenberg (1982) state that calcite precipitation may be expected from all solutions where SIc >0.3. From the water analysis the charge balance error is -1.3% and there is an excess of 39μeq/l anions. Assuming that the cation concentrations determined by ion chromatography are accurate as shown by the error/repeat analysis, and that the measured proportions of anions are correct, the 39 μeq/l excess is split proportionately and subtracted from the observed figures in order to obtain perfect charge balance (Table 3.5). Two scenarios are examined to account for the evolution of these perfect charge balance waters.

Table 3.5 Composition of perfect charge balance waters for the subglacial stream (July 27th, 1994)

Anions	μeq/l	Cations	μeq/l
SO_4^{2-}	1317	Ca^{2+}	1373
HCO_3^-	258	Mg^{2+}	150
		Na^+	44
		K^+	8
sum	1575	Sum	1575

Scenario 1.

In Scenario 1 it is assumed that there is simply calcite and gypsum dissolution occurring and that there is no calcite precipitation. If it is assumed that pure $CaCO_3$ is being dissolved then all of the HCO_3^- is balanced with Ca^{2+}. The remaining cations would be balanced with SO_4^{2-} giving the gypsum composition (assuming congruent dissolution) shown in Table 3.6.

Table 3.6 Theoretical cation composition of the gypsum following scenario 1

Species	%
Ca^{2+}	84.6
Mg^{2+}	11.4
Na^+	3.5
K^+	0.5
Total	100

This level of impurity in gypsum is highly unlikely. Gypsum has an almost constant composition and reported levels of impurities are c.<3% (Deer *et al.*, 1965, p. 206). Moreover, anhydrite (from which gypsum is formed) also has a relatively constant composition and reported levels of impurities are low c.<4% (Deer *et al.*, 1965, p. 221). Conversely, it is highly unlikely that pure calcite will exist as the bedrock mineral since impurities in calcite are extremely common (Ford and Williams, 1989). Thus this scenario would seem unlikely.

Scenario 2

In scenarios 2A and B it is assumed that there is both carbonate and gypsum dissolution to account for the HCO_3^- and SO_4^{2-} in the waters. However, it is also assumed that there is some precipitation of calcite since the SIc is >0.3. In the following calculations it is also assumed that all the Mg^{2+} comes from the congruent dissolution of either dolomite or impure calcite. The other impurity minerals, Na^+ and K^+ are assumed to come from gypsum dissolution. In scenario 2A all of the Mg^{2+} is assumed to come from congruent dolomite dissolution.

A) Dolomite

In this scenario, Mg^{2+} and Ca^{2+} must be produced in equal quantities (1:1 in the bulk rock). Hence, there are 150μeq/l Mg^{2+} and 150μeq/l Ca^{2+} from dolomite dissolution. To balance these cations requires 300μeq/l HCO_3^- to be in solution. However, only 258μeq/l HCO_3^- were measured. Therefore, 42μeq/l HCO_3^- have been precipitated from solution. Since SIc is 0.3 and SId is -0.55 it appears that calcite precipitation is occurring and that 42μeq/l of Ca^{2+} have also been precipitated. Converting the value of 84μeq/l for calcite precipitation into a weight gives precipitation of 3.4mg/l calcite to account for the HCO_3^- deficit.

B) Impure calcite

In scenario 2B it is assumed that all of the Mg^{2+} comes from the congruent dissolution of impure calcite. If it assumed that the Ca/Mg ratio in the marginal stream is representative of the bulk rock, then a ratio of 10:1 is appropriate for the following calculations. If the source of Mg^{2+} is from calcite dissolution then 1500 μeq/l Ca^{2+} and 1650 μeq/l HCO_3^- must also be dissolved. Only 258 μeq/l HCO_3^- were measured in the waters (Table 3.5). Hence, precipitation of 1392μeq/l of HCO_3^- must have occurred. If calcite precipitation is occurring then 1392 μeq/l of Ca^{2+} must also have been precipitated.

Converting the value of 2784μeq/l into a weight yields 112.77mg/l of calcite precipitation. The ratio of 10:1 Ca/Mg in the marginal stream may also reflect a mixture of sources i.e. low Mg-calcite and dolomite. To more accurately estimate the proportions of Mg^{2+} in the calcite would require acid dissolution of bulk rock samples.

With either scenario it is clear that there is initial dissolution of calcite/dolomite. As gypsum dissolution occurs then the waters become saturated with respect to calcite due to the common ion effect. In this case, the common ion in gypsum and calcite is Ca^{2+}. Accordingly, there is precipitation of calcite from the waters. Scenario A possibly represents minor dedolomitisation of the carbonate bedrock driven by gypsum dissolution (c.f. Bischoff *et al.*, 1994). In scenario B considerably more calcite precipitation is occurring than in scenario A. In both scenarios, however, congruent dissolution of the mineral is assumed, however, it is likely that incongruent dissolution of both calcite and dolomite may occur (I. Fairchild pers.comm., 1995) favouring the preferential input of Mg^{2+} into solution. Therefore, these results must be treated with some caution.

Dissolved oxygen variations in the meltwaters

The level of DO in the waters is an important control on the occurrence of oxidation reactions. The most important oxidation reaction in the glacial environment is that of sulphides (Tranter *et al.*, 1993). Table 3.7 shows the mean DO values in the five meltwater streams studied. No data exist for dissolved oxygen variations in the east marginal stream.

There is little variation in the DO content of the water either within an individual stream or between streams. (Table 3.7) All streams are extremely close to atmospheric values regardless of the stream flow routing or the predominant weathering reaction. Two useful conclusions can be drawn from this information. First, if there is significant pyrite oxidation occurring in any of the streams then it is occurring at a rate equal to that of the supply of O_2 to the water from the atmosphere. Second, it appears that both snowmelt and

icemelt-derived waters rapidly attain DO values close to equilibrium with the atmosphere.

Table 3.7 Mean and coefficients of variation of dissolved oxygen saturation levels in the five meltwater streams studied (Barker, 1995).

Stream	mean % saturation of dissolved O_2	coefficient of variation (%)
Supraglacial	92	4.3
Proglacial (a) and (c)	93	4.7
Proglacial (b)	96	4.2
West Marginal	91	4.4
Fountain	92	4.8
Subglacial	94	5.8

Sulphide oxidation as a proton source for weathering reactions

In alpine glacial meltwaters sulphide oxidation has been shown to be an important proton source in the distributed drainage system where water residence times are relatively high (Tranter *et al.*, 1993). Hence, it might be expected that in the subglacial environment especially, sulphide oxidation may be a possible proton source.

Sulphide oxidation in type 1 waters

If sulphide oxidation was occurring in type 1 waters then, following equation (10), it would be expected that elevated levels of sulphate, and lower pH values would be observed. If the solution was undersaturated with respect to calcite and there was particulate material available for weathering, it would be expected that the aqueous protons would be consumed in the weathering of calcite (Vear and Curtis, 1981; Raiswell

and Thomas, 1984; Sharp, 1991).

$4FeS_{2(s)} + 14H_20 + 15O_2 + 16CaCO_3 \rightarrow 4Fe(OH)_{3(s)} + 8SO_4^{2-} + 16Ca^{2+} + 16HCO_3^-$ (23)
pyrite

If this were the dominant proton source for calcite weathering, one would expect the SO_4^{2-} : HCO_3^- ratio to be 1:1 (where concentrations are measured in μeq/l) (Fairchild *et al.*, 1994). In the marginal streams where calcite dissolution is the dominant weathering reaction and gypsum dissolution appears minor, the average SO_4^{2-}:HCO_3^- ratio is 1:7.15 (east) 1:4.43 west. The proglacial stream has a SO_4^{2-}:HCO_3^- ratio of 1:4.38 prior to the subglacial input and a ratio of 1:2.28 afterwards. Hence, in the majority of these environments sulphide oxidation does not appear to be the dominant proton source for weathering reactions. However, in the proglacial (c) environment it cannot be ruled out as a significant source.

Sulphide oxidation in type 2 waters

In the subglacial environment it is not really possible to determine whether sulphide oxidation is occurring using the (HCO_3^-/SO_4^{2-} ratio) because gypsum dissolution provides a large quantity of SO_4^{2-} to the waters. If sulphide oxidation was happening on a large scale it would be expected that the level of dissolved O_2 in the subglacial waters would be reduced relative to the input (supraglacial) waters. This is not the case (see table 3.5). If there is significant sulphide oxidation occurring in the subglacial streams then it is occurring at a rate equal to that of the supply of O_2 to the water from the atmosphere and melting basal ice.

Sulphide sources in the catchment

From Figure 2.5 it is clear that the carbonate rocks outcropping on the valley sides continue beneath the glacier. If it assumed that the composition of the carbonate rocks in the marginal environment is similar to those in the subglacial environment and that sulphide oxidation does not appear to be an important weathering process in the marginal environment, it seems unlikely that there would be a significant sulphide source in the subglacial environment. However, it may simply be that sulphide is present in both the marginal and subglacial environments but that water-rock contact times in the marginal environment are not long enough for the reaction to take place. It is also possible that sulphide may be present in the subglacial environment since pyrite (FeS_2 - Iron sulphide) is a mineral occasionally found in association with gypsum (Deer *et al.*, 1965, p. 215). A very useful and relatively simple technique employed by Bischoff *et al.* (1994) to determine the relative proportions of aqueous SO_4^{2-} derived from gypsum and pyrite weathering sources is to measure the δ34S of the pyrite and the gypsum in the catchment (which differ by >10‰). Comparison of these values with the δ34S of the SO_4^{2-} in the catchment waters allows assessment of the relative proportion of SO_4^{2-} derived from each source. Such an analysis would be useful in subsequent studies on the water chemistry of John Evans Glacier.

Conclusions

At John Evans Glacier it is clear that waters can follow two distinct weathering pathways. Type 1 waters (supraglacial, proglacial, marginal) are dominated by the weathering of calcite. Type 2 waters (subglacial) are dominated by the weathering of gypsum. In both type 1 and type 2 waters limited weathering of dolomite is also likely. In type 2 waters there is also precipitation of calcite due to the common ion effect caused by gypsum dissolution. In both weathering environments the primary source of aqueous protons for the weathering of carbonates is likely the carbonation reaction. Evidence for sulphide oxidation as a major proton source is not recorded although it cannot be ruled out

completely. The weathering processes recorded in type 1 waters are not significantly different from those recorded in Alpine glacial catchments in carbonate areas (cf. Fairchild *et al.*, 1994). However, suspended sediment concentrations are significantly lower at John Evans Glacier (c. 0.1g/l cf 1.0g/l or greater in Alpine catchments). This seems to limit the total concentrations of solute in Type 1 waters. The results of the subglacial weathering processes are very important, especially in terms of providing a mechanism of subglacial calcite precipitation. Hallet (1976) suggested that the calcite deposits in the forefields of retreating glaciers are formed by calcite precipitation when solutes are rejected during the refreezing stage of the regelation process. At John Evans Glacier the precipitation of calcite appears to be occurring as an almost continuous process in subglacial waters due to the common ion effect. However, the proportion of the precipitated calcite that is deposited subglacially and the proportion that is transported from the glacier as suspended sediment remains unknown.

Implications

The implications of the findings are twofold. First, the subglacial waters at John Evans Glacier have a distinctive chemical signature when compared to supraglacial, proglacial and ice marginal waters. Subglacial waters are dominated by a Ca^{2+}/SO_4^{2-} chemistry, but also have higher Mg^{2+} and K^+ concentrations than the subaerial streams. Moreover, Na^+ concentrations indicate that there is a crustal weathering source for Na^+ in the subglacial environment, which is not evident in the marginal environment. The distinctiveness of the subglacial waters is important for determining hydrological pathways and will be examined in more detail in Chapter 4. Second, in terms of testing the assumptions of Gibbs and Kump (1994), about the degree of subglacial and proglacial chemical weathering occurring at the margins of former mid-latitude ice sheets, the following points can be made:

1) There is significant chemical weathering occurring at the base of a large polythermal Arctic valley glacier. Therefore, it is likely that chemical weathering occurred beneath the Pleistocene ice sheets in areas where polythermal ice conditions existed.

2) There is significant chemical weathering occurring in the proglacial area. When dilute supraglacial meltwaters come into contact with proglacial sediments, rapid weathering of calcite (driven by the carbonation reaction), results in the drawdown of atmospheric CO_2. It is also likely that the mixing of the saturated subglacial waters (possibly containing fine grained rock flour and reprecipitated calcite) with dilute supraglacial waters will result in post-mixing reactions (Brown *et al.*, 1994). Post-mixing reactions are observed in Alpine glacial meltwaters when concentrated subglacial water is mixed with dilute supraglacial waters in major drainage channels where large amounts of suspended sediment can be entrained. They involve the renewal of weathering reactions and net addition of solute to the mixed waters. (Brown *et al.*, 1994). If post-mixing reactions are driven by the carbonation reaction, this will cause a further increase in CO_2 consumption. This process could be simulated for the waters from John Evans Glacier using the chemical speciation model MIX (Plummer *et al.*, 1975).

CHAPTER 4 : SUBGLACIAL HYDROLOGICAL VARIATIONS

Introduction

In chapter 3 it has been established that waters draining subglacially from John Evans Glacier have very different chemical characteristics to waters draining subaerially. The aim of this chapter is to describe and account for the manner of outflow of the subglacial waters during the meltseason since this is a poorly understood phenomenon in high Arctic glaciers.

Observations on the hydrology of glaciers in the Canadian Arctic

Studies on the pattern of runoff from glaciers in the Canadian Arctic are extremely limited, with records lasting a maximum of two consecutive years. Furthermore, the glaciers studied vary greatly in areal extent and geographic location. In spite of these differences, common features observed in runoff patterns are as follows:-

1) Discharge is highly seasonal, with surficial runoff being restricted to the months when there is meltwater generation (May - August). Due to the problems of inhospitable conditions and 24 hour darkness, observations on runoff during the winter months have not been conducted. However, when air temperatures are significantly below zero degrees and there is no insolation, melt and therefore, surficial runoff will be zero. However, large icings in front of some glaciers on Bylot Island, N.W.T., suggest runoff of stored water after melt has ended (B. Moorman pers. comm., 1994).

2) Discharge hydrographs are dominated by diurnal oscillations reflecting variations in the melt rate of snow and ice in the basin. (Adams, 1966; Ostrem *et al.*, 1967; Ballantyne and McCann, 1980; Wolfe, 1995).

3) Superimposed on this pattern of runoff are short-lived discharge fluctuations of irregular periodicity and magnitude, which arise from the temporary damming of ice marginal streams by ice, slush or snow barriers (Adams, 1966; Maag, 1969; Church, 1972; Ballantyne and McCann, 1980)

Some of the above studies discuss flow routing of the meltwaters (e.g. Maag, 1969; Ballantyne and McCann, 1980), while others do not (e.g., Ostrem *et al.*, 1967). In the studies where flow routing is discussed, drainage is considered to be supraglacial and ice marginal rather than subglacial.

Observations on the hydrology of ice sheets

Studies on the pattern of runoff on parts of the Greenland ice sheet (e.g., Thomsen *et al.*, 1988) indicate that there is drainage of supraglacial waters into moulins. However, outflow of these waters and the nature of the subglacial hydrological system are not documented or discussed. Sudden release of waters from larger ice masses has been observed in Greenland (Russell, 1990), and Antarctica (Goodwin, 1988). Only Goodwin (1988), however, has good evidence to show water storage at the bed. The observations made were often incidental to other fieldwork programs, and thus documentary evidence is limited (e.g., Goodwin, 1988). Therefore, the release of water from beneath these ice masses remains a poorly understood phenomenon.

Indirect evidence for the existence of a subglacial drainage system beneath an Arctic glacier is presented by Mũller and Iken (1973). They observed increased summer ice flow velocities in the ablation zone of White Glacier, Axel Heiberg Island, N.W.T., and attributed these to seasonal basal motion. This implies that the basal ice is at the melting point and that surface meltwaters penetrate to the bed, even though the bulk of the ice is well below melting point. Iken (1972) argued that meltwater flowing down moulins penetrated to the bed and spread out over an area large enough to affect the basal velocity. Subsequent studies by Blatter (1987) and Blatter and Hutter (1991) show White Glacier has a polythermal regime, such that there is a central core of temperate ice at the bed, surrounded by cold ice at the surface, margins and glacier snout. Meltwater that does reach the bed will initially be limited spatially to the zone of basal ice at the pressure melting point. However, where water exits from the glacier, it must breach the cold ice barrier. Discharge of turbid "englacial" water was observed from both the eastern and

western margins of the glacier, but not from the glacier snout (Iken, 1974). This suggests that at White Glacier the barrier of cold ice at the glacier snout is more effective in preventing the drainage of such waters than the cold ice barriers at the margins.

Water storage mechanisms in polythermal ice masses

Following Blatter (1987), it appears that some Arctic glaciers are polythermal and that surficial water reaching the glacier bed is restricted to the basal zone where ice is temperate. If the basal hydraulic gradient is directed downglacier, basal water will flow towards the snout, being ponded behind the cold ice barrier. The growth of the water pocket will depend on the rate of input of supraglacial waters and on the permeability of the underlying substrate, which controls groundwater outflow. In sub polar glaciers groundwater may flow beneath the permafrost at the glacier margin (Shoemaker, 1994). If meltwater input significantly exceeds the output then water storage will occur until a critical point is reached when Pw (subglacial water pressure) is close enough to Pi (ice overburden pressure) to create separation of the cold ice from the bed and thus breach the cold ice dam. Release of the stored water will be controlled by the size of the breach of the ice dam relative to the size of the water store and how effectively the passage through which the water drains through the cold ice is maintained. Release of the stored water is more likely initially to resemble a sudden outburst - break flood (Haeberli, 1983) similar to that of water pocket ruptures in Alpine glaciers than a jökulhlaup. Water release in jökulhlaups is explained by the progressive enlargement of the outflow channels by melting of the channel walls. If the water temperatures are very close to zero it is difficult to envisage rapid channel enlargement in cold ice by wall melting, since a much greater amount of heat energy is required to warm the ice to zero before melting can occur. The process may occur but at a significantly slower rate than in temperate ice. If the ice is thinner at the margins than the snout, or the hydraulic gradient is steeper towards the margins than towards the snout, then subglacial water may exit ice marginally (e.g., White Glacier; Iken, 1974). The overall size of the water pocket and the subsequent flood will be controlled by the meltwater flux, the subglacial bedrock geometry and the

thickness of the cold ice barrier. If annual water fluxes are low and the ice barrier is thick, interannual storage of water may occur.

Catastrophic flood types

Catastrophic floods of glacially derived water fall into two main categories, jökulhlaups and outburst-break type floods (Haeberli, 1983). Each flood type has a very different and distinctive hydrograph (Figure 4.1). In each category, the reservoir of water that drains may be ice marginal or subglacial. However, in jökulhlaups the flood waters are always routed subglacially. The manner of water release by jökulhlaups, whether sourced ice marginally (e.g., Collins 1986) or subglacially (e.g., Rist, 1973, 1976, 1984, 1992), has been modelled theoretically (Nye, 1976; Mathews, 1973; Clarke, 1982) and the distinctive hydrograph shape has been explained by progressive enlargement of the outflow channel(s) by wall melting followed by a rapid decline in the water supply as the reservoir of water is emptied. The duration of the jökulhlaup will depend on the size of the outflow channels relative to the size of the reservoir of water, but is usually on the order of a few days (Figure 4.1).

In a study on hazard prediction in the Swiss Alps, Haeberli (1983) documents numerous sudden-outburst break type floods in glaciated catchments. The source of the stored water released in the flood events is ice marginal in some cases and subglacial in others. Haeberli (1983) examines the morphology of the glaciers and notes that where there are known water-pocket ruptures and hence subglacial storage of water, the glaciers are relatively steep. Otherwise, there do not seem to be any simple, discernible, morphological characteristics which make such glaciers recognisable. Of the 20 water-pocket ruptures documented, 19 occurred during the months of June-September. In Alpine glaciated catchments the summer meltseason is the time of maximum meltwater production, due to glacier ablation. Hence, there appears to be a link between the flood events and times of maximum meltwater production. Despite the above distinction, it is common for all types of glacier flood events to be described as jökulhlaups, even when the pattern of water

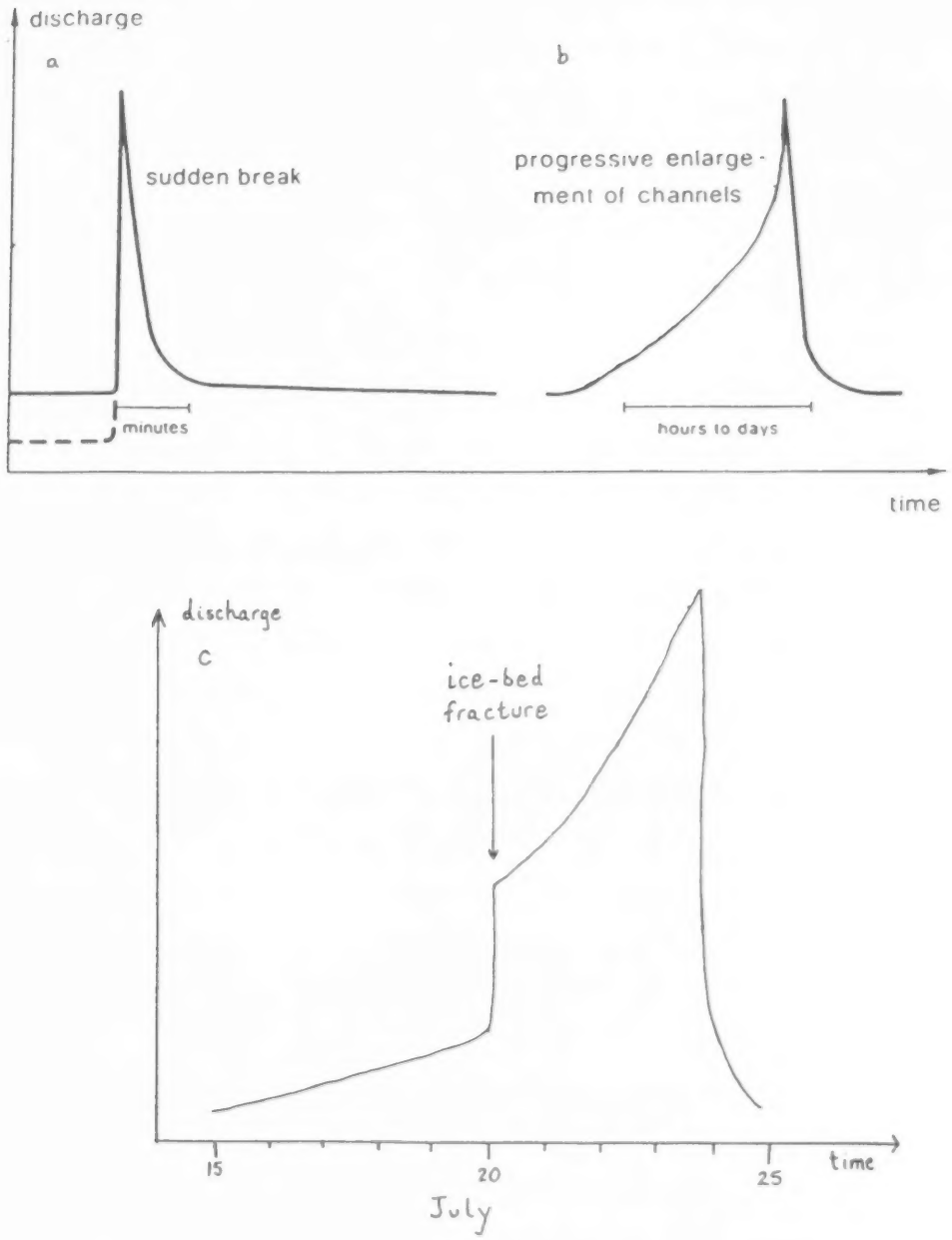

Figure 4.1 Characteristic hydrographs for a) sudden break outburst flood, b) jökulhlaup and c) schematic diagram of a "stepped" jökulhlaup.

release resembles an outburst-break type flood (e.g., Goodwin, 1988). Correctly describing and documenting the manner of water release is important in terms of understanding the subglacial hydrological conditions and the likely causes of the water release. Here is presented the first record of a sudden-break outburst event, followed by a jökulhlaup, from a high Arctic glacier involving subglacially stored water.

Field methods

The 1994 field season commenced on June 15th (JD166), and ended on August 7th (JD219). During that period water quality measurements were made on six meltwater streams draining the glacier. The supraglacial and west marginal streams were monitored for the duration of the field season, and the proglacial, fountain, east marginal and subglacial streams for parts thereof (Figure 2.8). During the period when streams were sampled, measurements were made at least once daily, apart from when high discharges in the east marginal stream prevented access to the other streams. Discharge and electrical conductivity (EC) - a measure of solute concentration - of the proglacial stream were both measured manually at least once a day, and continuously from June 15th - August 6th. Manual measurements of discharge in the subglacial stream were made at least once daily from July 27th-August 7th.

Results

Mode and location of water release

On July 9th both the initiation of the artesian water fountain and a premonitory release event (prior to the outburst) of subglacial water into the proglacial stream occurred simultaneously. The artesian fountain exited from the glacier c. 20 m above the glacier bed, c. 50 m from the snout and c. 250 m to the west of the proglacial stream channel (see Figures 2.3 and 4.2). Note that the artesian fountain occurs almost directly above the point of efflux of the 'subglacial' stream on July 15th. The fountain was initially 1-2 m

in height, but its height declined over the subsequent four days. The fissure from which the water exited was aligned perpendicular to the glacier snout and was approximately 10 cm wide by 30 cm long.

The main outburst of subglacial waters flowing into the proglacial stream channel occurred on July 10th, a day after the initiation of the artesian fountain and the premonitory event. The subglacial waters exited from the glacier over a c. 30 m wide zone at the ice-sediment interface at the base of the glacier by upwelling through the sediments (Figure 4.3). The outflowing subglacial waters became channelised within c. 10 m of the snout, as the waters occupied large pre-existing channels. Figures 4.4 and 4.5 show the proglacial stream channel and surrounding area both before and during the outburst event on July 8th, 9th, 10th, 11th, 12th, and 13th. The photographs were taken from a point on the glacier snout almost directly above the point of efflux of the subglacial waters (see Figure 2.3).

On the evening of July 15th turbid water was observed for the first time flowing from the glacier in a well defined channel c. 250 m to the west of the proglacial stream (defined as the 'subglacial' stream). Subglacial waters still drained into the proglacial channel at this point in time. On the morning of July 16th significant subglacial input to the proglacial stream ceased. For the remainder of the field season subglacial waters exited the glacier via the 'subglacial' stream. However, during the high discharge event on July 22nd, 23rd and 24th (JD203, 204, 205) a number of additional channels opened up at the base of the glacier across a c.30 m wide zone to the east of the main channel. These channels were broad low conduits with a height to width ratio of 1:7 and were only occupied during the high discharge event.

Figure 4.2 The artesian fountain on 9th July, 1994

Figure 4.3 Upwelling of subglacial waters through sediments at the ice-sediment interface 10th July, 1994.

Figure 4.4 View of the proglacial stream channel on a) July 8th, b) July 9th, c) July 10th.

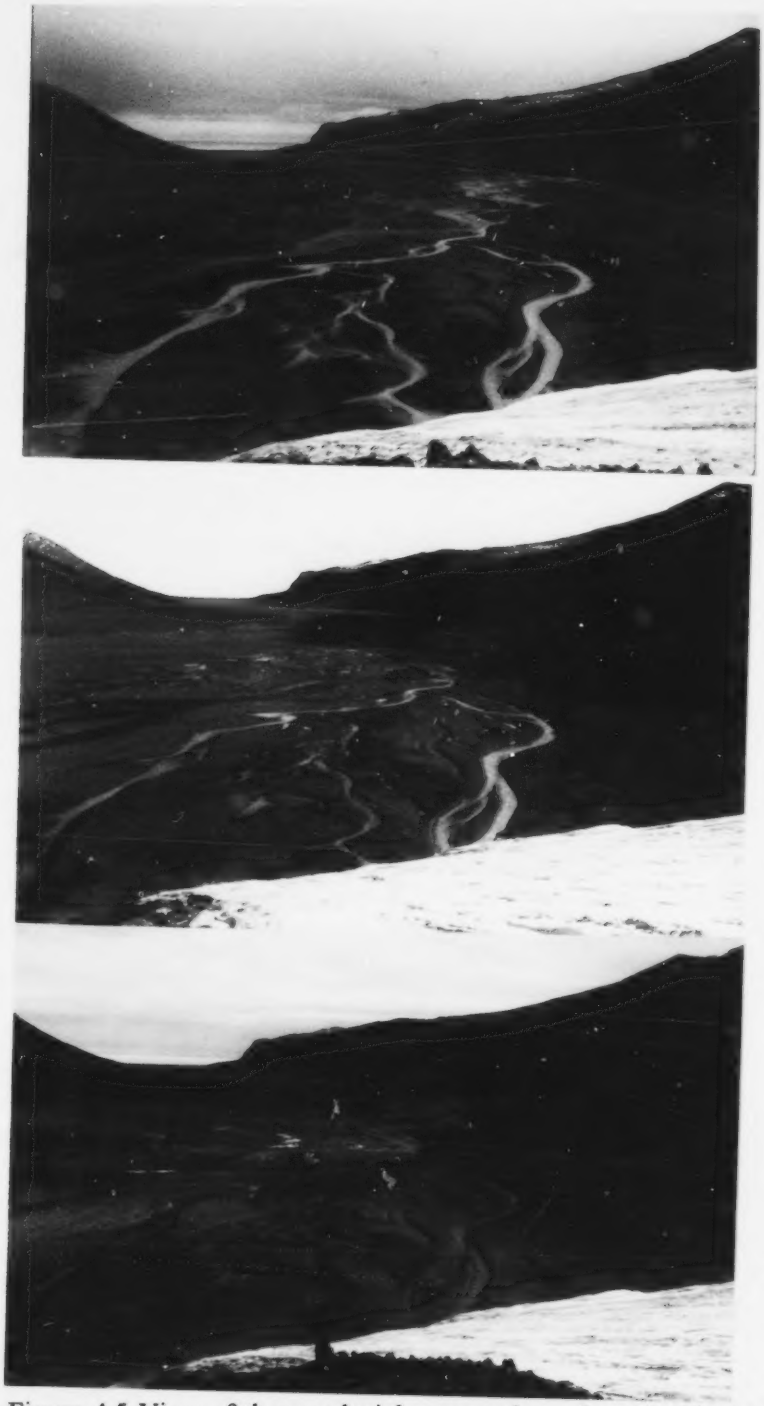

Figure 4.5 View of the proglacial stream channel on a) July 11th, b) July 12th, c) July 13th.

Proglacial stream

Figure 4.6 shows the continuous records of discharge and electrical conductivity (EC), and the record of suspended sediment concentrations (SSC) from manual samples collected from the proglacial stream. The combined results of discharge, EC and SSC allow the meltseason to be divided into three main phases; (i) pre-outburst, June 15th - July 9th (JD166-190), (ii) outburst, July 10th - July 15th (JD 191- 196) and (iii) post - outburst, July 16th - July 22nd (JD197- 208).

The pre-outburst and post-outburst phases showed very similar patterns of variation in discharge, EC and SSC and thus will be discussed together. During these periods both EC and discharge exhibited clear diurnal cycles and SSC's were close to zero. The proglacial stream is fed primarily by a large supraglacial stream which is the source of the diurnal discharge variations. The diurnal pattern of supraglacial runoff is controlled by the melt rate which is dependent principally on net radiation fluxes and sensible heat transfer at the glacier surface. Thus discharge is higher during the day when the melt rate is at a maximum. Diurnal variations of EC are inverse to those of discharge, with maximum EC coinciding with minimum discharge and vice versa. At maximum discharge, streamflow velocities are higher and residence time in the proglacial environment is thus limited,as are water-rock contact times. Hence solute acquisition may be expected to be limited. By contrast, at low discharge, water-rock contact times are increased and more solute acquisition may occur.

Outburst event

The outburst event was marked by an order of magnitude increase in discharge, EC and SSC over the period 10th-15th July. The main outburst was preceded on July 9th by a premonitory increase in EC. On July 10th, EC and discharge rose rapidly and simultaneously to 450 $\mu s\ cm^{-1}$ and 3.58 m^3s^{-1}. Subsequently, discharge declined rapidly over the three days following the peak, although there were two smaller discharge

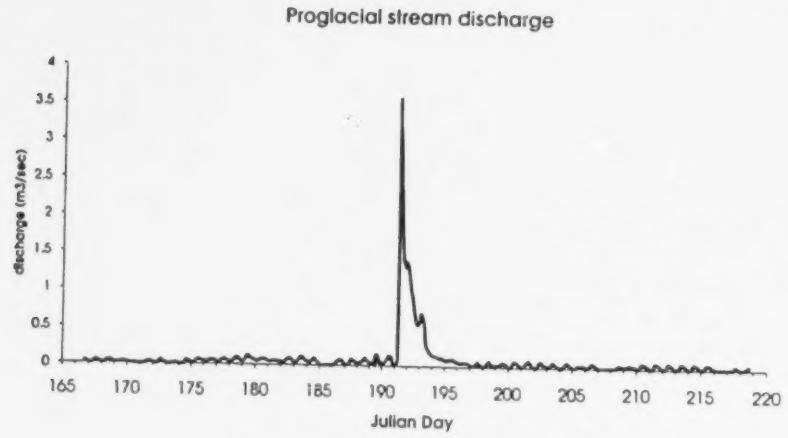

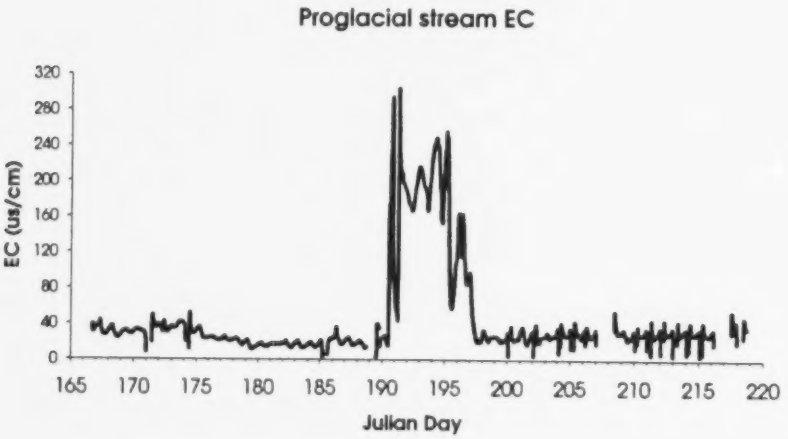

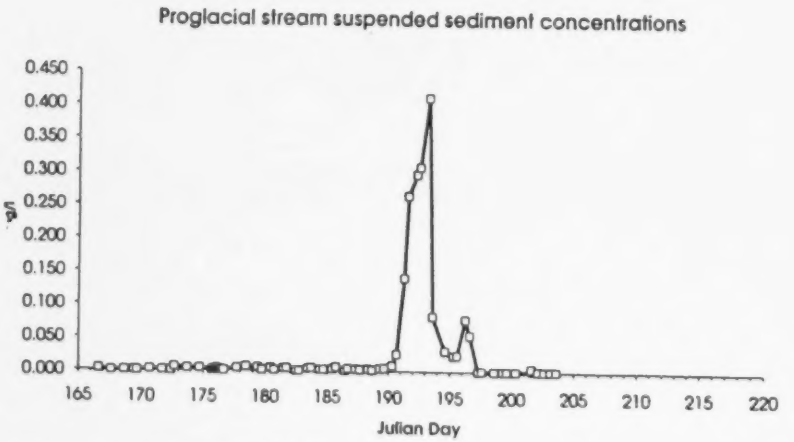

Figure 4.6 a) Discharge, b) EC and c) SSC variations in the proglacial stream June 15th - August 6th, 1994.

peaks superimposed on the overall decline. By contrast, EC remained at a high level for four days following the peak, oscillating around a mean value of 220 $\mu s\ cm^{-1}$ before declining in a stepwise fashion over the next three days. The peak in SSC lagged the peak in both discharge and EC by two days.

The discharge hydrograph for the outburst event is similar in shape to those observed by Haeberli (1983) for sudden outburst-break floods from temperate alpine glaciers (see Figure 4.1). The outburst events described by Haeberli (1983) are relatively short-lived and have durations of minutes to hours. Due to the switch in the point of efflux of the subglacial waters which occurred six days after the initial burst it is not possible to accurately ascertain the "end " of the outburst event. However, it is clear that the outburst event lasted for at least six days. On the basis of the hydrograph shape it seems reasonable to interpret the event as a sudden outburst-break type flood but of significantly longer duration. The slower release of waters and their continued outflow for the remainder of the fieldseason at John Evans Glacier compared to the bursts from Alpine glaciers, suggest that the water reservoir which supplied the drainage event was much larger than the finite water pockets involved in the Alpine events. Fluctuations in discharge of the subglacial stream, which lag air temperature variations, suggest that this reservoir continued to be fed by supraglacial streams and that it did not drain completely during the outburst.

The peaks superimposed on the proglacial discharge hydrograph occurred at 0100 July 11th (JD 192) and 0130 July12th (JD193). Analysis of the discharge record in the pre - outburst phase indicates that between 0000 and 0100 discharge was virtually zero, hence it is unlikely that direct supraglacial water input to the stream at the snout is the source of the discharge peaks. The timing of the peaks suggest that they occurred c. 6 hours after peak supraglacial runoff was observed. Therefore, the peaks may reflect the lag time for changes in input to be observed in the outflow from the subglacial system.

Although there are oscillations in EC, the overall trend is one of decline after the peak in the initial burst waters. This reflects the gradual dilution of the higher conductivity subglacial waters by more dilute supraglacial waters. The rate of dilution increases as the proportion of subglacial waters in the total discharge decreases. The diurnal cycles in EC simply reflect the diurnal input of supraglacial water to the overall discharge of the proglacial stream. The low points in the EC cycles all occur between 1400-1800 hours which coincide with maximum supraglacial water input.

To explain the large lag time between the discharge peak and the SSC peak it is necessary to plot SSC against discharge and consider possible hysteresis effects (Figure 4.7a). It is evident that the initial increase in discharge results in an increase in SSC. However, as discharge falls SSC continues to rise until it reaches a maximum of 0.4g/l. After this it declines abruptly in comparison to the concurrent decline in discharge. Relationships between EC and SSC during the burst event are shown in Figure 4.7b For only a very slight rise in SSC there is a large rise in EC. As SSC's rise rapidly and then fall rapidly EC remains fairly constant, suggesting that the waters initially had high solute concentrations and that solute acquisition by weathering of suspended sediment is not an important process.

The subglacial waters exited through the basal sediments at the ice-bed interface, which are a fairly restrictive medium to water flow, in comparison to channelised drainage. If one considers this outburst event as being piston type water flow through the sediments then the input of water into the sediment produces a kinematic wave which propagates through the sediments such that the actual input waters are not the initial output waters. Water input likely occurred to the sediments when the downglacier propagating reservoir connected with and started to introduce water to a subglacial aquifer. The initial outburst waters will have been percolating through the sediments at very low flow velocities and are thus unlikely to have entrained significant quantities of suspended sediment. The waters input into the sediment from the reservoir will flow through the sediment faster than the initial output water did, because the throughflow of the water through the

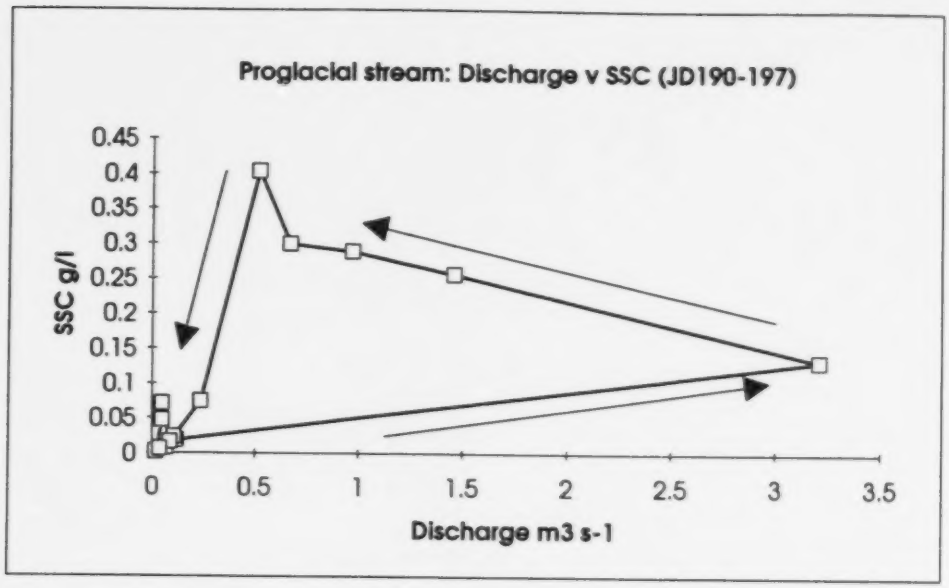

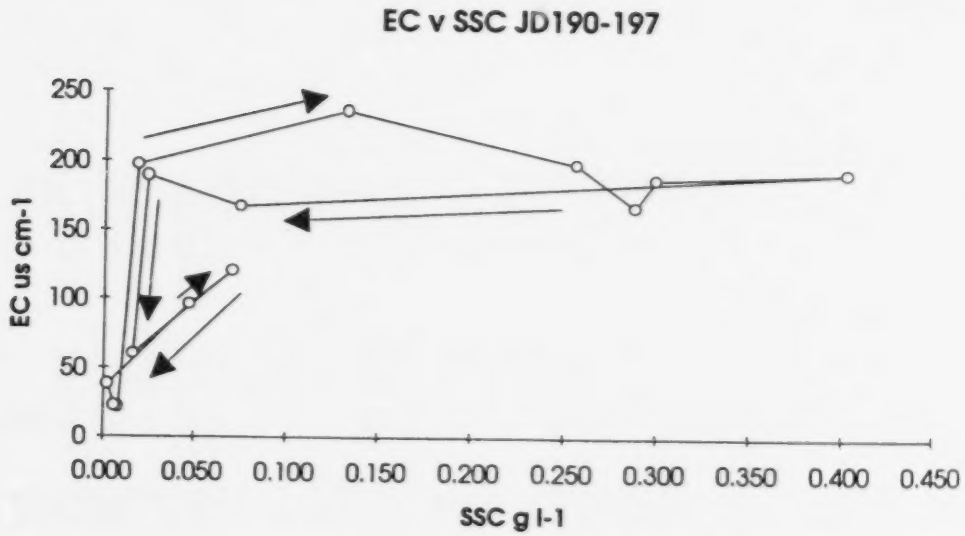

Figure 4.7 a) Discharge v SSC for the proglacial stream July 10th - July15th
b) EC v SSC for the proglacial stream July 10th - July15th

sediment will gradually mobilise the sediment, beginning with the finest fractions thus increasing the permeability of the sediments. As more fines are removed the permeability of the sediment and therefore the rates of water throughflow will increase and at higher velocities more entrainment of suspended sediment is likely. Solute concentrations were initially high and remained relatively constant for at least four days and were unaffected by changing SSC suggesting the waters in the downglacier propagating reservoir already had high concentrations of solute prior to their passage through the sediments.

Fountain

Figure 4.8 shows the EC and SSC variation in the waters from the artesian fountain. Apart from the initial values it appeared that SSC declined over time whereas EC showed a gradual rise. The chemistry of the outflowing waters was very similar to that of the "piston flow" waters through the subglacial sediments. This suggests that as outlined above that during the downglacier propagation of the subglacial reservoir the waters acquire high levels of solute. Hence the fountain is most likely a pressure "vent" for the subglacial reservoir and not the result of piston-flow water through the sediments. No quantitative discharge data are available for the fountain stream, however, the fountain declined in height over the four days that it flowed. However, without quantitative data on the discharge variations of the fountain explanation of the EC and SSC variations would be purely speculative and thus they will not be discussed further.

Subglacial stream

Figure 4.9 shows the variations in discharge, EC and SSC in the subglacial stream. Very high subglacial discharges were observed on July 21st, July 22nd, 23rd and 24th as determined by qualitative means. Prior to these days the stream had a low enough discharge that crossing was relatively easy. On July 21st and July 22nd stream crossing was possible but increasingly difficult. On July 23rd and 24th it was not possible to stand up in the channel let alone cross the stream, due to the extremely high rate of discharge.

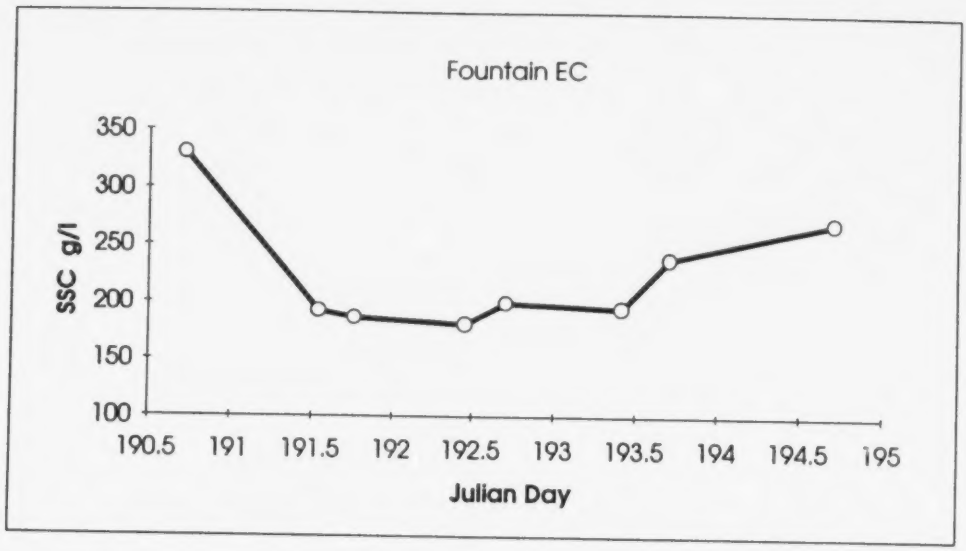

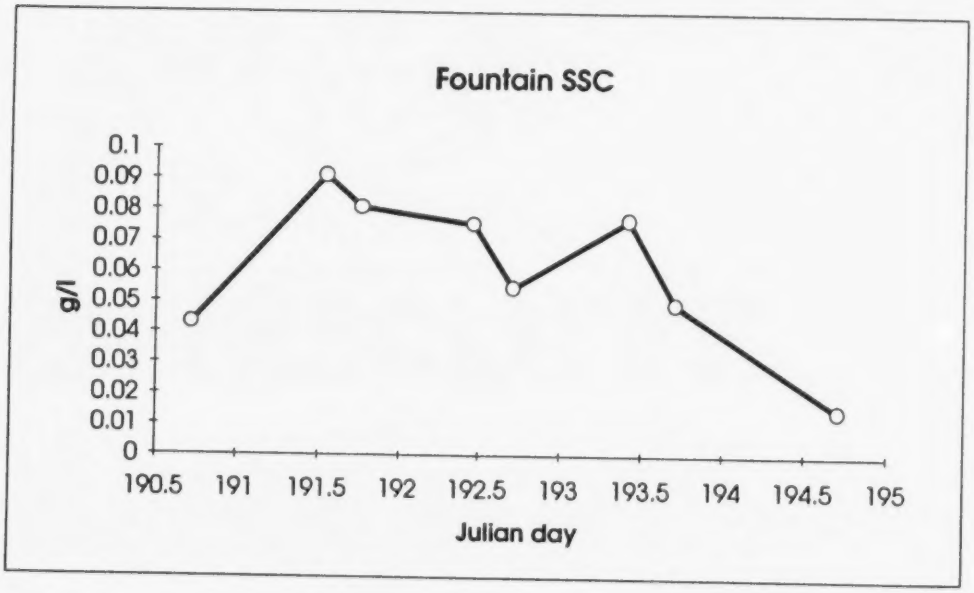

Figure 4. 8 SSC and EC variations in the fountain stream July 9th - July13th

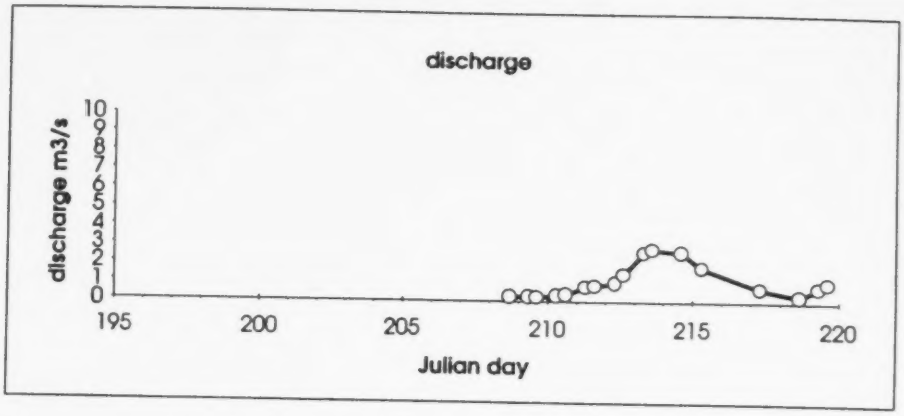

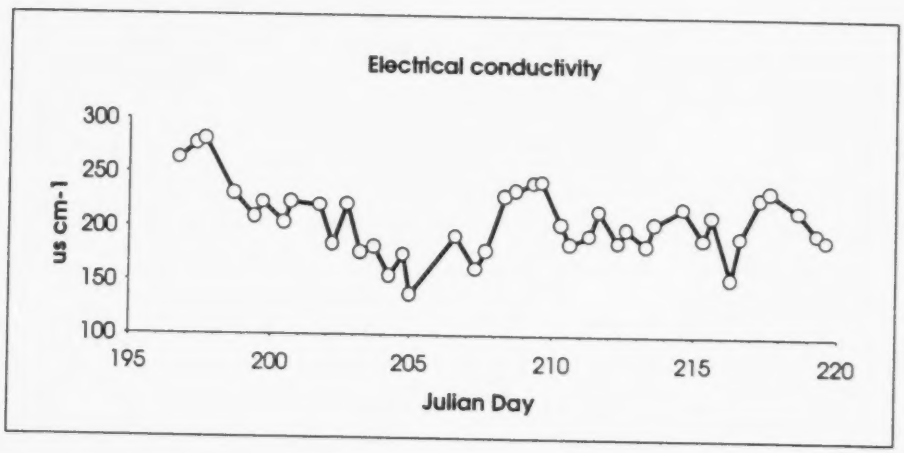

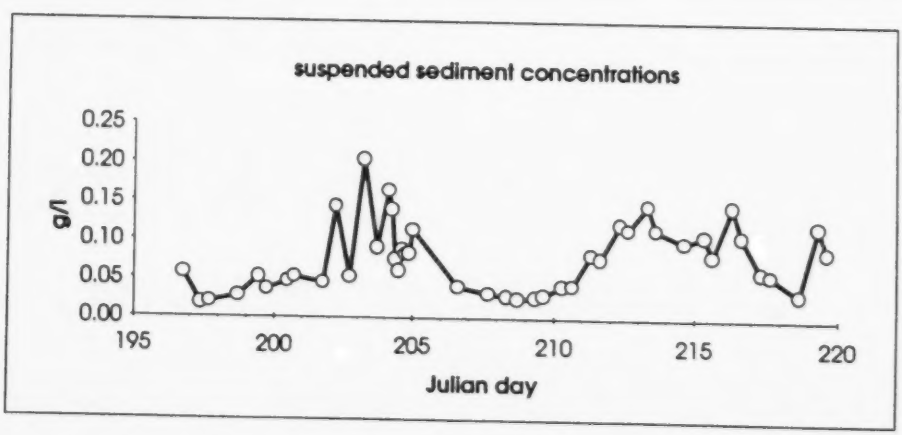

Figure 4.9 a) Discharge, b) EC and c) SSC variations in the subglacial stream July 15th - August 7th, 1994.

It was possible to cross the stream again with ease at 0800 on July 25th.

During the measured period of discharge no diurnal variations were evident. This suggests that the subglacial reservoir was large enough to filter out diurnal variations in input, or that the sampling frequency was too low to detect diurnal variations in discharge. Discharge (Q) and SSC variations are very similar, suggesting a positive association between the variables. In contrast, EC variations generally show an inverse relationship to Q. Combining these observations, it appears that there is a negative association between SSC and EC. The observations on Q/SSC and Q/EC relationships are similar to those observed in Alpine glacial meltstreams, i.e., that there is a positive association between SSC and Q (Gurnell, 1987) and that there is an inverse association between EC and Q (Fenn, 1987). Clearly, then, there is a significant difference between Q/SSC and Q/EC variations in the subglacial stream and those in the outburst of subglacial waters into the proglacial stream. The differences in these relationships are most likely related to the mode of outflow of the waters.

The chemical composition of the subglacial waters.

In Chapter 3 it was established that waters in the fountain, proglacial (b) and subglacial streams have a similar chemical composition (Type 2 waters), but one which is fundamentally different from the chemical composition of waters flowing ice marginally and supraglacially (Type 1 waters) (Table 3.2). Type 2 waters have high levels of Ca^{2+} and SO_4^{2-} indicating significant gypsum/anhydrite dissolution whereas type 1 waters have high levels of Ca^{2+} and HCO_3^- indicating calcite dissolution. The high levels of crustal solute in the subglacial waters indicate that water flow occurred at the glacier bed. High levels of NO_3^- are also observed in the initial subglacial water input into the proglacial stream and there is a consistent presence of nitrate in the subglacial waters for the remainder of the fieldseason (Figure 4.10).

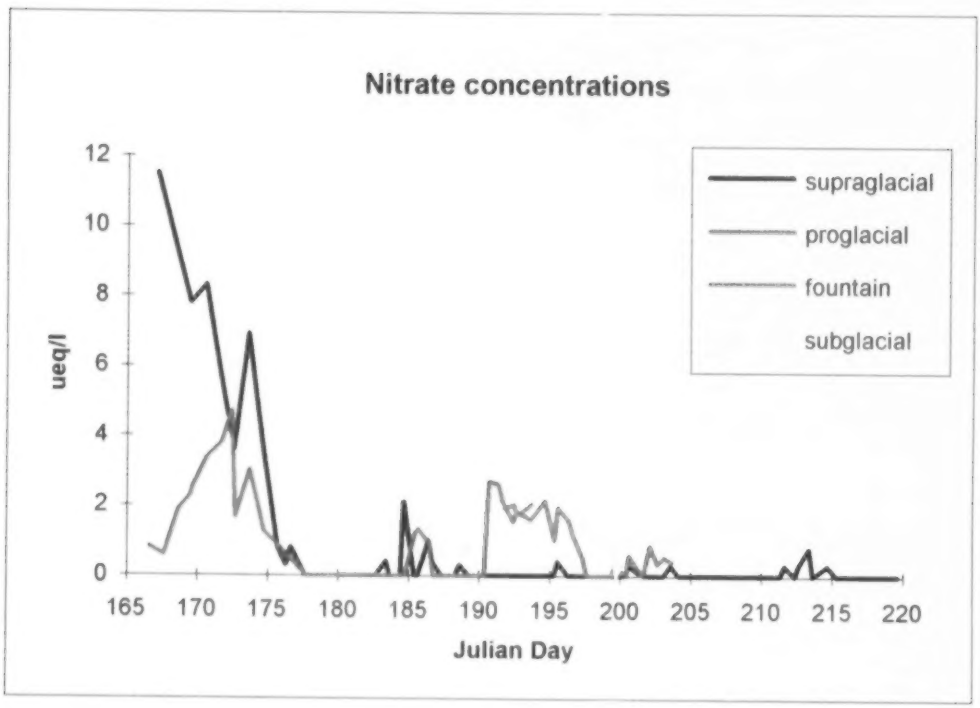

Figure 4.10 Nitrate concentrations in the supraglacial, proglacial, fountain and subglacial streams from June 15th - August 7th 1994.

Tranter et al, (1994) note that nitrate is deposited in glacial catchments as nitric acid aerosol in precipitation. From earlier analysis it has been established that nitrate concentrations in icemelt at John Evans Glacier are effectively zero. Therefore, the main sources of nitrate will be from snowmelt and from precipitation events during the meltseason. The high concentrations of nitrate (3μeq/l) in the initial burst waters suggest that these probably originated as early season snowmelt waters. Such high concentrations were observed in the supraglacial/proglacial waters at the snout 15 days earlier. However the precipitation event on July 5th was of sufficient intensity that sufficient water was collected at our base camp near the glacier snout for chemical analyses. Levels of nitrate in the precipitation were 4.5 μeq/l and significantly higher than observed in the supraglacial/proglacial streams. Since this was a major glacier wide precipitation event it is likely that this contributed to the nitrate source for the subglacial waters, but is unlikely to be the source for all the burst water due to the large volume of burst water involved. No subsequent precipitation events were observed between July 5th and July 10th.

The virtually constant nitrate concentrations in the stream waters suggest that there is always a snowmelt input to the subglacial waters and that this input remains relatively constant over a wide range of discharges. During the meltseason the snowline retreats up glacier and in 1994 was calculated to be at an elevation of 1150 m at the end of the meltseason. A possible explanation for these observations is as follows. The area elevation distribution (Figure 2.4) in the central drainage basin (Figure 2.2b), which is the source area for runoff into the crevasse zone and the probable input of water to the subglacial system, is such that as the snowline retreats to higher elevations the area of the melting snowpack will remain high relative to the area of melting ice. In addition it may be that NO_3^- concentrations in the snowpack at higher elevations are greater than at low elevations on the glacier since the air masses carrying the nitric acid aerosol will be far travelled and thus at high altitude, favouring precipitation at higher elevations. In contrast the snowpack at lower elevations may contain higher concentrations of ions from the seasalt aerosol since precipitation by local air masses may be more favoured at lower

elevations.

Comparison of the modes of outflow

The release of water into the proglacial stream as a sheetflow at the ice-sediment interface and through the upwelling of water through the sediment suggests that the ice dam was frozen to the base of the glacier and that it provided an effective seal against direct water outflow. If it is assumed that the waters in the fountain stream are from the same reservoir as the waters flowing into the proglacial stream, this indicates a) that at that point where the artesian fountain occurred on the glacier snout the easiest route for the water to escape was initially not at the ice bed interface but through the ice, due to the frozen seal and b) that the reservoir of water might be as wide as the distance between the artesian fountain and the proglacial stream channel c. 250 m (see Figure 2.3).

The change in the point of efflux of subglacial waters from the proglacial stream marks a radical change in the mode of water outflow, since the outflow of waters in the subglacial stream occurred in a well defined channel, both in the ice and in the proglacial area. The discharge of the waters was initially very low, but rose progressively over the next five days. This suggests that there may have been gradual enlargement of the channel by melting of the ice walls. This process of enlargement is likely to have been slow because the ice in the channel walls was 'cold', and a large amount of heat had to be conducted into the ice to raise its temperature to zero before melting could occur. On July 20th a major change in the configuration of the outflowing subglacial stream channel occurred. A number of tributary channels immediately to the west of the main channel were opened, such that drainage occurred across a c. 30 m wide section of the glacier in broad low conduits. Discharge of the stream then rose progressively from July 20th - 0000 July 24th. By 0800 on July 25th, stream discharge had returned to very low levels. The outflow of the water in broad low conduits and the sudden initiation of these conduits suggests that they formed when the subglacial water pressure (Pw) was high enough to force localised separation of the ice from the bed, breaking the frozen seal at the ice-bed

interface. Given the thermal conditions in the ice it is difficult to envisage broad low conduits forming by frictional melting. The manner of water release appears qualitatively to resemble that of a jökulhlaup, with a long rising limb, including a stepwise increase in discharge in response to the opening of the broad flat conduits, followed by a rapid fall from the peak flow (Figure 4.1).

Interannual variability of the subglacial drainage system

The location of the **'subglacial'** stream in 1994 was the same as that of the highly turbid stream issuing from the glacier on the aerial photographs taken on 05/07/1959. Moreover, photographs of the glacier snout taken on July 17th 1995 by Rod Smith indicate that turbid waters were exiting from the glacier in this location. From the 1995 photographs it is evident that there was no flow of turbid water in the "proglacial" stream channel on July 17th, but that there was a large artesian fountain exiting from the glacier c. 20 m above the glacier bed and c. 50 m to the *east* of the proglacial channel. This is c. 300 m east of the location of both the subglacial stream and the location of the fountain in 1994. Geyser-like water spouts on the surface of the glacier were also observed in July 1991 (G. Henry pers. comm., 1994). The observations suggest that there may be reoccupation of an existing subglacial outflow channel on an interannual basis, but that the location of artesian fountains is more variable from year to year. Whether subglacial drainage is an annual occurrence remains unknown at present.

Conclusions

From the above discussion it is clear that there are many unanswered questions about the configuration of the subglacial drainage system and possible changes in its configuration during the meltseason. However, the main points to note from the paper are as follows;-

a) There is good evidence for subglacial water storage at the bed of a high Arctic glacier.

b) Release of this water occurred simultaneously at two different places on the glacier snout via different modes of outflow, with the main burst of piston-type flow lagging the initiation of the artesian fountain by one day.

c) Release of the water was initially as an outburst-break type flood through the subglacial sediments as the downglacier-propagating reservoir connected to the permeable aquifer. The outburst event was of significantly longer duration than those observed in Alpine glaciers.

d) The efflux point of subglacial waters changed six days after the initial burst event and occurred as channelised drainage when a new and more efficient connection was made between the reservoir and the glacier margin. This release of subglacial waters resembled a "stepped" jökulhlaup.

e) Ion chemistry of the waters suggests that the stored water probably has a residence time of c.15 days prior to the initial burst, and a snowmelt source.

f) There may be interannual occupation of the same outflow channels by subglacial streams and thus possible stability of the subglacial drainage system for c. 35 years.

CHAPTER 5 : CONCLUSIONS

The hydrological and hydrochemical observations made during the 1994 field season provide good evidence for the existence of a subglacial drainage system beneath John Evans Glacier. The extent of the drainage system is unknown, but it is likely that water penetrates to the bed in a large crevasse field at an elevation of 500 m c. 4 km up-glacier from the glacier snout. Whether the water input reaches the bed directly at that elevation and then flows subglacially for the subsequent 4 km is unknown at present. However, it is clear from the chemistry of the initial 'burst' waters that storage of water at the bed occurs on the timescale of c. 15 days. Later in the fieldseason it is clear that the volume of the subglacial reservoir is large enough to filter out diurnal variations in the water input.

Drainage of water from the store is complex and three modes of water outflow are observed in different locations; an artesian fountain, upwelling of waters through the subglacial sediments and channelised subglacial drainage. The chemistry of the waters outflowing in these three locations is very similar, indicating a similar and singular source. The initial release of water from the store has a hydrograph similar in shape to that of a sudden outburst-break flood but of significantly longer duration. With a switch in the point of efflux of subglacial waters, the outflow hydrograph resembles a jökulhlaup but with a stepped rising limb. From this evidence it is clear that catastrophic drainage of the stored water is the dominant release mechanism. From photographs of the glacier, taken in 1959 and 1995 and from field observations made in 1994 it appears that subglacial waters exit the glacier in the same outflow channel in all three years. However, the 1994 and 1995 observations suggest that the location of artesian water fountains may be different from year to year.

The chemistry of the meltwaters indicates that waters routed subaerially in the supraglacial, proglacial and marginal streams (Type 1 waters) have a dominant Ca^{2+}/HCO_3^- chemistry. By contrast waters routed subglacially are dominated by Ca^{2+}/SO_4^{2-},

reflecting the dissolution of anhydrite/gypsum in the subglacial environment. Analysis of the subglacial waters indicates that the process of gypsum-driven dedolomitisation is occurring subglacially and results in the precipitation of calcite from the subglacial waters.

The observations at John Evans Glacier are probably not common to the majority of small glaciers in the high Arctic since size appears to be an important factor for a) generating polythermal ice conditions and b) generating sufficient runoff to allow development of a subglacial drainage system. However, it would appear that it is a good small scale analogue for the processes occurring at the margins of the mid-latitude ice sheets and thus provides a good location for observing hydrological processes in polythermal ice masses.

Implications

Hydrology

The study is the first to document subglacial drainage in the Canadian Arctic and the first to clearly demonstrate the storage and outflow modes of the waters. The fact that drainage occurs first as an outburst-break event in one location, followed by a jökulhlaup type event in another location suggests that the drainage system is relatively complex. It appears that the frozen seal at the cold ice - bed interface is a key component in controlling storage and mode of release of the subglacial waters. Initially the seal is strong enough to prevent a direct drainage pathway through the cold ice. Thus, water is released beneath the seal through permeable sediments, and above it, through the cold ice, as an artesian fountain. A more permanent channel is then established between the reservoir and the margin probably exploiting a fracture in the seal. This channel is very slowly enlarged by melting of the cold ice walls, however the channel does not grow rapidly enough to effectively drain the growing subglacial reservoir. Eventually the subglacial water pressure is high enough to break the seal and major fracture occurs across a part of the ice sediment interface allowing catastrophic drainage of the waters as a jökulhlaup.

The observations at John Evans Glacier provide direct evidence of hydrological conditions beneath polythermal ice masses and information about the modes of water storage and outflow. They may be useful for the debate about catastrophic release of water from the mid- latitude ice sheets in the late Wisconsinan. (Rains *et al.*, 1993; Shaw, 1994)

Hydrochemistry

The study is the first to examine in detail the chemistry of the meltwaters draining a Canadian Arctic glacier, and the first to document the chemical composition of subglacially stored waters derived from polythermal ice masses. It is also the first study to examine subglacial weathering processes in a catchment with an evaporite/carbonate geology. The results have important implications for understanding the processes of calcite precipitation in the subglacial environment. Hallet (1976) suggested that the calcite deposits in the forefields of retreating glaciers were formed by calcite precipitation which occurred when solutes were rejected during the refreezing stage of the subglacial regelation process. This process occurs where there is a thin water film between the glacier and the bed, and thus where throughflow velocities are slow. At John Evans Glacier, by contrast, the precipitation of calcite due to the common ion effect with gypsum appears to occur in environments where water velocities and discharges are high.

In relation to the debate over the role of chemical weathering in regulating atmospheric CO_2 concentrations, it can be seen that at John Evans glacier CO_2 is being both consumed and added to the atmosphere due to calcite dissolution and precipitation reactions. Since HCO_3^- is present in the outflowing waters it indicates that dissolution of calcite is greater than precipitation, however, the actual amounts of precipitation and dissolution remain unknown. However, the precipitation of calcite and thus CO_2 release to the atmosphere is occurring very rapidly and within the glacial catchment rather than being delayed if the calcite was precipitated in the ocean.

For workers modelling chemical erosion rates during the last glaciation the results obtained show that chemical weathering is an active process in subglacial, proglacial and ice marginal environments at a polythermal ice mass located in an area where the mean annual air temperature is -18°C. These observations may, therefore, be a good analogue for the processes occurring at the margins of the mid-latitude ice sheets during deglaciation. If so, one might infer that chemical weathering was likely occurring in these areas and thus may be an important factor to consider in assessing atmospheric CO_2 variations over the glacial/interglacial transition.

REFERENCES

Adams, W.P. (1966) Ablation and run-off on the White Glacier, Axel Heiberg Island, Canadian Arctic Archipelago. Glaciology No.1 Axel Heiberg Research reports, McGill University, Montreal. Jacobsen-McGill Arctic Research Expedition 1959-1962 77p.

Andreason, J.O. (1984) Glacier meltwater chemistry at two - subpolar glaciers in West Greenland. Rapport Grønlands Geologiske Undersøgelse, **120**, p105-108

Arendt, A. (1995) Mass balance simulations using a positive degree-day model for John Evans Glacier, N.W.T., Canada. Unpublished term paper. University of Alberta

Arnold, N. (1994) Modelling the influence of glacier hydrology on the dynamics of the Scandinavian ice sheet. Unpublished PhD thesis. Cambridge University, U.K.

Bales, R.C. (1992) Snowmelt and the ionic pulse. In *Encyclopedia of Earth System Science*, **1**, Academic press p199-207.

Ballantyne, C.K. and McCann, S.B. (1980) Short-lived damming of a high-Arctic ice-marginal stream, Ellesmere Island, N.W.T., Canada. Journal of Glaciology, **25**, p477-481.

Barker, J. (1995) A study of the dissolved oxygen in the meltwaters of John Evans Glacier, N.W.T., Canada Unpublished BSc. thesis. University of Alberta

Bischoff, J.L., Julia, R., Shanks, W.C. and Rosenbauer, R.J. (1994) Karstification without carbonic acid: Bedrock dissolution by gypsum-driven dedolomitization. Geology, **22**, p995-998.

Blatter, H. (1987) On the thermal regime of an Arctic valley glacier : a study of White Glacier, Axel Heiberg Island, N.W.T. Canada. Journal of Glaciology, **33**, p 200-211

Blatter, H. and Hutter, K. (1991). Polythermal conditions in Arctic glaciers. Journal of Glaciology, **37**, p261-269.

Bøggild, C.E., Reeh, N. and Oerter, H. (1994) Modelling ablation and mass-balance sensitivity to climate change of Storstrømmen, N.E. Greenland. Global and Planetary Change, **9**, p79-90

Bond , G. and 13 others (1992). Evidence for massive discharges of icebergs into the North Atlantic ocean during the last glacial period. Nature, **360**, 245-249

Brown G.H., Sharp M., Tranter M., Gurnell A.M. and Nienow P. (1994) Impact of post-mixing chemical reactions on the major ion chemistry of bulk meltwaters draining the Haut Glacier d'Arolla, Valais, Switzerland. Hydrological Processes, **8**, 465-480.

Church, M. (1972) Baffin Island Sandurs: A study of Arctic fluvial processes. Geological Survey of Canada Bulletin, **216**, 208p.

Clarke, G.K.C. (1982) Glacier outburst from "Hazard Lake", Yukon Territory, and the problem of flood magnitude prediction. Journal of Glaciology, **28**, p3-21.

Clark, P.U. (1994) Unstable behaviour of the Laurentide Ice Sheet over deforming sediment and its implications for climate change. Quaternary Research, **41**, p19-25.

Collins, D.N. (1986) Characteristics of meltwaters draining from the portal of an Alpine Glacier during the emptying of an ice marginal lake. Alpine Glacier Project Working Paper Series, 4, Department of Geography University of Manchester 28pp.

Dansgaard, W., Johnsen, S.J., Clausen, H.B. Dahl-Jensen, D., Gundestrup, N.S., Hammer, C.U., Hvidberg, C.S., Steffensen, J.P., Sveinbjörnsdottir, Jouzel, J. and Bond, G. (1993) Evidence for general instability of past climate from a 250-kyr ice-core record. Nature, **364**, p218-220.

Deer, W.A., Howie, R.A and Zussman, J. (1965) *Rock-Forming Minerals*, Vol. 5. Longmans. London, 333pp.

Denton, G.H., Armstrong, R.L. and Stuiver, M. (1970) Late Cenozoic glaciation in Antarctica: The record in the McMurdo Sound region. Antarctic Journal of the United States, **5**, p15-21.

Fairchild, I.C., Bradby, L., Sharp, M. J. and Tison, J-L. (1994) Hydrochemistry of carbonate terrains in alpine glacial settings. Earth Surface Processes and Landforms, **19**, p33-54.

Fenn C. (1987) Electrical conductivity. In Gurnell A.M. and Clark M.J. (eds.) *Glacio-fluvial sediment transfer : An alpine perspective*. Chichester, John Wiley and Sons p377-414.

Ford, D.C. and Williams, P. (1989) : *Karst Geomorphology and Hydrology*, Unwin Hyman, London, 601pp.

Freeze, R.A. and Cherry, J.A. (1979) *Groundwater*. New Jersey: Prentice-Hall.

Gardiner, V. and Dackcombe, R. (1983) *Geomorphological Field Manual*, Allen & Unwin, London, 254pp.

Garrels, R.M. and Christ, C.L. (1965) *Solutions, minerals and equilibria*, New York: Harper and Collins.

Gibbs, M.T. and Kump, L.R., (1994) Global chemical erosion during the last glacial maximum and the present: Sensitivity to changes in lithology and hydrology. Paleoceanography, **9**, p529-543

Goodwin, I.D. (1988) The nature and origin of a jökulhlaup near Casey Station, Antarctica. Journal of Glaciology, **34**, p95-101.

Gurnell, A. (1987) Suspended sediment, in Gurnell A.M. and Clark M.J. (eds.) *Glacio-fluvial sediment transfer : An alpine perspective*. Chichester, John Wiley and Sons, p305-354.

Haeberli, W. (1983) Frequency and Characteristics of glacier floods in the Swiss Alps. Annals of Glaciology, **4**, p85-90.

Hagen, J.O., Korsen, O.M. and Vatne, G. (1991) Drainage pattern in a subpolar glacier: Broggerbreen, Svalbard. in Gjessing, Y., Hagen, J.O., Hassel, K.A., Sand, K and Wold, B., eds. Arctic hydrology. Present and future tasks. Norwegian National Committee for hydrology report no.23, p121-131.

Hallet, B. (1976) Deposits formed by subglacial precipitation of $CaCO_3$. Bulletin, Geological Society of America, **87**, p1003-15.

Hallet, B. and Anderson, R.S. (1980) Detailed glacial geomorphology of a proglacial bedrock area at Castleguard Glacier, Alberta, Canada. Zeitschrift für Gletscherkunde und Glazialgeologie, **16**, p171-184.

Hansen, J., Johnsen, D., Lacis, A., Lebedeff, S., Lee, P., Rind, D., and Russell, G. (1981) Climate impact of increasing atmospheric carbon dioxide. Science, **213**, p957-966.

Heinrich, H. (1988) Origin and consequences of cyclic ice rafting in the Northeast Atlantic Ocean during the past 130,000 Years. Quaternary Research, **29**, p142-152.

Hemm, J. D. (1982) Conductance: a collective measure of dissolved ions In Minear, R.A. and Keith, L.H. (eds.) *Water analysis Vol.1 Inorganic species. Part 1.* New York Academic Press.

Hodgkins, R. (1994) The seasonal evolution of meltwater discharge, quality and routing at a high-Arctic glacier. Unpublished PhD thesis. University of Cambridge, U.K. 246p.

Hodson, A. (1994) Climate, hydrology and sediment transfer process interactions in a sub-polar glacier basin, Svalbard. Unpublished PhD. thesis, University of Southampton, U.K.

Holland, H.D. (1978) *The Chemistry of the Atmosphere and the Oceans*, Wiley-Interscience, New York

Holmlund, P. (1988) Internal geometry and evolution of moulins, Storglaciären, Sweden. Journal of Glaciology, **34**, p242-248.

Humphrey, N., Raymond, C.F. and Harrison, W.D. (1986) Discharges of turbid water during mini-surges of Variegated Glacier, Alaska, U.S.A. Journal of Glaciology, **27**, p407-421.

Iken, A. (1972) Measurements of water pressure in moulins as part of a movement study of the White Glacier, Axel Heiberg Island, Northwest Territories, Canada. Journal of Glaciology, **11**, p53-58

Iken, A. (1974) Velocity fluctuations of an Arctic valley glacier, a study of the White Glacier, Axel Heiberg Island, Canadian Arctic Archipelago. Axel Heiberg Island Research Reports, McGill University, Montreal. Glaciology No.5 116p.

Iken, A. (1981) The effect of the subglacial water pressure on the sliding velocity in an idealised numerical model. Journal of Glaciology, **27**, p407-421.

Iken, A., Röthlisberger, H., Flotron, A. and Haeberli, W. (1983) The uplift of the Uneraargletscher at the beginning of the meltseason -a consequence of water storage at the bed? Journal of Glaciology, **29**, p28-47.

Iken, A. and Bindschadler, R. A. (1986) Combined measurements of subglacial water pressure and surface velocity of the Findelengletscher, Switzerland: conclusions about the drainage system and sliding mechanism. Journal of Glaciology, **32**, p101-109.

Iken, A., Echelmeyer, K., Harrison, W. and Funk, M. (1993) Mechanisms of fast flow in Jakobshavns Isbrae, West Greenland: Part I. Measurements of temperature and water level in deep boreholes. Journal of Glaciology, **39**, p15-25.

Iverson, N., Hanson, B., Hooke, R. Le B. and Jansson, P. (1995) Flow mechansims of glaciers on soft beds. Science, January.

Johannessen, M. and Henriksen, A. (1978) Chemistry of snow meltwater : changes in concentration during melting. Water Resources Research, **14**, p615-619.

Jouzel, J., Lorius, C., Petit, J.R., Genthon, C., Barkov, N.I., Kotlyakov, V.M. and Petrov, V.M. (1987) Vostok Ice core: a continuous isotope temperature record over the last climatic cycle (160,000 years). Nature, **329**, p403-408.

Kamb, W.B. (1987) Glacier surge mechanism based on linked cavity configuration of the basal conduit system. Journal of Geophysical Research, **92 (B9)**, p9083-9100.

Kamb, W.B. and Engelhardt, H. (1991) Antarctic ice stream B: conditions controlling its motion and interactions with the climate system. In Glaciers-Ocean-Atmosphere interactions (Proceedings of the International Symposium held at St. Petersburg, September, 1990) IAHS Publication **208**, p145-154

Kerr, J.W. (1972) Map 1358A Geology: Dobbin Bay, District of Franklin 1:250000, Geological Survey of Canada.

Koerner, R.M. (1979) Accumulation, ablation and oxygen isotope variations on the Queen Elizabeth Islands Ice Caps, Canada. Journal of Glaciology, **22**, p25-41.

Kump, L.R., and Alley, R.B. (1994) Global chemical weathering on glacial time scales, in *Material Fluxes on the surface of the Earth*. (eds.) Usselman, T.M. and Hay, W.W., National Academy Press, Washington, D.C.

Letreguilly, A., Reeh, N. and Huybrechts, P. (1991) The Greenland ice sheet through the last glacial-interglacial cycle. Palaeogoegraphy, Palaeoclimatology, Palaeoecology, **90**, 385-p394.

Maag, H. (1969) Ice dammed lakes and marginal glacial drainage on Axel Heiberg Island, Canadian Arctic Archipelago. Axel Heiberg Island Research Reports, McGill University, Montreal. 147p.

Mathews, W.H. (1973) Record of two jökulhlaups. International Association of Hydrological Sciences Publication, **95** (Symposium on the hydrology of glaciers. Proceedings of the Cambridge Symposium, 7-13 September 1969) p99-110.

Mathews, W.H. (1974) Surface profiles of the Laurentide ice sheet in its marginal areas Journal of Glaciology, **13**, p37-44.

Müller, F. (1963) Englacial temperature measurements on Axel Heiberg Island, Canadian Arctic Archipelago. International Association of Hydrological Sciences Publication, 61 p168-180.

Müller, F. and Iken, A. (1973) Velocity fluctuations and water regime of arctic valley glaciers. International Association of Hydrological Sciences Publication, **95** (Symposium on the hydrology of glaciers. Proceedings of the Cambridge Symposium, 7-13 September 1969), p165-182

Nienow, P.W. (1994) Dye tracer investigations of glacier hydrological systems. Unpublished PhD thesis. Cambridge University, U.K.

Nye, J.F. (1976) Water flow in glaciers: Jökulhlaups, tunnels and veins. Journal of Glaciology, **17**, p181-207.

Nye, J.F. (1973) Water at the glacier bed. International Association of Hydrological Sciences Publication, 95 (Symposium on the hydrology of glaciers. Proceedings of the Cambridge Symposium, 7-13 September 1969), p189-194.

Ommanney, C.S.L. (1969). A study in glacier inventory. The ice masses of Axel Heiberg Island, Canadian Arctic Archipelago. Glaciology. No.3 Axel Heiberg Island Research Reports. McGill University, Montreal. 105p.

Østrem, G., Bridge, C.W. and Rannie, W.F. (1967) Glaciohydrology, discharge and sediment transport in the Decade glacier area, baffin Island, N.W.T., Geografiska Annaler, **49A**, p268-282.

Oswald, G.K.A. and Robin, G. de Q. (1973) Lakes beneath the Antarctic Ice Sheet. Nature, **245**, p251-254.

Palmer, A.N. (1984) Geomorphic interpretation of karst features. In La Fleur, R.G. (ed.) *Groundwater as a geomorphic agent* , Allen and Unwin, London,p173-209.

Paterson, W.S.B. (1994) *The Physics of Glaciers*, 3rd Edition, Permagon, Oxford, 480pp.

Plummer, L.N. and Busenberg, E. (1982) The solubilities of calcite, aragonite and vaterite in CO_2-H_2O solutions between 0 and 90°C, and an evaluation of the aqueous model for the system $CaCO_3$-CO_2-H_2O. Geochimica Cosmochimica Acta, **46**, 1011-40.

Plummer, L.N., Parkhurst, D.L. and Kosiur, D.R. (1975) MIX2, a computer program for calculating chemical equilibria in natural waters United States Geological Survey, Water Resources Investigations Report, **61** 75pp

Pohjola, V.A. (1994) TV-video observations of englacial voids in Storglaciären, Sweden. Journal of Glaciology, **40**, p231-24.

Punkari, M. (1982) Glacial geomorphology and dynamics in the eastern parts of the Baltic Shield interpreted using Landsat imagery. Photogrammetric Journal of Finland, **9**, p 77-93.

Rains, B., Shaw, J., Skoye, R., Sjogren, D. and Kvill, D. (1993) Late Wisconsin subglacial megaflood paths in Alberta. Geology, **21**, p323-326.

Raiswell, R. (1984) Chemical models of solute acquisition in glacial meltwaters. Journal of Glaciology, **30**, p49-57.

Raiswell, R. and Thomas, A.G. (1984) Solute acquisition in glacial meltwaters. I. Fjallsjökull (south-east Iceland): bulk meltwaters with closed-system characteristics. Journal of Glaciology **30**, p35-43

Rehak, J. and Rehak, J. (1995) New information on the interior drainage of subpolar glaciers of southwest Spitsbergen. In Griselin, M. (ed.) Annales litteraires de l'université de Besancon No 561, Série Géographie No. 34, Besancon, p93-100.

Reynaud, L. and Moreau, L. (1995) Moulins glaciares des glaciers tempérés et froids de 1986 à 1994 (Mer de Glace et Groenland). In Griselin, M. (ed.) Annales litteraires de l'université de Besancon No 561, Série Géographie No. 34, Besancon, p109-113.

Rist, S. (1973) Jökulhlaupaannall 1971, 1972 og 1973 Jökull, **23**, p56-60.

Rist, S. (1976) Jökulhlaupaannall 1974, 1975 og 1976 Jökull, **26**, p75-79.

Rist, S. (1984) Jökulhlaupaannall 1981, 1982 og 1983 Jökull, **34**, p165-172.

Rist, S. (1992) Jökulhlaupaannall 1984-1988 Jökull, **42**, p73-80.

Rollins, L. (1989) User's guide to DATAGEN4 and WQ4F.

Röthlisberger, H. (1972) Water pressure in intra- and subglacial channels. Journal of Glaciology, **11**, p177-203.

Russell, A.J. (1990) Extraordinary melt-water run-off near Sondre Stromfjord, West Greenland. Journal of Glaciology, **36**, p353.

Russell, A.J. (1993) Supraglacial lake drainage near Sondre Stromfjord, Greenland. Journal of Glaciology, **39**, p431.

Scholtz, H., Schreiner, B. and Funk, H. (1988) Der einfluss von gletscherlaufen auf die schmelzwasserablagerungen des Russell-gletschers bei Sondre Stromfjord (Westgrønland). Zeitschrift für Gletscherkunde und Glazialgeologie, **24**, p55-74.

Schroder, J. (1995) Hans Glacier moulins observed from 1988 to 1992. In Griselin, M. (ed.) Annales litteraires de l'université de Besancon No. 561, Série Géographie No. 34, Besancon, p31-40.

Sharp M.J. (1991) Hydrological inferences from meltwater quality data : the unfulfilled potential. Proceedings, BHS 3rd National Hydrology Symposium, Southampton 5.1 - 5.8.

Sharp, M., Gemmell, J.C. and Tison, J.L. (1989) Structure and stability of the former subglacial drainage system of the Glacier de Tsanfleuron, Switzerland. Earth Surface Processes and Landforms, **14**, p119-134.

Sharp, M., Tranter, M., Brown, G.H. and Skidmore, M. (1995) Rates of chemical denudation and CO_2 drawdown in a glacier-covered alpine catchment. Geology, **23**, p61-62.

Shaw, J. (1989) Drumlins, subglacial meltwater floods, and ocean responses, Geology, **17**, p853-856.

Shaw, J. (1994) A qualitative view of sub-ice-sheet landscape evolution. Progress in Physical Geography, **18,** p159-184.

Shaw, J., Kvill, D. and Rains, B. (1989) Drumlins and catastrophic subglacial floods. Sedimentary Geology, **62**, p177-202.

Shoemaker, E.M. (1986) Subglacial hyrology for an ice sheet resting on a deformable acquifer. Journal of Glaciology, **32**, p20-30.

Shoemaker, E.M. (1991) Water sheet outburst floods from the Laurentide Ice Sheet Canadian Journal of Earth Sciences, **29**, p1250-1264.

Shoemaker, E.M. (1992) Subglacial floods and the origin of low-relief ice-sheet lobes. Journal of Glaciology, **38**, p105-112.

Shoemaker, E.M. (1994) Sub-permafrost water storage beneath subpolar ice sheets. Cold Regions Science and Technology **23** p83-91

Stumm, W. and Morgan, J.J. (1981) *Aquatic Chemistry*, 2nd Edition, Wiley Interscience, New York, 780pp.

Sugden, D.E. and John, B.S. (1976) *Glaciers and Landscape. A geomorphological approach*. Edward Arnold, London, 376pp.

Sugden, D.E., Clapperton, C.M. and Knight, P.G. (1985) A jökulhlaup near Sondre Stromfjord, West Greenland, and some effects on the ice sheet margin, Journal of Glaciology, **31**, p366-368.

Thomas, A.G. and Raiswell, R. (1984) Solute acquisition in glacial meltwaters II. Argentière (French Alps): bulk meltwaters with open system characteristics. Journal of Glaciology, **30**, p44-48.

Thomsen, H. H., Thorning, L. and Braithwaite, R.J. (1988) Glacier-hydrological conditions on the Inland Ice north-east of Jakobshavn, central West Greenland. Rapport Grønlands Geologiske Undersøgelse, **138**, map with text

Tranter, M., Brown, G., Raiswell, R., Sharp, M.J. and Gurnell, A. (1993) A conceptual model of solute acquistion by Alpine glacial meltwaters. Journal of Glaciology, **39**, p573-581.

Tranter, M., Brown, G.H., Hodson, A., Gurnell, A.M. and Sharp, M. (1994) Variations in the nitrate concentration of glacial runoff in Alpine and sub-Polar environments. Snow and Ice Cover: Interactions with the Atmosphere and Ecosystems (Proceedings of Yokohama Symposia J2 and J5, July 1993). IAHS Publication no.223. p299-311.

van Donk, J. (1976) An ^{18}O record of the Atlantic Ocean for the entire Pleistocene. In Investigation of late Quaternary paleoceanography and paleoclimatology, Cline R.M. and Hays, J.D. (eds.) p145-163 Geological Society of America Memoir 145. Boulder, Colorado: Geological Society of America

Vear, A. and Curtis, C.D. (1981) A quantitative evaluation of pyrite weathering Earth Surface Processes, **6**, p191-198

Walder, J.S. (1986) Hydraulics of subglacial cavities. Journal of Glaciology, **32**, p439-445.

Walder, J.S. and Fowler, A. (1994) Channelised subglacial drainage over a deformable bed. Journal of Glaciology, **40**, p3-15.

Weertman, J. (1972) General theory of water flow at the base of a glacier or ice sheet. Reviews of Geophysics and Space Physics, **10**, p287-333.

Willis, I.C., Sharp, M.J. and Richards, K.S. (1990) Configuration of the drainage system of Midtdalsbreen, Norway, as indicated by dye tracing experiments. Journal of Glaciology, **36**, p89-101.

Wolfe, P.M. (1995) Hydrometeorological investigations on a small valley glacier in the Sawtooth Range, Ellesmere Island, N.W.T. Unpublished M.A. thesis, Wilfrid Laurier University.

Zotikov, I.A. (1986) The thermophysics of glaciers. D. Reidel, Dordrecht. 275p.

APPENDICES

APPENDIX 1

JULIAN DAY CALENDAR

	1	2	3	4	5	6	7	8	9	10	11	12	13	14	15	16	17	18	19	20	21	22	23	24	25	26	27	28	29	30	31
Jan	1	2	3	4	5	6	7	8	9	10	11	12	13	14	15	16	17	18	19	20	21	22	23	24	25	26	27	28	29	30	31
Feb	32	33	34	35	36	37	38	39	40	41	42	43	44	45	46	47	48	49	50	51	52	53	54	55	56	57	58	59	60		
Mar	*60*	*61*	*62*	*63*	*64*	*65*	*66*	*67*	*68*	*69*	*70*	*71*	*72*	*73*	*74*	*75*	*76*	*77*	*78*	*79*	*80*	*81*	*82*	*83*	*84*	*85*	*86*	*87*	*88*	*89*	*90*
Apr	*91*	*92*	*93*	*94*	*95*	*96*	*97*	*98*	*99*	*100*	*101*	*102*	*103*	*104*	*105*	*106*	*107*	*108*	*109*	*110*	*111*	*112*	*113*	*114*	*115*	*116*	*117*	*118*	*119*	*120*	
May	*121*	*122*	*123*	*124*	*125*	*126*	*127*	*128*	*129*	*130*	*131*	*132*	*133*	*134*	*135*	*136*	*137*	*138*	*139*	*140*	*141*	*142*	*143*	*144*	*145*	*146*	*147*	*148*	*149*	*150*	*151*
Jun	*152*	*153*	*154*	*155*	*156*	*157*	*158*	*159*	*160*	*161*	*162*	*163*	*164*	*165*	*166*	*167*	*168*	*169*	*170*	*171*	*172*	*173*	*174*	*175*	*176*	*177*	*178*	*179*	*180*	*181*	
Jul	*182*	*183*	*184*	*185*	*186*	*187*	*188*	*189*	*190*	*191*	*192*	*193*	*194*	*195*	*196*	*197*	*198*	*199*	*200*	*201*	*202*	*203*	*204*	*205*	*206*	*207*	*208*	*209*	*210*	*211*	*212*
Aug	*213*	*214*	*215*	*216*	*217*	*218*	*219*	*220*	*221*	*222*	*223*	*224*	*225*	*226*	*227*	*228*	*229*	*230*	*231*	*232*	*233*	*234*	*235*	*236*	*237*	*238*	*239*	*240*	*241*	*242*	*243*
Sep	*244*	*245*	*246*	*247*	*248*	*249*	*250*	*251*	*252*	*253*	*254*	*255*	*256*	*257*	*258*	*259*	*260*	*261*	*262*	*263*	*264*	*265*	*266*	*267*	*268*	*269*	*270*	*271*	*272*	*273*	
Oct	*274*	*275*	*276*	*277*	*278*	*279*	*280*	*281*	*282*	*283*	*284*	*285*	*286*	*287*	*288*	*289*	*290*	*291*	*292*	*293*	*294*	*295*	*296*	*297*	*298*	*299*	*300*	*301*	*302*	*303*	*304*
Nov	*305*	*306*	*307*	*308*	*309*	*310*	*311*	*312*	*313*	*314*	*315*	*316*	*317*	*318*	*319*	*320*	*321*	*322*	*323*	*324*	*325*	*326*	*327*	*328*	*329*	*330*	*331*	*332*	*333*	*334*	
Dec	*335*	*336*	*337*	*338*	*339*	*340*	*341*	*342*	*343*	*344*	*345*	*346*	*347*	*348*	*349*	*350*	*351*	*352*	*353*	*354*	*355*	*356*	*357*	*358*	*359*	*360*	*361*	*362*	*363*	*364*	*365*
	Add 1 to figures in italics during leap years																														

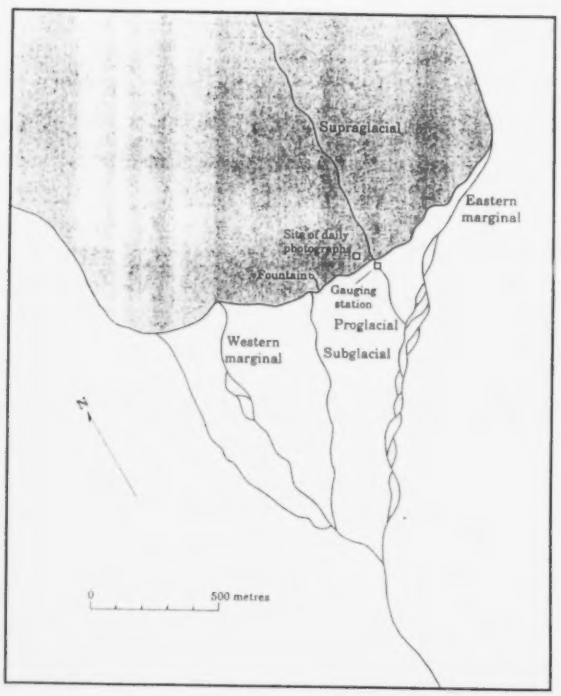

APPENDIX 2. CONFIGURATION OF THE STREAMS AT THE GLACIER SNOUT